5-2020

Receptor Tyrosine Kinases-Mediated Acquired Parp Inhibitor Resistance In Breast Cancer

MEI-KUANG CHEN

RECEPTOR TYROSINE KINASES-MEDIATED ACQUIRED PARP INHIBITOR RESISTANCE IN BREAST CANCER

By

Mei-Kuang Chen, M.S.

APPROVED:

Dihua Yu, M.D., Ph.D.
Advisory Professor

Mien-Chie Hung, Ph.D.
Co-advisory Professor

Jennifer L. Litton, M.D.

Shiaw-Yih Lin, Ph.D.

Bin Wang, Ph.D.

Jeffrey T. Chang, Ph.D.

Paul J. Chiao, Ph.D.

APPROVED:

Dean, The University of Texas MD Anderson Cancer Center UTHealth Graduate School of Biomedical Sciences

RECEPTOR TYROSINE KINASES-MEDIATED PARP INHIBITOR RESISTANCE IN BREAST CANCER

A

DISSERTATION

Presented to the Faculty of

The University of Texas

MD Anderson Cancer Center UTHealth

Graduate School of Biomedical Sciences

in Partial Fulfillment

of the Requirements

for the Degree of

DOCTOR OF PHILOSOPHY

by

Mei-Kuang Chen, M.S.

Houston, Texas

May 2020

Copyright

Chapter I-2 is based on contents published in FEBS Journal.

License Number 4796220018447.

“Chen MK, Hung MC. Proteolytic cleavage, trafficking, and functions of nuclear receptor tyrosine kinases. FEBS J. 2015 Oct;282(19):3693-721. PubMed PMID: 26096795; PubMed Central PMCID: PMC4591179.”

Chapter I-3 is based on contents published in American Journal of Cancer Research.

“Chen MK, Hung MC. Regulation of therapeutic resistance in cancers by receptor tyrosine kinases. Am J Cancer Res. 2016 Mar 15;6(4):827-42. eCollection 2016. PubMed PMID: 27186434; PubMed Central PMCID: PMC4859887.”

The reuse of these materials are under copyright policy of American Journal of Cancer Research: *“Once the paper is published, the copyright will be released by the publisher under the “Creative Commons Attribution Noncommercial License”, enabling the unrestricted non-commercial use, distribution, and reproduction of the published article in any medium, provided that the original work is properly cited.”*

Dedications

This thesis is dedicate to my dearest parents, Shu-Chin Wang and Shan-Tarng Chen, also to my husband, Gong-Her Wu, my family, and my family in law.

Acknowledgements

During my Ph.D. training period, my most sincerely acknowledgment goes to both Dr. Mien-Chie Hung and Dr. Dihua Yu, for they always being extremely supportive to my research and to my life. I joined Dr. Mien-Chie Hung's group before he retires from MD Anderson Cancer Center. He had multiple administrative positions in the institute, but he still made time to discuss my projects with me whenever I need, and he also tracked my progress regularly to make sure I was on the right track. After Dr. Hung retired, Dr. Yu took me in and supports me to continue my project. I remember clearly that when I told her I will survive from the Ph.D. training, she told me "Sweetheart, you will not only survive, you will thrive." Both of my advisors are so considerate that they not only support my research, they also remind me to spend time with my family, and they encourage me to join school events and spend time with my friends. In the hard time during global pandemic, the first thing they asked me is to stay healthy and safe, and they told me that is the most important thing and should be my highest priority. I feel so lucky that I have both of them as advisor. I also want to thank all my committee members for always being there for me, and they offered generous help to my project. They always give me suggestions and point out my blind spots to improve my critical thinking. It is a great relief for this 6 year in graduate school knowing my committee members are on my side and they aim on transforming me to professional researcher in this field.

I also want to express my grateful of having my parents, my family, and my family in law. Studying aboard is never easy to anyone, especially living alone without family under the same roof. They called me everyday and I can share all my feelings with them. Although I stay in a foreign country, I know I always have home to go to. They make me strong to face challenges and they support me with unconditional love. My smart friends, Shu-hong Lin and Jackie Shen, sharing creative thoughts and scientific insights with me. We shared a lot of crazy idea, especially in science, that keeps us thinking outside of the box. My food squad, Cavan Bailey, Danielle Little, Aparna Padhye and Monica Wen, spent a lot of time with me sharing the ups and downs in graduate school, and they always know the food that bring me comfort after a long day. I also want to thank all my friends, too many to list here, for being there for me, reading my posts and telling me how much they support me.

I also appreciate GSBS deans and staffs, they provide resources to answer all my questions about graduate program and secure awards to support GSBS students. Last, but not least, I want to acknowledge all donors and agencies that provide the following fellowships to support my projects: Jesse B. Heath, Jr. Family Legacy Award; Larry Deaven Ph.D. Fellowship in Biomedical Sciences; T32 Training Grant in Cancer Biology at MD Anderson Cancer Center; and, Scholarship for Excellence in Biochemistry and Molecular Biology at MD Anderson.

Abstract

RECEPTOR TYROSINE KINASES-MEDIATED ACQUIRED PARP INHIBITOR RESISTANCE IN BREAST CANCER

Mei-Kuang Chen, B.S., M.S.

Advisory Professors: Dihua Yu, M.D., Ph.D. and Mien-Chie Hung, Ph.D.

Leveraging compromised DNA damage repair (DDR) pathways commonly found in tumor cells, a classic strategy in cancer therapy is inducing excessive DNA damage to cause cancer cell death. Small molecule poly(ADP-ribose) polymerase (PARP) inhibitors (PARP-is) have been approved for clinical use in treating breast cancer and ovarian cancer patients bearing DDR-deficient tumors with mutations in breast cancer susceptibility genes (*BRCA*^{m}). However, accumulating evidences show that both intrinsic and acquired resistances to PARP-is exist in clinic and pre-clinical animal models. Therefore, I developed panels of cells with acquired PARP-is resistance from PARP-is-sensitive triple negative breast cancer (TNBC) cell lines, and used these cells to screen for common traits that can be targeted with feasible therapeutic agent combinations to overcome PARP-is resistance. Since TNBC lacks of effective targeted therapy so far, I focused on developing and using a panel of PARP-is-resistant TNBC cells in this study. Among the molecular mechanisms known contribute to PARP-is resistance, oncogenic kinase activations, including several hyper-activated receptor tyrosine kinases (RTKs), are involved in enhancing

DNA damage repair and decreasing affinity of PARP-is to PARP1. Among the candidate RTKs, MET has more small molecules inhibitors that can target it, and thus, my colleagues and I made it a priority in investigating synergism between MET inhibitor and PARP inhibitor in multiple cancer types and demonstrated that combinations of PARP-is and MET inhibitors possess moderate to strong synergism in the different cancer types we studied. In this thesis, I systematically screened for activated RTKs as common traits in the PARP-is-resistant cells I developed. Through non-biased antibody array screening, I found MET phosphorylation is also high in the TNBC cells with acquired PARP-is resistance. However, there are several activated RTKs have higher prevalence than MET, including FGFR, EGFR and IGF1R. Therefore, in this thesis, I extended my study from MET to other candidate RTKs and demonstrated that MET is not the only RTK contribute to PARP-i-resistance in TNBC, and I found that RTKs have different working mechanisms toward PARP-i-resistance. In conclusion, RTKs contribute to PARP-i-resistance through multiple mechanisms and it is worthwhile to investigate these mechanisms to unveil more targeted therapeutic strategies for cancer patients with PARP-i-resistance.

Table of Contents

List of Illustrations

List of Tables

Chapter I. Research Background

1. Subtypes of Breast Cancer

Breast cancer can be categorized into many subtypes according to the molecular traits of cancer cells. Popular molecular traits used is expression of hormone receptors for determining clinical hormone therapy's treatment strategy, breast cancer can be group into different subtypes according to their hormone molecule expression status examined based on histology (reviewed in [1, 2]). Breast cancer that express estrogen receptor (ER) (ER-positive) or progesterone receptor (PgR) (PR-positive) are defined as hormone receptor positive group. Around 70 % - 75 % of breast cancers belong to this hormone receptor positive group, and expression levels of ER and PgR can be identified mainly through immunohistochemistry (IHC) staining of tumor biopsy [1, 2]. Beside ER and PgR, HER2 is another receptor commonly examined to classify breast cancer subtype due to distinct clinicopathologic feature and survival outcomes related to these receptors [1-4]. HER2 is a receptor tyrosine kinase (RTK) which promotes cancer cell growth and can serve as prognostic factor [5, 6]. Approximately, around 15% of breast cancers express excessive HER2 receptor or having multiple copies of *HER2* gene are group into HER2-positive subtype [1, 2]. HER2-positive breast cancer can be either hormone receptor positive or negative [4]. In clinical, HER2-positive subtypes is predominantly diagnosed by analyzing IHC and HER2 *in situ* hybridization results while HER2 phosphorylation

status is a raising alternative defining method (reviewed in [7]). Beside the hormone-positive and HER2-positive subtypes, HER2-negative and hormone receptor negative breast cancers are group into triple negative breast cancer (TNBC) [8]. In clinic, most of the hormone therapy targeted receptor positive patients are treated with targeted medications, such as tamoxifen or aromatase inhibitors, that specifically block hormone signaling or can reduce estrogen production [9, 10]. Most of HER2-positive patients will be treated with anti-HER2 agents such as trastuzumab (Herceptin), pertuzumab (Perjeta) or TDM1 (Kadcyla) [10]. Depends on the methods and threshold used for diagnosis and on racial identities, around 10 - 25% of breast cancer are grouped into TNBC subtype [11]. TNBC are generally more aggressive than other subtypes, which has worst patient survival rate and rapid resistance to chemotherapy [3, 12]. However, because of lacking target for hormone receptor targeted therapy, TNBC patients often are recommended with chemotherapy treatment instead of targeted therapy [10, 12].

In addition to histological classification, a set of 550 genes were also be used to classify breast cancers according to their molecular subtypes [2]. With different gene expression clusters, breast cancer can also grouped into at least five molecular subtypes: luminal A, luminal B, HER2-enriched, basal-like and normal-like [2, 13]. For hormone-positive subtypes, most of breast cancers in this group express gene profile as luminal breast epithelial cell [14], therefore, it can also be referred as luminal type. Luminal type can be further divided into

two groups: luminal A and B, where luminal B type expresses higher mitosis or proliferation genes and higher lymph node involvement [15].

2. Transportation of Receptor Tyrosine Kinase into Cell Nucleus

This section is based upon the review article published in FEBS Journal. "Chen MK, Hung MC. Proteolytic cleavage, trafficking, and functions of nuclear receptor tyrosine kinases. FEBS J. 2015 Oct;282(19):3693-721. PubMed PMID: 26096795; PubMed Central PMCID: PMC4591179."

In the past, a majority of studies have focused on the canonical RTK signaling from cell surface via the following sequential events (Fig. 1): (1) The receptor binds with its ligand. (2) The receptor then undergoes conformational changes and forms homo- or hetero- oligomers that are essential to activate the kinase activity of the receptor. The tyrosine kinase domain then undergoes *trans* autophosphorylation that greatly elevates the receptor's catalytic activity. (3) The phosphotyrosine residues serve as docking site for cytoplasmic adaptor proteins containing Src homology-2 (SH2) and phosphotyrosine-binding (PTB) domain to form signal transduction complex that determines and initiates the corresponding signaling cascade to regulate cellular processes in response to ligand stimulation [16-22].

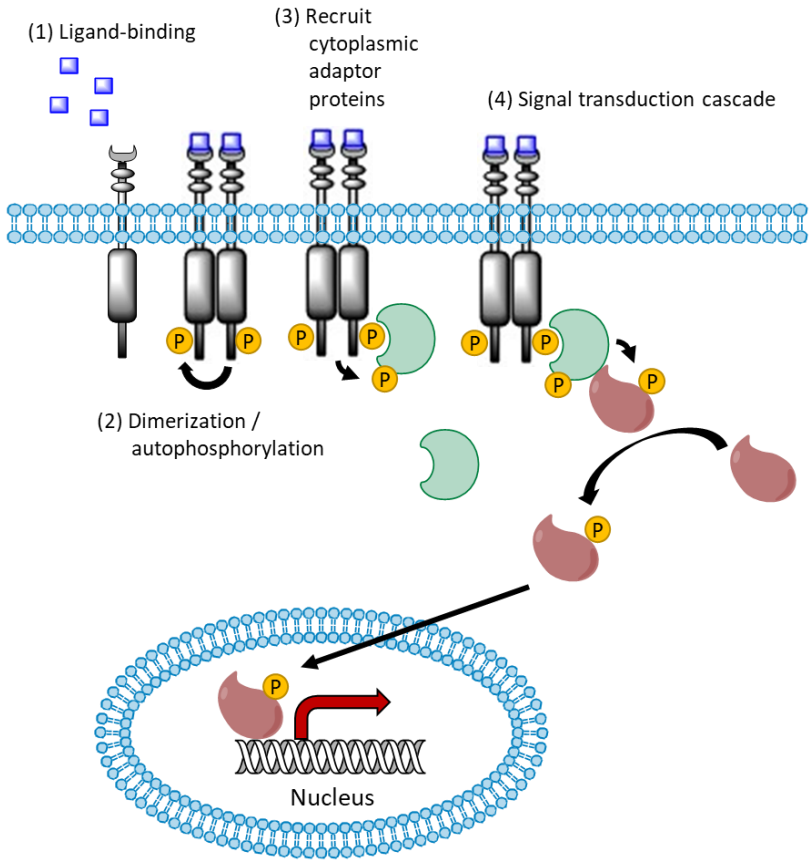

Figure 1. Canonical RTK signaling cascade

This figure illustrates the canonical RTK signal transduction pathway stepwise. The canonical RTK signaling begins with (1) the receptor binding with its ligand. (2) The receptors then undergo oligomerization and *trans* auto-phosphorylation. (3) The phosphor-tyrosine residues on receptor served as docking sites for the secondary messenger proteins containing either SH2 and/or PTB domain (shown as green crescent-shape molecule) which are subjected to be phosphorylated by the RTK. (4) The secondary messenger proteins recruit and activate its downstream proteins (illustrated as oval shape molecule) which serve as envoys delivering the signal into nucleus to regulate gene transcription.

Interestingly, members of the RTK subfamilies are also present in the nucleus and they are referred to as membrane receptor in nucleus or MRIN [23, 24]. Accumulating evidence indicates that at least 12 RTK families contain MRINs that exist either as holoreceptor or truncated form with novel non-canonical functions in transcriptional regulation, cell proliferation, DNA damage repair as well as cancer cell invasion [24-28]. In various cancer types, nuclear RTK expression is associated with poor prognosis [29-32]. Generally, after ligand-induced activation, membrane-bound MRINs are internalized from cell surface through endocytosis and transported into the nucleus. However, RTKs can be proteolytically cleaved to release an active RTK fragment that is also transported from the cell membrane to subcellular compartments, including the nucleus.

2.1. RTK internalization and endosomal retrograde trafficking to the Golgi and ER

Cell surface receptors are also found in many subcellular compartments, including the Golgi apparatus, mitochondria, ER, and nucleus. Upon ligand activation, RTK is rapidly internalized and translocated into endosomal compartments for signaling, recycling, or degradation by a clathrin-mediated or -independent pathways, depending on the different coat proteins in the membrane region that form the endocytic vesicles (reviewed in [33]). The endocytic vesicles are then sent to different subcellular compartments based on the associated

cargo proteins such as Rab proteins [34] or clathrin-binding adaptor proteins (AP) [35] (Fig. 2).

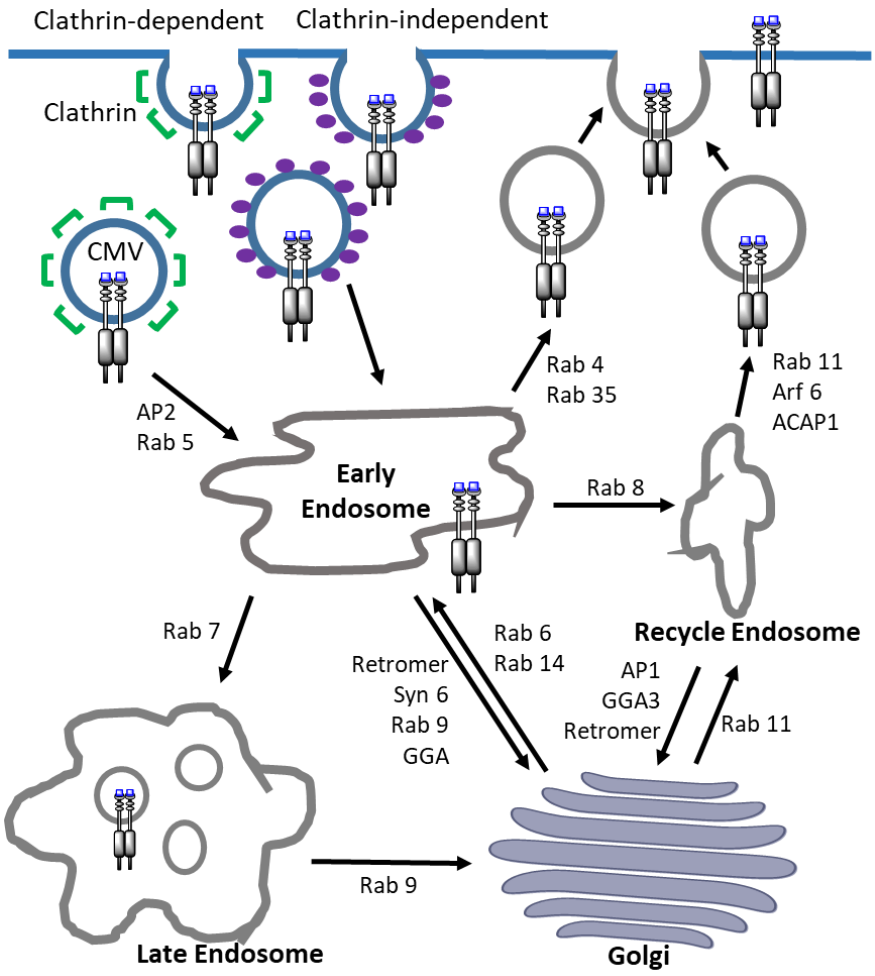

Figure 2. Endosomal vesicle trafficking of internalized RTK.

The RTK are internalized through either clathrin-dependent or clathrin-independent pathways. In clathrin-dependent endocytosis mechanism, the internalized membrane vesicle is coated with clathrin (green). Meanwhile, caveolin-mediated endocytosis, which is the main clathrin-independent RTK endocytic mechanism, is initiated at the membrane region that contain caveolin-rich lipid raft (purple).

The endocytic vesicles from both pathways are sent to early endosome for sorting. Based on the component of coating proteins, the vesicles are then transported to different endosomal components, including recycle endosome, late endosome and *trans* Golgi network. Several important coating proteins that guide vesicle transportation direction, including Rab proteins, clathrin-dependent adaptor proteins (AP), retromer, syntaxin 6 (Syn 6), and Golgi-associated, gamma adaptin ear containing, ARF binding protein (GGA) are indicated.

Clathrin-mediated endocytosis (CME) from the non-lipid raft membrane domains is the predominant mechanism for RTK internalization. Prior to RTK activation, auto-inhibition of clathrin prevents the recruitment of cytosolic adaptor protein. Upon RTK activation, clathrin recognizes specific posttranslational modifications, such as ubiquitination and acetylation, at the C-terminus of activated RTK [36, 37]. The clathrin complex then recruits cargo-specific adaptors, e.g., AP2, which can also interact with phosphatidylinositol (4,5)-biphosphate (PIP2) to bring in the phospholipids on adjacent plasma membrane and undergo conformational change that promotes the formation of clathrin-coated pit through membrane curvature, clathrin polymerization, and internalization of the RTK-containing pit from the plasma membrane [38]. Moreover, CME is a highly selective process that forms only after recognition of the cargo protein sequence by AP. For example, AP2 specifically recognizes the YXXΦ and LL motif ([ED]XXXL[LI]) consensus sequence on the cargo protein (reviewed in [39]). In

EGFR, the LL motif is important for AP-2 phosphorylation, which further facilitates the interaction between AP-2 and EGFR, and subsequent internalization of EGFR via CME [40].

Posttranslationally modified RTKs, such as from ubiquitination, can also be internalized for transport to various compartments but the process occurs via a clathrin-independent endocytic pathwya [41]. There are several clathrin-independent endocytic mechanisms, including phagocytosis, macropinocytosis, and lipid raft-mediated (e.g., caveolin-mediated) endocytosis, and among them, macropinocytosis and lipid raft-mediated endocytosis are more common in RTK internalization. Macropinocytosis is a growth factor-induced and actin-mediated transient endocytic process that begins from all membranous regions such as those of the lipid rafts in larger vesicles containing extracellular fluid and plasma membrane-bound components. Unlike clathrin-dependent endocytosis, caveolae-mediated endocytosis does not require a specific coat protein and is usually associated with lipid raft membrane regions containing caveolin-1 protein (reviewed in [42]). Recently, Boucrot *et al.* reported a new clathrin-independent endocytic mechanism called endophilin-mediated endocytosis (FEME) which does not required AP2 or clathrin [43]. Renard *et al.* further showed the FEME uses endophilin-A2 as membrane scissor to release the endocytic vesicles [44]. Endocytosis of membrane receptors, including RTKs such as EGFR, MET, VEGFR, PDGFR, IGF-1R, and TrkA via FEME requires ligand activation [43]. The binding of endophilin by CIN85 and Cbl are important in FEME, further sup-

porting that RTKs are subjected to FEME after ligand-induced activation. However, take EGFR for example, the EGFR FEME is observed mainly under high concentration EGF treatment, and FEME was suggested to more related to RTK canonical signaling down regulation [43].

After RTK internalization, the receptors are routed to the early endosomes, where the fate of cargo is determined. In general, RTKs can be degraded or recycled or can undergo retrograde trafficking to the Golgi apparatus (Fig. 2). Although it has been reported that in EGFR is recycled after stimulation by high concentrations of ligand in A431 cells, which express high levels of EGFR with 80% of EGFR internalized [45], not all endocytic receptors are subjected to recycling or degradation. Instead, a small portion of them undergoes retrograde transport which is the influx of protein and lipid from cell surface to Golgi or from Golgi to ER. The *trans* Golgi network (TGN)-targeting coat proteins, including Rab9, syntaxin 6, and GGA, guide fusion of the endosomal vesicle with TGN [46]. *Du et al.* demonstrated that inhibition of dynein or knockdown of dynein or syntaxin 6 attenuates EGFR accumulation in the Golgi apparatus and nucleus [47]. These findings indicated that the EGFR detected in these subcellular compartments is from the cell surface. Many reports have indicated that internalized RTKs via CME can also be transported to TGN for further sorting through coated vesicle transport, including EGFR [47], c-MET [48], and fibroblast growth factor receptor (FGFR)-1 [49, 50]. However, endocytic RTKs that undergo retrograde transport do not necessarily stop at TGN as they can be fur-

ther routed back to the ER and even the nucleus. In general, COPI vesicles mediate retrograde transport between the Golgi network and ER as exemplified by the Golgi-to-ER translocation of EGFR [50].

2.2. Nuclear trafficking of MRINs from ER

After reaching ER, the endocytic RTKs can be further transported into the nucleus via two importin-β-mediated pathways, integral trafficking from the ER to the nuclear envelope transport (INTERNET) and integrative nuclear FGFR-1 signaling (INFS) (Fig. 3) [51]. The major difference between the two is that the receptor remains membrane bound and is localized to inner nuclear membrane (INM) before nuclear translocation in INTERNET whereas FGFR-1 becomes a soluble protein after its release from ER or ER-derived membrane vesicle before translocation into the nucleus in INFS [51].

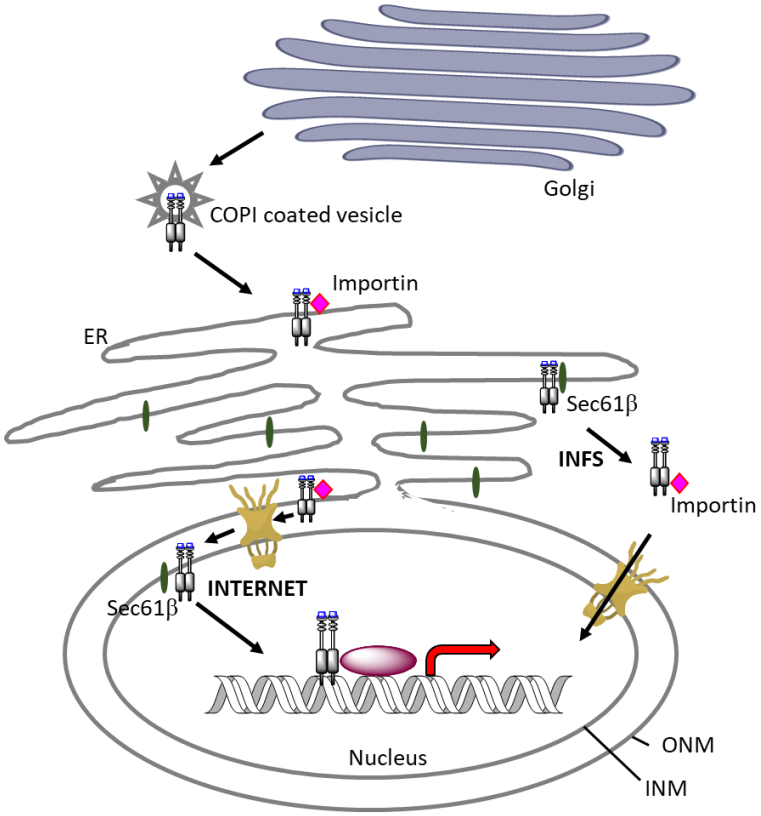

Figure 3. Retrograde and nuclear transportation mechanisms of membrane-bound RTKs.

The RTKs are retrograde transported from Golgi to ER through COPI-coated vesicles. The ER to nuclear transportation are divided into two pathways, INFS and INTERNET. For the INFS pathway, the RTK are pumped through Sec61 complex into cytosol where it binds to cytosolic Importin complex and transported into nucleus by the importin-NPC interaction. For the INTERNET pathway, the RTK are trafficking along ER and translocate from ONM to INM through NPC by binding with ER-associated Importin, and the RTK were released from INM by Sec61 complex into nucleoplasm. For both pathways, the nuclear localized RTK can interact with transcription factors and functions as transcription regulator.

Both EGFR and ErbB-2 contain a typical NLS that attracts NLS-harboring molecules and form complex with importin-β [52]. It has been shown that EGFR and ErbB-2 are transported from the ER to the outer nuclear membrane (ONM) and then to the NPC where the receptors enter the INM with the help of importin-β [51, 53]. As demonstrated with digitonin-permeabilized cells, detection of importin-β in the non-nuclear extract suggest that the INTERNET mechanism depends on membrane-associated importin-β to transport EGFR and ErbB-2 from the ONM into the INM [51, 54]. As demonstrated by Wang *et al.*, Sec61β translocon is required for releasing INM-bounded EGFR into the nucleus [55]. Because EGFR and ErbB-2 both contain NLS which can interact with membrane-bound importin-β, we hypothesized that INTERNET pathway predominantly mediates nuclear translocation of NLS-containing RTKs. Given that NLS is conserved among most of RTKs and that nuclear translocation of another NLS-containing RTK, c-MET, also follows the INTERNET pathway (unpublished data), it is likely that INTERNET is more commonly shared mechanism for RTK nuclear trafficking. However, further investigation of the nuclear transport mechanism of other RTKs is required to define this notion.

Via the INFS pathway, FGFR-1 is released as soluble protein from ER or ER-derived membrane vesicle into the cytosol through the Sec61 channel. FGFR-1 then associates with importin-β in cytoplasm before being transported into the nucleus [56]. Notably, even though FGFR-1 does not contain a consensus NLS sequence, it can still translocate into the nucleus by association with NLS-containing proteins, such as NLS-containing ligand, FGF-2 [56].

3. Regulation of Therapeutic Resistance in Cancers by Receptor Tyrosine Kinases

This section is based upon the review article published in American Journal of Cancer Research. "Chen MK, Hung MC. Regulation of therapeutic resistance in cancers by receptor tyrosine kinases. Am J Cancer Res. 2016 Mar 15;6(4):827-42. eCollection 2016. PubMed PMID: 27186434; PubMed Central PMCID: PMC4859887"

DNA damage stimuli can be divided into two classes, endogenous and environmental, based on the site of the stimulus' origin [57]. Endogenous DNA damage generates chemical changes in DNA structure leading to mutagenic events such as deamination of bases resulting from hydrolytic and oxidative events inside the cell. Environmental DNA damage can result from either physical or chemical agents outside the cells [57]. The incidence of DNA damage occurs frequently in normal cells. It is estimated that the error rate of the DNA replication machinery is at least 10^{-8} in *Escherichia coli* and human [58, 59]. In addition to replication errors, DNA breaks mainly caused by reactive oxygen species (ROS) are estimated to be 10^5 events per day [60, 61]. Thus, DNA damage response (DDR) is required to correct mistakes in DNA and is also responsible for eliminating cells with irreparable deleterious damage.

DNA damage and DDR are highly related to the formation and treatment of cancer. During carcinogenesis, the inefficiency and infidelity of the DDR pathway are the main causes of oncogenic events, such as DNA mutations, translocations, and epigenetic modifications, which correlate DDR to cancer risks [57, 62-65]. In cancer treatment, both radiotherapy and chemotherapy utilize DNA damaging agents that eliminate cancer cells by inducing DDR. Capitalizing on the deficiency of DDR in cancerous cells, the treatment of cancer with DNA damaging agents is an effective means of inducing massive DNA lesions and programmed cell death in the cells unable to resolve the damage. However, resistance to these types of treatment is reported in patients, and the crosstalk between DDR and altered receptor tyrosine kinase (RTK) signaling pathways in solid tumors is thought to be an important contributor to the development of chemotherapy resistance [66-69]. Overexpression of RTKs also contributes to tumor progression through promotion of cell survival, metastasis and stimulation of angiogenesis [70]. While many inhibitors targeting RTKs are already in clinical trials or clinical use [70], it is important to understand how RTKs promote cell survival upon DNA damage to develop combination therapies to enhance treatment efficacy.

3.1. DNA damage response

Once the DNA damage sensor protein machinery detects DNA damage lesions, it recruits mediators and numerous transducer and effector proteins to

ensure that the transcription and translation processes are paused by cell cycle arrest and to initiate DNA damage repair or apoptosis (Fig. 4 and Table 1) [57].

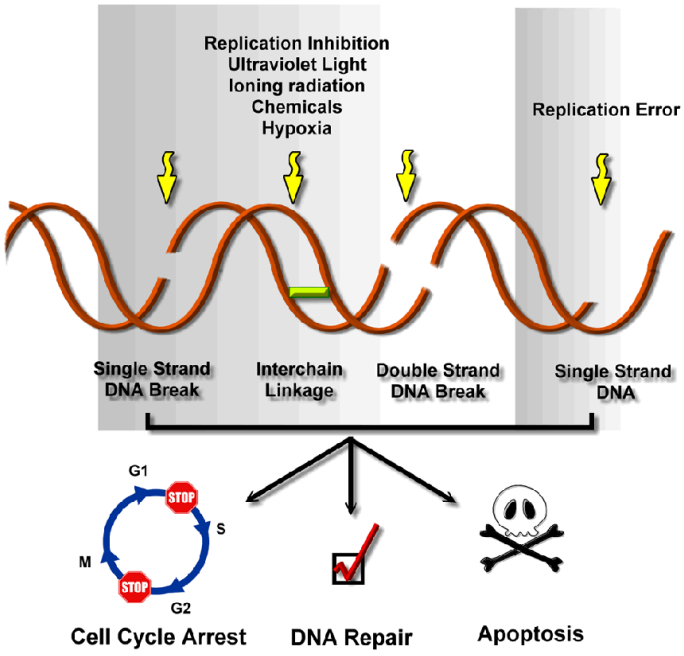

Figure 4. DNA damage reagents and DNA damage response.

DNA is vulnerable to both exogenous and endogenous DNA damage reagents, including replication error, replication inhibition, ultraviolet (UV) light and cancer treatments such us irradiation therapy and chemotherapy. Exposure to these DNA damage reagents leads to DNA damage including DNA single-strand break (SSB), DNA inter strand cross-linking (ICL), DNA double-strand break (DSB) as well as single strand DNA lesion (ssDNA). The DNA damage lesions then trigger the signal cascade which results in DDR primarily through delayed cell cycle from G1 to S phase (G1/S arrest) or from G2 to M phase (G2/M arrest) and as well as triggering DNA damage repair pathways. After successfully re-paired, the cell cycle arrest is released and the cells will survive. However, the severe DNA damage adducts or DNA damage repair failure will eventually leads to apoptotic cell death.

Table 1. Sources of DNA damage and major repair pathways

Table 1. Sources of DNA damage and major repair pathways

Sources of damage	Spontaneous reactions AAs	X-ray ROS AAs 5-FU	UV Aromatic groups Hydrocarbons		Replication inhibitor UV IR Platin ROS Hypoxia				Replication errors
DNA damage types	O^6mG Pyrimidine dimer	8-oxoG AP site Uracil	CPD 6,4-P.P. DNA crosslink		DNA crosslink dsDNA break				Base mismatch Insertion Deletion
Repair pathway	Direct reverse	BER	NER		HR		NHEJ		MMR
			GG-NER	TC-NER	ATR	ATM	C-NHEJ	A-NHEJ	
Sensor/Initiator	MGMT AGT	OGG1 PARP	XPE XPC HR23B	RNA Pol I/II CSA CSB PARP	ATRIP	MRN PARP	Ku70 Ku80	PARP	MSH2 MSH3 MLH1
Transducer/Effector		XRCC1 APE1/2	RPA XPA XPC TFIIH XPB XPD XPG XPF ERCC1		ATR Chk1	ATM Chk2	DNA-PK WRN Artemis XRCC4 XLF	Fan1 PNKP XRCC1	
					MRN Rad51 BRCA 1/2 XRCC 2/3 P53 Rad52 Rad54				
Elongation/Ligase		PCNA DNA Polβ Lig III	PCNA RFC FEN1 Lig I DNA Pol δ/ε		PCNA Lig I DNA Pol δ/ε		DNA Polβ Lig IV	Lig III	RFC PCNA EXO1 DNA Pol δ Lig I/IV

Abbreviations: AAs, alkylating agents; ROS, reactive oxygen species; 5-FU, 5-Fluorouracil; IR, ioninzing radiation; O^6mG, O6-methylguanine; 8-oxoG, 8-oxoguanine; CPD, cyclo-butane pyrimidine dimer; 6,4-P.P, 6-4 photoproduct.

The main mediators in DDR pathways are members of the phosphatidyl-inositol 3-kinase-like protein kinases family, including ataxia-telangiectasia mutated (ATM), ATM and Rad 3-related (ATR), and DNA-dependent protein kinase (DNA-PK). When DNA damage lesions are recognized by a sensor protein, these mediators are recruited to the damage site and phosphorylate downstream proteins that are involved in all aspects of DDR. In addition to these mediators, poly (ADP-ribose) polymerases (PARPs), a large enzyme family with multiple functions, also play important roles in DDR [71, 72]. PARP1 and PARP2

are activated by DNA single-strand break (SSB) and DNA double-strand breaks (DSB) and can poly(ADP-ribos)ylate (PARylate) different substrates under different genotoxic stress to further elevate DDR response [73].

3.1.1. Cell cycle arrest

The cell cycle is subdivided into G1, S, G2, and M phase. In brief, cells increase in size and prepare for DNA synthesis during G1 phase and undergo DNA replication during S phase. Then, cells continue to grow and prepare for mitosis in G2 phase before dividing in M phase. To ensure genomic stability, eukaryotic cells develop cell cycle checkpoints that pause cell division in response to environmental stress, DNA damage, and improper DNA replication [74]; this process is referred as cell cycle arrest. In mammalian cells, there are two major signaling pathways that control cell cycle arrest in response to DNA damaging stress: the ATM pathway, which is responsible for DSB throughout the cell division cycle and the ATR pathway, which is responsible for both DSB as well as replication forks [74, 75].

3.1.2. DNA damage repair and therapeutic DNA damaging agents

In 1974, researchers had already realized that the integrity of DNA is vulnerable and that the repair mechanisms are crucial to maintain genomic stability. Dr. Francis Crick stated in *The double helix: a personal view* that "… one could hardly discuss mutation without considering repair at the same time" [76]. The DNA damage repair pathways are composed of base excision repair (BER),

nucleotide excision repair (NER), mismatch repair (MMR), single-strand annealing (SSA), homologous recombination repair (HR) and non-homologous end joining repair (NHEJ) [57].

3.1.2.1. Repair of base alternation and small DNA damage adducts

Base alternation and small DNA damage adducts, covalent DNA-chemical binding structures, can be caused by low concentration of reactive oxygen species (ROS) as well as alkylation agents and DNA crosslinking agents. Small DNA damage adducts can be easily repaired in normal cells compared with DSBs, but the failure to repair these adducts' fidelity may lead to oncogenic mutations. In cancer treatment, low doses of ionizing radiation (IR) and low linear energy transfer γ-radiation [77] can generate low concentrations of ROS whereas a large number of chemotherapeutic drugs are alkylating agents, including nitrogen mustards (mechlorethamine, cyclophosphamide, and ifosfamide), nitrosourease (streptozocin, carmustine and lomustine), alkyl sulfonates (busulfan), triazine (dacarbazine and temozolomide) and ehylenimines (thiotepa and altretamine) [78].

Base excision repair. BER is mainly responsible for small lesions caused by endogenous DNA damage, such as oxidation, hydroxylation, deamination, or methylation, and is considered to be the most frequently used DNA damage repair pathway [57, 79]. Abnormal DNA bases are detected and excised by lesion-specific DNA glycosylases, such as OGG1 and MYH, creating apurinic, apyrimidinic, or abasic sites (AP sites) [57]. For AP sites limited to a single base, the short patch BER endonuclease APE1 generates a single nucleotide gap at the

AP site and recruits DNA polymerase β as well as XRCC1-DNA ligase to fill the gap. For extensive AP sites (2-10 bases), long patch BER with FEN1 endonuclease and proliferating cell nuclear antigen (PCNA)-DNA polymerase δ/ε complex are used to repair the lesions [57]. Genetic variants of ADPART, XRCC1, APE1 proteins in BER are reported to increase the risk of squamous cell carcinoma [80, 81] and bladder cancer [82]. APE1 and XRCC1 polymorphisms have been reported to correlate with gastric cancer [83] and with risk of lung adenocarcinoma [84, 85], respectively. The nitrogen (*N*-) and oxygen (*O*-) alkylated DNA bases caused by alkylating agents as well as oxidative DNA bases induced by ROS are repaired by BER [86].

PARP participates in many DNA repair pathways including BER, NER, HR and NHEJ [87, 88] but predominantly functions in the BER pathway. Although PARP is not essential in the BER pathway, the treatment of PARP inhibitor has successfully converted the base lesion into a SSB [89], which is a more severe type of DNA damage that can be developed into lethal DSB lesions during DNA replication [71, 90]. PARP inhibitors, for example, olaparib, can induce synthetic lethality in DSB repair-deficient cancer cells, such as *BRCA*-mutated cells, and benefit patients with *BRCA1*/*2*-mutated breast or ovarian cancer [71, 91-93].

Nucleotide excision repair. NER mainly tackles a variety of helix-distorting lesions that impede transcription and replication by interfering with base pairing [57, 79]. Global genome NER (GG-NER) repairs helix-distorting lesions and prevents mutagenesis. Transcription-coupled NER (TC-NER) repairs transcription-blocking lesions to prevent perturbed gene transcription. The damage

recognition steps are different between these NER mechanisms: in GG-NER, the lesions are detected by XPC/hHR23B and XPE protein complex, whereas the RNA polymerase/CSA/CSB/HMGN1 protein complex is responsible for lesion detection in TC-NER [57]. After lesion recognition, XPA proteins are recruited and bind to DNA around 20 base pair upstream of the DNA damage adduct. The DNA double helix around the DNA damage adduct is then unwound by a multi-protein complex, TFIIH. Single-stranded DNA (ssDNA) resulting from the unwinding process is stabilized by the RPA protein, and the DNA adduct excision steps are completed by the XPF-ERCC1 and XPG proteins. NER repairs DNA lesions caused by various endogenous and environmental DNA damaging agents, including UV irradiation [94], platin-based chemotherapy drugs, e.g., cisplatin and carboplatin [95], and carcinogens, such as benzopyrene [96]. Defects in NER result in diseases, such as xeroderma pigmentosum (XP), Cockayne syndrome, and trichothiodystrophy [57]. Among the NER-related diseases, XP patients, but not Cockayne syndrome or trichothiodystrophy patients, exhibit a higher incidence of skin cancer. For example, XP group A patients, a subpopulation of XP patients, are more prone to basal cell and squamous cell carcinoma, and melanoma [97, 98].

Mismatch repair. MMR is designed to resolve mispaired or modified bases as well as insertion or deletion loops. Heterodimers of the MSH2/MSH6 complex recognize mismatched pairs and single-base loops whereas the MSH2/MSH3 complex recognizes insertion/deletion loops. This damage recog-

nition complex then recruits and interacts with MLH1/PMS2 and EXO1 endonuclease to excise the newly synthesized strand after mismatch/loop. DNA is then resynthesized by PCNA, RPA, and DNA polymerase δ/ε complex [57]. Germline mutations in MLH1 and MSH2 have been shown to contribute to hereditary non-polyposis colorectal cancer [99], and defects in MSH6 are known to cause atypical hereditary non-polyposis colorectal cancer. Germline variants in DNA polymerase ε are also associated with MMR-deficient colorectal cancer [100]. MMR deficiency testing can predict the prognosis of colorectal cancer and stratify patients for adjuvant chemotherapy [101].

3.1.2.2. Repair of DNA double-strand breaks

DSBs are considered to be lethal DNA damage lesions that must be repaired before cell continues to grow and proliferate. Currently, radiotherapy and most chemotherapies aim at creating irreparable DSBs in cancerous cells. In cancer treatments, radiotherapies, such as ionizing radiation, induce high concentrations of ROS [77]. Topoisomerase poisons, such as doxorubicin and daunorubicin, can cause DSBs [102].

Non-homologous end joining (NHEJ). NHEJ is important for DSB repair in DNA damage repair as well as for V(D)J recombination in T and B cells [103]. NHEJ functions in DSB repair throughout the cell cycle, especially in G0/G1 phase, and is highly conserved from prokaryotes to eukaryotes, demonstrating its mechanistic flexibility and tolerance for various structures of DNA ends [104-106]. NHEJ is a highly mutagenic repair pathway in that it ligates two ends at the DSB site together regardless of the homology of the DNA sequence [106].

NHEJ can be divided into two pathways, canonical NHEJ (C-NHEJ) and alternative NHEJ (A-NHEJ), according to the resection of DNA ends at the breakage site and the proteins involved [103]. For C-NHEJ, Ku proteins bind to the broken ends of DSBs and recruit DAN-PK as well as 53BP1 and the Mre11 complex to the damage site. The breakage sites are then processed by Artemis and are simply ligated in *cis* by the XRCC4/Ligase IV/XLF complex [103]. The direct ligation process in C-NHEJ alters the DNA sequence at the damage site, resulting in more mutations as extra nucleotides are excised before ligation. For A-NHEJ, the DNA breakage ends are recognized by PARP1, which recruits the Mre11 complex to the damage site before a few nucleotides are excised by CtIP-mediated end resection. The gap can then be filled and ligated by the XRCC1/Ligase III/Ligase I complex [103].

Homologous recombination repair (HR). HR repair is the predominant type of DSB repair that occurs in late S and G2 phases of the cell cycle [107]. The HR pathway utilizes a DNA template strand with significant sequence homology to the damaged strand; therefore, this repair pathway is considered to be error-free and non-mutagenic [57]. The regulation and flexibility of the Mre11 nuclease activities are important in controlling the repair pathway choice during DSB repair [108]. The HR pathway initiates binding of the Mre11-Rad50-Nbs1 protein complex (MRN) to the DSB site and the cyclin-dependent kinase (CDK)-dependent activation of the CtIP protein, which regulates Mre11-mediated end resection of DNA [108, 109]. After initial resection, the Exo1-DNA2-Sgs1 complex is responsible for further DNA resection, and the ssDNA is protected by the

RPA proteins [107]. The RPA proteins are then replaced by Rad51 in a BRCA1/BRCA2 dependent strand invasion process, and the pairing of homologous sequence is completed and extended with the help of Rad52, Rad54 and WRN complex proteins [110]. The junctions at homologous pairing site are then resolved by the BLM/TOPIII/Mus81 complex [110].

Cancer cells are highly proliferative and divide more frequently than cells in normal tissue. Genomic integrity in S and G2 phase is required before cells divide; therefore, inhibiting HR and initiating DSB in HR-deficient cells are both efficient ways to inhibit cancer cell proliferation by trapping cells in the G2/M cell cycle checkpoint. Chemicals that serve as HR inhibitors are often involved in regulating protein expression, nuclear localization, and recruitment of HR proteins. For example, inhibitors of histone deacetylation and HSP90 can block HR by diminishing the expression of BRCA2 [111] and Rad51 [112]. There are also cancer cells that have HR-deficiency. For example, *BRCA1*/*2* germline mutations are reported in many patients with solid tumors, especially in hereditary breast and ovarian cancer patients [113, 114]. The deficiency of HR leads to sensitization of patients to DNA damaging agents such as cisplatin and PARP1 inhibitors [115-119].

Single-strand annealing. SSA is an error prone repair mechanism that is initiated when DSBs occur between two repeated intra-strand DNA sequences. The ERCC1/XPF complex is responsible for the DNA excision step in SSA [120]. After excision of the 5´-ends and exposing regions of homology, the homologous strands of DNA must be paired through SSA, as in HR. Unlike HR,

the RAD52 and RAD59 proteins play a predominant role in the SSA DNA binding step instead of RAD51 [121]. SSA is reduced in G1-arrested cells, but it is not clear whether the SSA pathway is cell cycle dependent because it is not under control of ATM, ATR, or DNA-PK [120]. Although SSA utilizes homologous pairing of repeated DNA sequence, it excises the repeated sequence closer to the site of the DNA break and could be mutagenic. However, the detailed mechanism and regulation of SSA is still unclear. Therefore, the importance of SSA in cancer formation and progression cannot be clearly addressed at this point in time.

3.2. Regulation of RTK signaling on DDR and therapeutic resistance

Mutations in the RTKs as well as dysregulation of its downstream signaling proteins can impair normal DDR. Some RTKs are reported to translocate into the nucleus and their nuclear substrates includes DDR related, RTKs have been implicated in DDR regulation as the canonical RTK downstream proteins have been shown to correlate with DDR regulation (Fig. 5). RAS constitutive activation and/or mutation are observed frequently in human cancers, and the K-RAS encoding gene is particularly vulnerable to chemical carcinogens [122, 123]. Oncogenic activation of K-RAS leads to an accumulation of replication stress by orchestrating wild-type H- and N-RAS signaling, and triggers the ATR/Chk1 pathways to evade G2 cell-cycle arrest [124]. Oncogenic K-RAS also promotes A-NHEJ by upregulating the expression of DNA ligase III, PARP1, and XRCC1 in leukemia cancer model [125]. The AKT-mediated signaling pathway

also regulates DDR. It has been reported that when cells are pretreated with Chk1 inhibitor, inactivation of AKT/PKB pathway can restore radiation-induced Chk1 activation at late G2 cell cycle arrest [126]. Other than Chk1, AKT is known to inhibit TopBP1 and BRCA1 even though it also positively regulates ATM, ATR, and DNA-PK (reviewed in [127]). In addition to the RAS and AKT pathways, some RTKs can also regulate DDR through other pathways as discussed in the following sections.

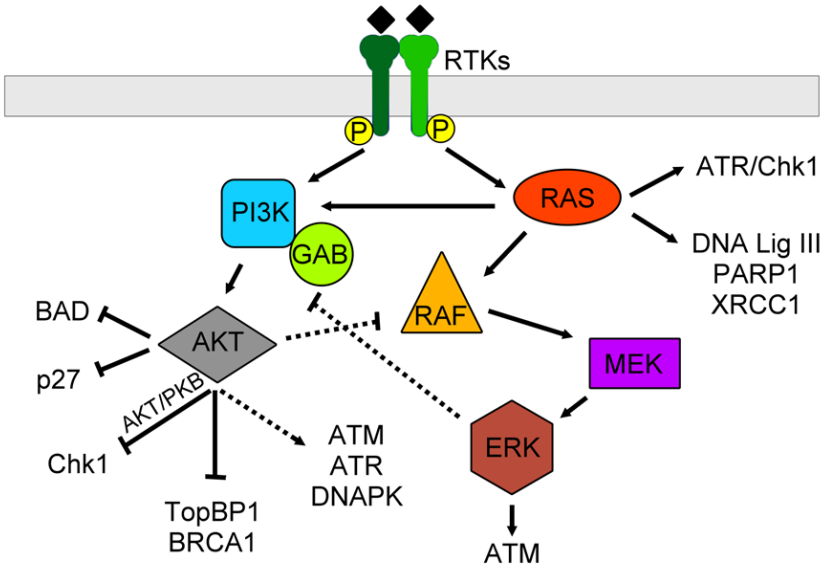

Figure 5. RTKs mediate DDR through canonical AKT and RAS pathways. In general, RTKs can activate both AKT and RAS pathways. Crosstalk between these two pathways can occur through AKT-RAF and ERK-GAB interactions. The downstream effects of the AKT pathway include inhibition of apoptosis through BAD and p27, inhibition of cell cycle progression through Chk1, down-regulation of DNA damage repair through BRCA1, and indirect upregulation of DNA damage repair through ATM, ATR and DNAPK. Meanwhile, RAS itself can

activate cell cycle arrest through ATR and Chk1 while promote DNA damage repair through expression of DNA ligase III, PARP1 and XRCC1. Also, the downstream of RAS pathway can activate ATM to promote DDR.

3.2.1. Regulation of DDR by the ErbB family

The ErbB family is composed of four receptors, ErbB1 (epidermal growth factor receptor, EGFR), ErbB2 (HER2), ErbB3 (HER3), and ErbB4 (HER4). Among them, EGFR and HER2 have been shown to regulate DDR and contribute to therapeutic resistance through both canonical and non-canonical signaling pathways. Using EGFR siRNAs and EGFR small molecule inhibitors, Wei *et al.* demonstrated that EGFR-mediated AKT/ERK pathway upregulates cell cycle regulatory proteins, including cyclin A, B, E, and CDK 1/2, in carcinogenic metal-induced proliferation of triple-negative breast cancer cells (Fig. 6) [128]. The RAS/MEK/ERK pathway promotes EGFR-mediated radioprotection [129] by affecting gene transcription of the DNA repair proteins. The expression levels of the base repair DNA ligase XRCC1 and the DNA adduct excision protein ERCC1 upregulated under radiation treatment can be attenuated by EGFR inhibitor [130, 131]. By utilizing small molecule inhibitors, radiation-induced and EGFR-mediated XRCC1 upregulation was shown to depend on the RAS/MEK/ERK pathway whereas normal XRCC1 expression is affected by EGFR-mediated PI3K/AKT pathway (Fig. 6) [132].

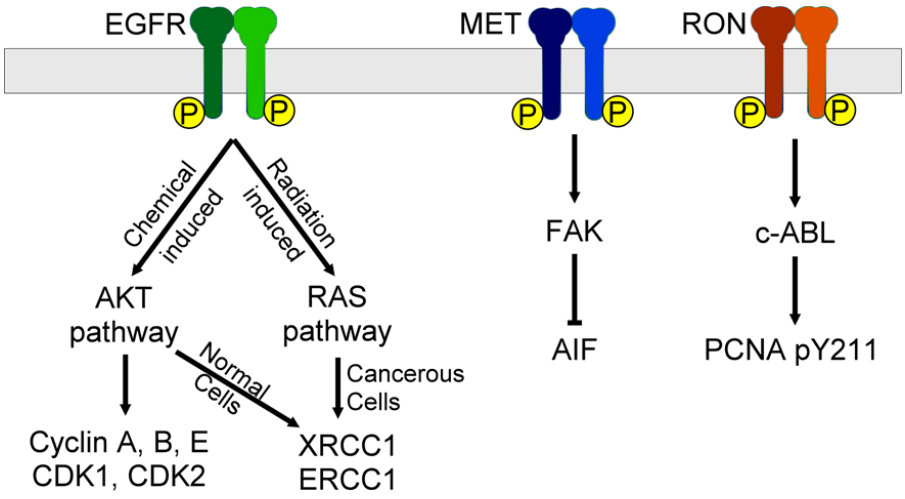

Figure 6. Some RTKs regulate DDR through specific canonical pathways. The chemical-induced EGFR activation will activate AKT pathway to upregulate the expression of cyclin A, B, E and CDK 1, 2 to promote cell cycle. On the other hand, the radiation-induced EGFR activation will activate RAS pathways to increase expression of XRCC1 and ERCC1 in cancer cells. MET can downregulate the expression of AIF specifically through the FAK pathway. Ron promotes PCNA Y211 phosphorylation through c-ABL mediated pathway.

Nuclear EGFR also plays an important role in DNA damage repair, including MMR, NHEJ and HR (Fig. 7). For instance, nuclear EGFR can phosphorylate histone H2B and histone H4. Specifically, EGFR phosphorylates histone H4 at Y-72 to regulate histone H4 methylation [133]. EGF, as well as arsenic, can stimulate nuclear EGFR-mediated phosphorylation and stabilization PCNA via Y211. Phosphorylated PCNA Y211, which has been shown to correlate with poor patient survival, promotes cell proliferation as well as inhibits the endonuclease activity of MutLα, which leads to inhibition of MMR [66, 134, 135]. Yu *et al.* demonstrated that PCNA-derived peptide blocks the EGFR-PCNA complex

and suppresses the growth of breast cancer cells [136]. Nuclear EGFR plays a role in HR in many aspects. EGFR phosphorylates ATM at Y370; depletion of EGFR abolishes ATM-mediated foci formation and HR; the ATM-EGFR interaction can be blocked by gefitinib, an EGFR inhibitor [137]. EGFR also interacts with BRCA1 to facilitate HR; the EGFR-BRCA1 interaction as well as BRCA1 nuclear translocation can be blocked by the EGFR inhibitor, lapatinib [138]. These interactions provide molecular basis for the combination therapy of EGFR inhibitor with PARP inhibitor, which induces synthetic lethality in tumor cells, as demonstrated in breast and ovarian cancers [138-140]. Radiation also enhances EGFR nuclear translocation [141, 142]. Nuclear accumulation of EGFR contributes to radio-protection and interferes with DNA repair through interacting and regulating activity of DNAPK [143-146]. Treatment of EGFR monoclonal antibody, cetuximab (C225), promotes the interaction between EGFR, DNAPK, and Ku proteins, which results in a redistribution of DNAPK from the nucleus to cytosol, a critical step in the radiosensitizing role of EGFR blockade [147-149]. EGFR blockade also inhibits cell growth via p27 and maintains cells in G1 phase, which has been shown to also contribute to the radiosensitizing effect of EGFR [150, 151]. In addition to EGFR, HER2 also regulates cell cycle regulation by binding to and colocalizing with cyclin B-bound CDC2 protein. Phosphorylation of CDC2 by HER2 at Y15 then delays entry of cells into M phase and contributes taxol resistance in HER2-overexpressing cancer cells [152]. Inhibition of HER3 also sensitizes cancer cells to radiation therapy by blocking AKT

phosphorylation [153], and dual inhibition of EGFR and HER3 can overcome cross-resistance to EGFR inhibition and radiation [154, 155].

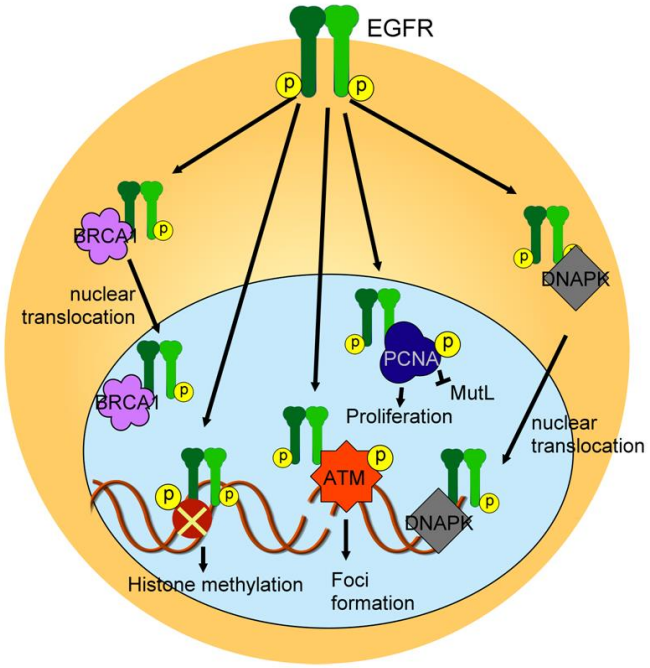

Figure 7. EGFR also mediates DDR through non-canonical signaling pathways.

EGFR interacts with BRCA1 and DNAPK to promote their translocation into the nucleus. EGFR can also phosphorylate histone, ATM and PCNA to promote histone methylation, foci formation, and proliferation whereas EGFR-mediated PCNA phosphorylation inhibits MutL activity.

3.2.2. MET family regulated DDR

Two RTKs in the MET family, MET (also known as hepatocyte growth factor (HGF) receptor) and Ron (also known as macrophage stimulating 1 (MST1) receptor) also regulate DDR. In lung adenocarcinoma, HGF-induced MET activation inhibits apoptosis through the canonical pathway. Chen *et al*. demonstrated that the $FAK^{-/-}$ mouse embryonic fibroblast cells express higher levels of apoptosis-inducing factor (AIF), which correlates with better therapeutic response to cisplatin treatment. Moreover, AIF expression and cisplatin sensitivity were increased in cells when binding of MET to FAK was impeded or when MET inactivated [156], suggesting that this FAK-regulated AIF expression is downstream of MET signaling in lung adenocarcinoma cells. MET is also reported to directly phosphorylate PARP1 at Y907 site [157]. Phosphorylated PARP1 is more resistant to the PARP inhibitor, veliparib, and the combination of MET inhibitor and veliparib increased breast cancer cell killing effect. Contrary to MET, Ron phosphorylates PCNA at Y211 through the canonical signaling pathway by activating Ron downstream kinase, c-Abl, an adaptor protein containing SH2 domain [158]. These findings suggested a functional redundancy between Ron receptor and nuclear EGFR on PCNA Y211 regulation.

4. PARP Inhibitors in Cancer Therapy

4.1. PARP Protein Family

Poly (ADP-ribose) polymerase (PARP) is an enzyme family contains 18 members with sequence homology in their catalytic domain. The structure of

PARP1 (113 kDa) contains 2 zinc-finger domains (ZnF I and II), a zinc binding domain (ZnFIII), BRCA1 C-terminal homology domain (BRCT), WGR domain and catalytic domain (CAT) (Fig. 2). PARP1 and PARP2 are activated immediately by DNA strand breaks. Single strand DNA (ssDNA) damage recognition step needs cooperation of both ZnFI and ZnFII domains of PARP1. PARP1 weakly interacts with and diffuses 3 dimensionally through undamaged DNA by its ZnFI domain to screen for damaged DNA, the discontinuity of ssDNA will allow additional PARP1-DNA binding through ZnFII domain of PARP1. ZnFII domain exhibit higher DNA-binding affinity than ZnFI, and the DNA-bounded ZnFI and ZnFII domains can form a heterodimer with ZnF1 and 2 domains from a second PARP1. After the formation of PARP1 dimer, one of the PARP1 can *trans*-autoPARylate the other PARP1 to activate its enzymatic activity. It is also reported that when encountering double strand DNA (dsDNA) breaks, PARP1 can interact with broken DNA with its ZnFI, ZnFIII and WGR domains [159]. The conformational change of PARP1 when binding to broken DNA will distort its CAT domain, and the destabilized CAT domain will increase its catalytic activity[160]. Although PARP participates in many DNA repair pathways, including BER, NER, HRR and NHEJ, it functions predominantly in the BER pathway [87, 88].

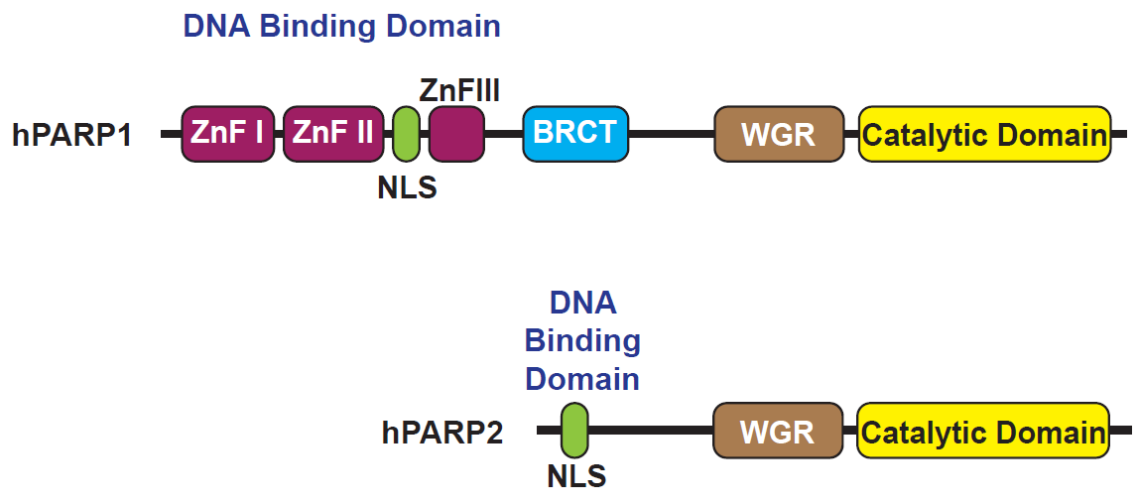

Figure 8. Domains of human PARP1 and PARP2 proteins.
Human PARP1 is a 113 kDa protein with 4 major domains including ZnF, BRCT, WGR and catalytic domains. PARP1 ZnFI to ZnFIII compose its N-terminal DNA binding domain. PARP1 also have nuclear localization sequence (NLS) in its N-terminal to lead the protein imported into cell nucleus. PARP2 is a 66 kDa protein with N-terminal DNA binding domain containing NLS, WGR and catalytic domain.

The enzymatic function of PARP1-5 is to post translationally poly(ADP-ribosyl)ate (PARylate) target proteins by consuming nicotinamide adenine dinucleotide (NAD+) and transfer its negative charged ADP-ribose (ADPr) onto PARP's target proteins. While PARP6-8, PARP10-12 and PARP14-16 can only mono-ADP-rybosylate (mARylate) target proteins; PARP9 and 13 are most likely to be catalytic inactive. The biological process affected by PARP largely depends on the function of its target proteins. Among PARP family, functions of PARP1 and PARP2 in DNA damage repair (DDR), chromatin modification, transcription regulation, cell death and inflammation regulation are most studied.

4.2. PARP1 and PARP Inhibitors in DNA Damage Response

When encountered structures of DNA breaks, PARP1 PARylates multiple DNA repair proteins including itself [160, 161]. In BER, PARP1 and PARP2-mediated PARylation facilitates recruitment of XRCC1 to DNA breaks and thus enhance repair efficiencies [161]. PARylated PARP1 also recruits DNA damage-binding protein 1 (DDB1)–DDB2 complex to bulky adducts of DNA to facilitate lesion detection for GG-NER [161]. Beside SSB repair mechanisms, PARP1 also plays a role as DNA break sensor in DSB repair through interacting with MRE11 and ATM proteins [161]. PARP1 recruits MRE11 to DSB sites, and it may also indirectly participated in BRCA1 recruitment by interacting with BRCA1-associated RING domain protein 1 (BARD1) to facilitate HR repair [161]. The PARP1 and MER11 interaction can also stimulate alternative NHEJ, a repair mechanism which utilizes microhomology between two strands at DSB region and using sequences around the microhomology sites as template to fill DNA gaps with DNA polymerase θ [161]. In conclusion, PARP1 plays important roles in both SSB and DSB repairs.

Small molecule PARP inhibitors (PARP-is) were developed as therapeutic agents for cancer treatment, because the deficiencies in DNA repair results in one of the hallmarks for cancer [162]. Among the PARP-is, at least three of them, olaparib, rucaparib, and niraparib, are approved by the United States Food and Drug Administration for treating *BRCA1/2*-mutated ($BRCA^m$) ovarian

cancer as single therapeutic agent or for maintenance support for platinum-sensitive patients [163]; two of them, olaparib and talazoparb, were approved for $BRCA^m$ breast cancer treatment [164]. PARP-is are designed to compete with NAD+ for catalytic pocket of PARP1 and, therefore, PARP-is can inhibit PARP1 PARylation activity [165]. Beside of inhibiting PARP1 enzymatic activity, most of the PARP-is can also immobilize PARP1 on damaged DNA, a phenomenon known as “PARP trapping” [166]. Because cytotoxicity of the PARP-is are not positively correlated to their capability of enzymatic inhibition, but more correlated to their capability of inducing PARP trapping, PARP trapping is considered as main working mechanism of PARP-is in eliminating DDR-deficient cells [166]. Repairing the PARP trapping-caused PARP1-DNA complex requires multiple DNA repair pathways. Deficiencies in either HR, topoisomerase, Fanconi anemia pathway, DNA polymerases, or NER can increase PARP-is sensitivities in cells [167]. Therefore, although PARP-is have currently be approved for $BRCA^m$ cancer treatment, these PARP-is may be effective targeted therapy for cancer patients bearing tumors with mutations in DDR proteins other than BRCA.

4.3. BRCA Mutation and BRCAness in Breast Cancer

Germline mutation of *BRCA1* and *BRCA2* genes are known contribute to increased risk of hereditary, early on-set breast cancers [168]. *BRCA1* mutated breast cancer often overlapped with TNBC subgroup (from 8.5% to 28% in different patient cohorts), while *BRCA2* mutation are found in 1% to 17% TNBC patients [169, 170]. Overall, around 66% of BRCA1 mutated breast cancer are

TNBC and average of 25% BRCA2 mutated breast cancer are TNBC. The gene mutations that induce pathological HR deficiency, the phenomenon mimicking the loss or mutation of BRCA1/2, are termed as “BRCAness” [171]. In general, BRCAness tumors are more sensitive to treatment using DNA damaging agents [171]. With the emerging of targeting defective DDR as cancer treatment strategy, breast cancer can also be grouped to *BRCAness* based on their mutation of DDR genes. In breast cancer patients, around 50% of patient are identified as BRCAness [172]. Therefore, PARP-is become an emerging targeted therapy for breast cancer treatment, especially for TNBC [173].

4.4. PARP-i Resistant Mechanisms and Current Strategies to Overcome Resistance.

Although PARP-is have been approved by the U.S. Food and Drug Administration for $BRCA^{m}$ ovarian cancer and breast cancer treatment, there are intrinsic, as well as acquired, PARP-i-resistance observed in clinical trials and pre-clinic animal models [174, 175] (Fig. 9).

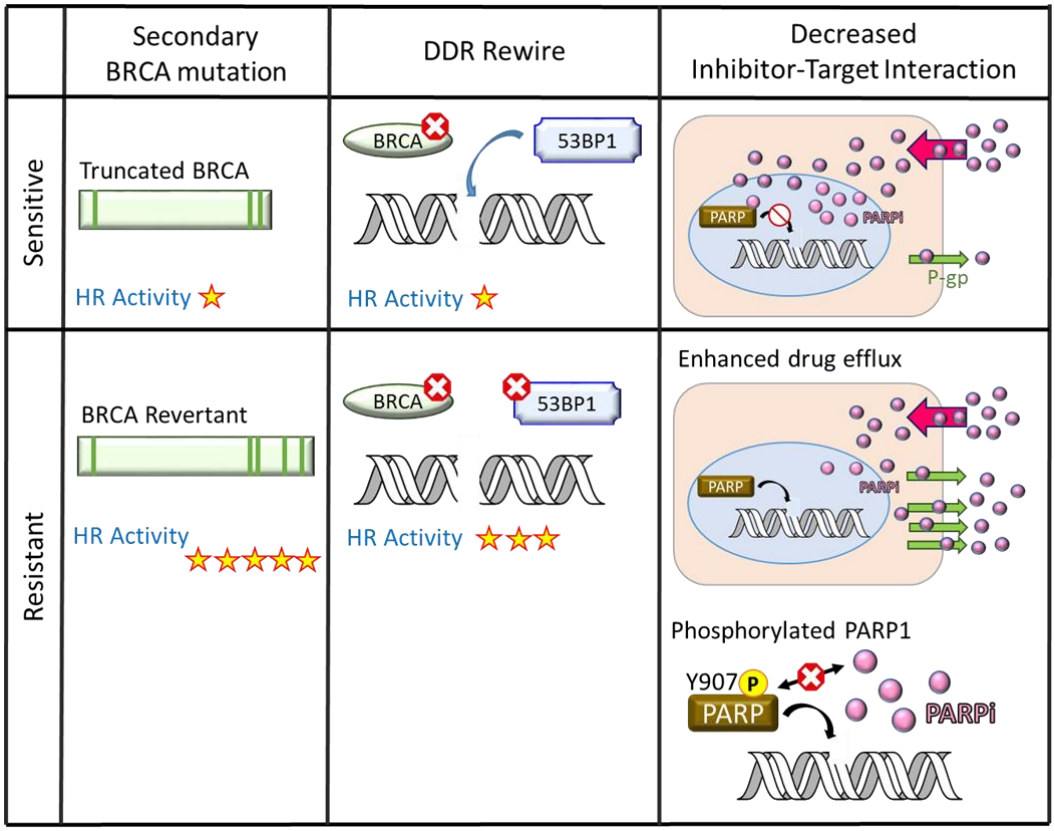

Figure 9. PARP-i resistant mechanisms.

Several mechanisms contribute to PARP-i-resistance have been identified in preclinical models and clinical observations, including secondary BRCA gene mutations, loss of 53BP1, upregulation of MDR proteins, and tyrosine phosphorylation of PARP1.

Surprisingly, it is estimated that around 50% of tumors may develop acquired resistance to PARP-is based on the observation that tumors acquired secondary mutation that restores function of BRCA1/2 [176, 177]. While BRCAness cells are more sensitive to PARP-is, most of the PARP-is resistance mechanisms identified are related to restoration of HR function. The HR restore due to secondary mutations in BRCA genes were observed in majority of PARP-

is resistant cells [174-177]. Besides the secondary BRCA mutations, inactivation of NHEJ also partially rescue BRCAness due to the low affinity of MRE11 to DSB while lacking of competing proteins such as TP53 binding protein 1 (53BP1) [178-180]. Moreover, mechanisms that decrease interaction between PARP1 and PARP-is also contribute to PARP-i-resistance. The upregulation of multiple drug resistant (MDR) proteins, such as P-glycoprotein (P-gp, also known as MDR1), induces efflux of PARP-is from cells and thus decrease PARP-is efficacy [181-183]. In addition, MET-induced PARP1 tyrosine 907 phosphorylation can also decrease binding affinity of PARP-is to PARP1 [157].

There are several strategies under investigation to overcome PARP-i-resistance, including development of new PARP-i to avoid being substrate of MDR proteins, reinstating BRCAness by targeting DDR proteins other than BRCA, and inhibiting cell cycle regulating proteins to prevent undergoing HR. While olaparib (AZD2281) is one of the substrate of MDR proteins, AZD2461, a PARP-i, which is a poor substrate for MDR proteins, was developed to overcome the MDR-mediated PARP-i-resistance [184]. Because cyclin-dependent kinases (CDK) 1 promotes HR through phosphorylating BRCA1 [185] and CDK12 promotes transcription of HR proteins including BRCA1 [186-189]. Inhibitors of cyclin-dependent kinases are introduced to PARP-i combination strategies that decrease HR activity and re-establish BRCAness. Also, inhibitor targeting DNA polymerase δ was developed to inhibit HR [190], and was therefore suggested to be combined with PARP-is in overcoming PARP-i-resistance. Inhibitors abro-

gating cell cycle checkpoint proteins and replication fork protection, such as targeting ATM, ATR, and WEE1, are under investigation as agents for overcoming PARP-i-resistance by preventing DNA repair and inducing more replication stress in cells[191-193]. Moreover, studies show that alternative NHEJ is utilized in cells acquired resistance to PARP-is [194], therefore, inhibitor targeting DNA polymerase θ is also suggested as a potential agent to overcome PARP-i-resistance [175].

5. Significance of this Study

Current strategies to overcome PARP-is resistance include inhibiting more DNA repair pathways in combination with PARP-is to enhance DNA damages [195], but these also affect normal tissues. To identify therapeutic agent combinations with wider therapeutic window between cancer and normal cells, we systematically screened $BRCA^{m}$ breast cancer cells with acquired PARP-i resistance for commonly activated receptor tyrosine kinases, for which there are feasible inhibitors in clinic and leveraging oncogenic addictions to these kinases for wider therapeutic window.

Chapter II. Materials and Methods

1. Cell Culture

SUM149 immortalized breast cancer cells were purchased from Asterand Bioscience (MI, USA) and maintained in 37°C CO_2 incubator with F-12K medium (ATCC 30-2004) supplied with 5% feral bovine serum (FBS), 10 mM HEPES, 1 µg/ml hydrocortisone, 5 µg/ml insulin and 100 U/ml penicillin-100 µg/ml streptomycin (P/S). MDA-MB-231 and BT-549 cells were maintained with DMEM/F-12 medium supplied with 10% FBS and P/S. MDA-MB-468 cells were maintained with DMEM/F-12 medium supplied with 10% FBS, P/S and L-glutamine. HCC70 and HCC1937 cells were maintained with RPMI1640 medium supplied with 10% FBS and P/S. Except for SUM149, all cell lines were purchased from ATCC. Cell lines were validated by short tandem repeat DNA fingerprinting using the AmpF_STR Identifiler kit according to the manufacturer's instructions (Applied Biosystems). Theshort tandem repeat profiles were compared with and matched to known ATCC fingerprints (ATCC.org) and to the Cell Line Integrated Molecular Authentication database (CLIMA) version 0.1.200808 (http://bioinformatics.istge.it/clima/).

2. Chemicals and Regents

Methyl methanesulfonate (MMS, cat no. 129925), 3-(4,5-Dimethylthiazol-2-yl)-2,5-Diphenyltetrazolium Bromide (MTT, cat no. M5655), polybrene was purchased from Millipore-Sigma Corporate (MO, USA). Talazoparib (BMN673),

olaparib, rucaparib, veliparib, PD173074, AZD4547 and Erdafitinib for *in vitro* experiments were purchased from Selleck Chemicals (TX, USA). Concentrated stock solutions of PARPi and kinase inhibitors were prepared with DMSO. Protease inhibitor cocktail (# B14001) and phosphatase inhibitor cocktail (# B15001) were purchased from Biomake (Houston, TX). Para-formaldehyde (16% stock solution, cat no.) were purchased from Electron Microscopy Sciences (Hatfield, PA, USA). pCMV-VSV-G (Addgene plasmid # 8454) and pCMV-delta 8.9 plasmids were a gift from Dr. Robert A. Weinberg.

The primary antibodies and dilution ratio for Western blotting analysis used in this study were: rabbit anti-FGFR3 (#ab137084; 1:2,000) and rabbit anti-Histone H4 (1:1,000) from Abcam; rabbit anti-PARP (#9532S; 1:1,000) from Cell Signaling Technology; rabbit anti-actin (#A2066; 1:5,000), mouse anti-tubulin (#T5158; 1:5,000), mouse anti—phospho-histone H2A.X (Ser139) (#05-636; 1:1,000), mouse anti-HA (clone 12CA5) (1:1,000), and rabbit anti–phospho-FGFR (Tyr653/Tyr654) (#06-1433; 1:1000) from MilliporeSigma; rabbit anti-lamin B1 (#sc-374015; 1:2,000), and mouse anti-GAPDH (#sc-32233; 1:1,000) from Santa Cruz Biotechnology.

3. Development of Acquired PARPi Resistant Clones

3.1 SUM149 Talazoparib Resistant Cells

As illustrated in Figure 10 below, SUM149 cells were treated with fresh 100 nM talazoparib every day for 5 consecutive days to eliminate most of the SUM149 cells. The cells were then maintained in 15 nM talazoparib for 3 days

before increased talazoparib concentration in culture media to 22.5 nM, 35 nM and 50 nM. Each colony remained in 50 nM talazoparib was picked and transferred into 96-well plate with one colony for each well and were then maintained with 50 nM talazoparib. Colonies stably proliferated in 50 nM talazoparib were then named as BR (BMN673-Resistant) cell #01 to #31.

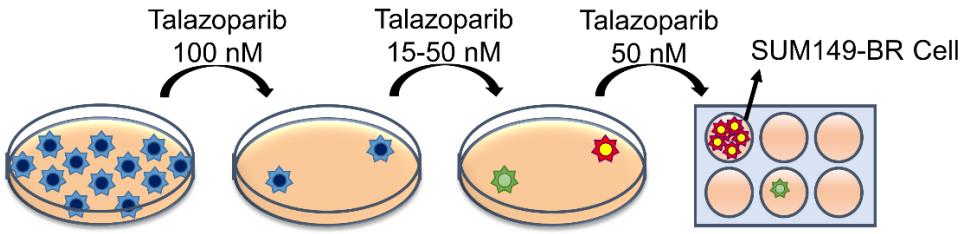

Figure 10. Development of talazoparib resistant SUM149 cells.
SUM149 cells were plated into 1,500 mm culture dishes a day before 100 nM talazoparib treatment. After 5-day 100 nM talazoparib treatments, cells were maintained in talazoparib with concentrations gradually raised from 15 - 50 nM. After 3-days of 50 nM talazoparib incubation, single clones were then picked and cultured in 96-well plate with 50 nM talazoparib until stable proliferation.

3.2 HCC1806-BR Cells

HCC1806 talazopairb resistant cell (HCC1806-BR) were a gift from Dr. Khandan Keyomarsi. HCC1806-BR cells were developed by treating HCC1806 with 1 μM talazoparib continuously for 9 months.

4. MTT Cell Viability Assay

Cells were seeded into 96 plate a day prior to PARP and kinase inhibitors treatments. Number of cells seeded were adjusted for reaching 90% confluence after 5-6 days of culture: MDA-MB-231 (1,000 cells/well), SUM149 (1,000 cells/well), SUM149-derived resistant clones (1,000 cells/well), BT549 (2,500 cells/well), HCC1937 (5,000 cells/well). Cells were treated with inhibitors indicated in different experiments in a volume of 200 µL/well and the medium containing inhibitors were refreshed every 3 days. MTT stock solution is made by dissolving 5 mg/mL MTT in PBS. After treatment, 20 µL MTT stock solution were added into each well and incubated for 1-2 h in 37 °C incubator. After MTT incubation, medium was removed and 50 µL DMSO were added into each well to dissolve formazan. The quantity of formazan is measured by recording absorbance of 595 nm using microplate reader.

5. Whole Cell Extract Preparation

Cells were cultured until reaching 80%-90% confluence in 10-cm cell culture dish before harvested for whole cell extract preparation. Cell culture medium was removed and cells were washed with PBS before washed again with protease inhibitor-containing PBS (PBS with 2 mM Na_3VO_4, 1 mM NaF and 1 mM PMSF) before scratching and centrifuging at 1,500x g for 5 min to collect cells. Cells were then homogenized in RIPA buffer (150 mM NaCl, 1% Triton X-100, 0.5% sodium deoxycholate, 0.1% SDS, 50 mM Tris, pH 7.5 and PIC) with

sonication (Bioruptor® Plus sonication device,10 sec on, 10 sec off, repeat 3 cycles) (Diagenode Inc. Denville, NJ, USA). Protein lysates were collected by centrifuging at 13,200 rpm for 10 min to remove pellet. Protein concentrations were then determined by using BCA Protein Assay kit (Pierce, cat no. 23225).

6. Co-Immunoprecipitation (co-IP)

Cells were treated with chemicals indicated in each experiments before whole cell extracts were collected for immunoprecipitation (IP). 500 µg of total proteins were diluted to 500 µL with RIPA buffer for IP, proteins were pre-cleaned by incubating with 1 µg IgG and 10 µL protein A/G agarose beads for 1 h at room temperature before supernatant were collected for IP after centrifuging at 2,500x g for 3 min. 2-5 µg primary antibodies were added into the samples and incubated for overnight rotating at 4 °C. For primary antibodies without agarose pre-conjugation, 10 µL protein A/G agarose beads were added into each sample and incubated on rotator for 1.5 h at room temperature. After incubation, agarose beads were collected by centrifuging at 2,500x g, 4 °C for 3 min and washed 3 times by rotating at 4 °C for 5 min with IP wash buffer (150 mM NaCl, 1% Triton X-100, 10 mM Tris, pH 7.5, 1 mM EDTA, 1 mM EGTA, 0.2 mM Na_3VO_4 and protease inhibitor cocktail). IP complex were released from agarose beads by boiling for 3 min in Laemmli buffer (2% SDS, 5% 2-mercaptoethanol, 10% glycerol, 0.005% bromophenol blue and 0.0625 M Tris, pH 6.8). After releasing, protein supernatants were collected after centrifuging at 2,500x g, 4 °C for 5 min and were loaded for Western blotting analysis.

7. Proximity ligation assay (PLA) and immunofluorescence staining

Cells were treated for 1 h with either 0.01% MMS, 0.1 μM talazoparib, or 10 μM PD173074 as indicated before fixed with 4% paraformaldehyde. 2-4 hours pre-treatment of PD173074 was introduced before combining with other chemicals to ensure FGFR3 was inhibited while inducing DNA damages. PLA (Duolink® In Situ Red, Sigma Aldrich) were performed following manufacture's instruction. Mouse anti-PARP1 (Sino Biological, #11040-MM04), rabbit anti-FGFR3 (Abcam, #ab137084), and mouse anti-phospho-Histone H2A.X (Ser139) (clone JBW301, MilliporeSigma, #05-636) primary antibodies for PLA were diluted at a ratio of 1:500 and incubated with samples overnight at 4 ℃. Immunofluorescence staining and confocal microscopy were performed as previously described[196]. Cells were treated with either DMSO (solvent control), talazoparib (125 nM for BR#09; 250 nM for BR#17), PD173074 (10 μM), or the combination of talazoparib and PD173074 for the time indicated. Primary antibodies were diluted in 5% BSA at a ratio of 1:500 for both anti—phospho-histone H2A.X and anti-FGFR3 and were incubated overnight. Secondary antibodies anti-mouse fluorescein isothiocyanate (FITC) and anti-rabbit Texas Red were diluted at a 1:1,000 ratio in 5% BSA. In both immunostaining and PLA assay, images of the cells were captured and analyzed with LSM 710 laser confocal microscope and Zeiss Zen software (Carl Zeiss) and foci counting was performed using BlobFinder [197].

8. Western Blotting

Cell extracts were boiled in Laemmi buffer (50 mM Tris-Cl pH 6.8, 2 % SDS, 10 % glycerol, 5% β-mercaptoethanol, 0.05 % bromophenol blue) for 10 min before Western blotting analysis. In Western blotting analysis, proteins were separated by electrophoresis in an 8%-10% SDS-PAGE gel with Western blotting running buffer (25 mM Tris base, 190 mM glycine, 0.1% SDS, pH 8.3) before transferred onto PVDF membrane in transfer buffer (25 mM Tris base, 190 mM glycine, 20% methanol, pH 8.3) for overnight at 4 °C. PVDF membrane were then blocked with 5% skim milk in TBST buffer (198.18 mM Tris base, 1.5 M NaCl, 0.1% Tween 20, pH7.5) at room temperature for more than 1 h. After blocking, the membrane was incubated with primary antibodies for overnight at 4°C before washing with TBST 3 times for 5 min each time. Primary antibodies were diluted with 5% bovine serum albumin (BSA)/TBST at the ratio indicated in Table 2. HRP-conjugated secondary antibodies (Rockland™, Limerick, PA, USA) were diluted with 5% skim milk/TBST and incubated with membrane for 1 h at room temperature before washing with TBST 3 times for 10 min each time. Pierce™ ECL Western Blotting Substrate (Thermo Scientific™) were prepared following manufactory's manual. Western blotting images were captured by using ImageQuant LAS 4000 system (GE Health Care Life Sciences, Pittsburgh, PA, USA) and quantified by using Image Studio Lite (Ver 5.2).

9. Colony Formation Assay

Cells were seeded into 12-well plate at optimized densities (600 cells/well for SUM149R #09, 800 cells/well for SUM149R #17 and 1,000 cells/well for BT549) a day before drug treatments. After cells attached to the plate, culture medium were refreshed with 800 µL drug-containing medium for each well. Drug-containing medium were refreshed every 48 h for the 10-14 days incubation. For quantitation, medium were removed from each well and the wells were washed with PBS twice before fixed with 4% paraformaldehyde at room temperature for 10 min. Colonies were stained by incubating in 0.5% crystal violet in methanol for at least 2 h at room temperature. Excess crystal violet was washed off under running tape water. The plate were then subjected to imaging and quantified by using Celigo Imaging Cytometer (Nexcelom Biosciences, MA, USA).

10. *In Vitro* Kinase Assay

Recombinant PARP1 protein (Lifespan, cat no. LS-G3996-10) and recombinant active FGFR3 kinase domains (Thermo Fisher, cat no. PV3145) are used for *in vitro* kinase assay. 1 µg PARP1, 1 µg FGFR3, 0.1 mM ATP and NEBuffer for Protein Kinases (New England Biotechnology, cat no. B6022S) were mixed together and incubated at 30 °C for 70 min. The reaction is stopped by adding Laemmli buffer into samples and boiled for 5 min. Samples were then subjected to Western blotting analysis or mass spectrometry analysis as indicated. For

Western blotting analysis, 4G10, PY20 and PY100 antibodies were mixed and applied as primary antibody to recognize phosphorylated tyrosine.

11. PARP Trapping Assay

Cells were pre-treated with, 10 μM PD173074 for 2 h before 0.01% MMS and 0.1 μM talazoparib treatment for the duration indicated in each experiment. After treatment, cells were harvested by trypsin and washed with ice-cold PBS twice before cell pellets were collected by 1,700 ×g centrifuge at 4 ℃. HDG150 buffer (20 mM HEPES-KOH [pH 7.4], 150 mM KCl, 0.5 mM DTT, 10% glycerol and protease inhibitor cocktail) [198] and tight dounce tissue grinder (Wheaton #357538) were used to isolate nucleus and cytoplasm fractions. Nuclei were collected after 1,700 ×g centrifuge at 4 ℃ and washed with 5 mL ice-cold HDG150 buffer twice. Cell nuclei were teared by using Bioruptor Twin (Diagenode, Denville, NJ) at the setting of 10-sec on, 10-sec off and 10 cycles. Chromatin-bound fraction were collected by 20,000 ×g centrifuge at 4 ℃. After washed once with 0.2 mL ice-cold HDG150 buffer, DNA were digested using 100 U/mL micrococcal nuclease (Life Technologies #88216) in HDG150 buffer containing 5 mM calcium chloride and rotated at 20 rpm for an hour at 4 ℃ cold room. Chromatin-bound proteins were then collected by 20,000 ×g centrifuge at 4 ℃ and supernatant were analyzed by Western blotting.

12. Lentivirus Infection and RNA Interference

Lentiviral plasmid containing short hairpin RNA (shRNA) were purchased from Millipore-Sigma (pLKO.1 sets), MD Anderson Cancer Center shRNA and ORF core facility (pGIPZ sets) and Dharmacon (SMARTvector inducible shRNA). PARP1 targeting shRNAs (shPARP1-1: TRCN0000007928; shPARP1-2: TRCN0000356550) and FGFR3 targeting shRNA (shFGFR3-1: TRCN0000000371; shFGFR3-2: TRCN0000196809) were purchased from Sigma Aldrich. Lentivirus particles were generated by transfecting HEK293T cells with pCMV-VSV-G (Addgene plasmid # 8454), pCMV- dR8.91 and either shRNA plasmids, PARP1 expressing plasmids or FGFR3 expressing plasmids in a 1:3:6 ratio. Scramble shRNA control plasmid pLKO.1 (Addgene plasmid #1864) was a gift from David Sabatini and pCMV-VSV-G was a gift from Dr. Bob Weinberg. For lentivirus production, HEK293T cells were transfected with pCMV-VSVG, pCMV-dR8.91and shRNA plasmid at the ratio of (1 : 5 : 10 µg). In brief, 12 µg plasmid DNA were packaged in 18 µL SN transfection reagent for each 10-cm plate of HEK293T. HEK293T cells were transfected with serum-free medium for 8 h before transfecting medium were replaced by complete culture medium. Virus particles-containing mediums were collected at 60 h post-transfection and were filtered by using 0.45 µm dish filter. The virus-containing mediums were mixed with lentivirus concentration solution (40% PEG-8000, 1.2M NaCl in PBS) at a ratio of 1:3 and incubated at 4 °C for more than 4 h. Virus particles were then pelleted by centrifuge at 1,600x g for 1 h at 4 °C and resuspended in PBS to make virus infection solution. Cancer cell lines were cultured

to reach 70% confluence for virus infection. Virus infection solutions were mixed with cell culture medium and supplied with 8 μg/mL polybrene (Millipore) for mammalian cell infection. Cells were incubated with the virus infection medium for 72-96 h before treated with antibiotic selection medium. Stable cells were selected and maintained in the selection medium containing 1 μg/ml puromycin (InvivoGen) or 500 μg/ml G418 (Thermo Fisher).

13. Cloning and mutagenesis

FGFR3-expressing plasmid pDONR223_FGFR3 (Addgene plasmid #23933) was a gift of Dr. William Hahn and Dr. David Root [199]; pDONR223_FGFR3_K650E (Addgene plasmid #82187) was a gift from Dr. Jesse Boehm, Dr. William Hahn, and Dr. David Root [200]. FGFR3 was subcloned from pDONR223-FGFR3 into pCDH-CMV-MCS-EF1-Neo (System Biosciences) by amplifying the *FGFR3* open reading frame with polymerase chain reaction. 3xFlag-tag was inserted by oligomer annealing. The same cloning strategies were used for generating $FGFR3^{K650E}$-expressing plasmid. HA-tagged PARP1 expression plasmid was described in our previous study [157]. $FGFR3^{K508R}$-, $PARP1^{Y158F}$-, and $PARP1^{Y176F}$-expressing plasmids were generated using site-directed mutagenesis polymerase chain reaction and HA-PARP1 plasmid [157].

Table 2. Sequences of primers for PARP1 mutagenesis.

Primer Name	Sequence
PARP1 Y158E-F	TGATTGACCGCTGGGAACATCCAGGCTG
PARP1 Y158E-R	CAAAGCAGCCTGGATGTTCCCAGCGGTCAAT
PARP1 Y158F-F	TAGGCATGATTGACCGCTGGTTTCATCCAGGCTG
PARP1 Y158F-R	CTTGACAAAGCAGCCTGGATGAAACCAGCGGTC
PARP1 Y176E-F	GTTTCCGGCCCGAGGAAAGTGCGAGTCAG
PARP1 Y176E-R	GAGCTGACTCGCACTTTCCTCGGGCCGGAA
PARP1 Y176F-F	GTTTCCGGCCCGAGGAAAGTGCGAGTCAG
PARP1 Y176F-R	CTTGAGCTGACTCGCACTAAACTCGGGCCGGAA
pCDH-EF1-F	CTCCACGCTTTGCCTGACCCTGCTT

14. Comet Assay

Cells were seeded into 60-mm cell culture dish at least 18 h before reaching 60% confluence for treatments. Cells were treated with 0.01% MMS, 100 nM talazoparib, and 10 μM PD173074 as indicated. When releasing cells from MMS, culture medium was removed and cells were washed with ice-cold PBS twice before adding fresh prepared inhibitor-containing medium for DNA repair. Alkaline comet assay was performed as described previously [201]. In brief, cells were harvested and diluted to $2x10^5$ cells/ml in PBS, and were embedded in 1.2% low-melting point agarose gel at 1:1 ratio. 80 μl mixture were applied to a 24 mm x 40 mm area and the slide was immersed in alkaline lysis buffer (10 mM Tris, 2.5 M NaCl, 100 mM EDTA, 1% Triton X-100, 10% DMSO, 1% sodium lauryl sarcosinate, pH 10.0) overnight. DNA damages were further digested with 2U formamidopyrimidine [fapy]-DNA glycosylase (fpg) (New England BioLabs, # M0240S) for 1 h before electrophoresis (22V, 300 mA, 20 min). Comet Olive moment were measured using CometScore v1.5 (TriTek).

15. Xenograft Mouse Models

Animal studies were performed following an MD Anderson Cancer Center Institutional Animal Care and Use Committee–approved protocol. Female nude mice were purchased from the MD Anderson Cancer Center Department of Experimental Radiation Oncology. For BR#09 and BR#17 xenograft mouse models, two million cells were mixed with 50% (v/v) growth factor reduced matrigel matrix (Corning) and inoculated into the mammary fat pads of a 6 to 8-week-old female nude mouse. For 4T1 model, female Balb/c mice were purchased from Jackson Laboratory. A total of 50,000 4T1 cells were mixed with matrigel matrix and inoculated into the mammary fat pad of a 6-week-old female Balb/c mouse. Inhibitors at the concentrations indicated in each experiment were dissolved in vehicle solvent containing 10% dimethylacetamide (Sigma-Aldrich), 5% Kolliphor HS 15 (Sigma-Aldrich), and 85% phosphate-buffered saline [202]. Inhibitor treatment started when tumor volume reached a mean of 120 mm^3. Mice were treated using oral gavage daily for 20 days followed by 3 days with no drugs to prevent severe weight loss. After the first cycle, treatment was continued on a schedule of 6 days on and 1 day off. Mouse weight and tumor volume were measured 3 times every week. Tumor volume was estimated using the following formula: volume (mm^3) = length (mm) × width (mm) × 0.5 width (mm), where length is the longest axis of the tumor. Mice were killed using CO_2 when tumor volume reached 2,000 mm^3. Mouse cardiac blood were collected and used for blood chemical tests that performed by veterinarians in MD Anderson Cancer Center Department of Veterinary Medicine and Surgery.

16. Tyrosine 158 Phosphorylated PARP1 Antibody Generation

Mouse anti-phospho-PARP1 Y158 antisera were generated by immunize 20 mice with phospho-PARP1-Y158 KLH hot peptide (KLH-C-EKPQLGMIDRW-pY-HPG-S-FVKNREE) once every 2 weeks. Binding affinities specificities of the antisera were evaluated by using ELISA and Western dot blot with hot peptide (C-EKPQLGMIDRW-pY-HPG-S-FVKNREE) and cold peptide (C-EKPQLG-MIDRW-Y-HPG-S-FVKNREE) and Western blotting. The homemade antibodies were prepared by Ms. Hung-Ling Wang and Dr. Shao-Chun Wang in Center for Molecular Medicine, China Medical University.

17. Statistics

For Western blotting signal quantifications, signal intensities were analyzed by using Image Studio Lite (version 5.2) (LI-COR Biosciences). Signals of PARP1, PAR, FGFR3, and phosphorylated FGFR were first normalized to house-keeping proteins (tubulin, actin, or GAPDH) of each sample before being normalized to the control groups. Every independent experiment repeat is quantified individually. Fold changes in Western blot signals were analyzed by a non-parametric Friedman test using the GraphPad Prism 8.0 software. A p value less than 0.05 was considered statistically significant. *, $p < 0.05$; **, $p < 0.002$; ***, $p < 0.001$. CI experiments were designed according to the Chou-Talalay method [203], and results were calculated using Compusyn software (http://www.combosyn.com).

Chapter III.

Fibroblast Growth Factor Receptor (FGFR) Inhibition Reinstates PARP Inhibitor Anti-tumor Efficacy in Breast Cancer with Acquired Resistance by Prolonging PARP Trapping

1. Fibroblast Growth Factor Receptors (FGFR) in Breast Cancer

Fibroblast growth factor (FGF) induced FGFR pathways are important in regulating cellular homeostasis. The FGF-FGFR pathways are known involving in multiple cellular regulations including cell proliferation, angiogenesis, cell differentiation, migration and survival (reviewed in). FGFR is a family of receptor tyrosine kinases (RTKs) containing 4 members, FGFR1, 2, 3, and 4. The FGFR members share conserved structure, including three extracellular immunoglobulin (Ig) domains, a single transmembrane (TM) helix, cytosolic tyrosine kinase (TK) domain and a short carboxy-terminal tail (reviewed in). There are 18 fibroblast growth factors (FGF) identified as ligand for FGFRs (reviewed in [204]). For FGFR1-3, alternative splicing results in generation of receptor isoforms, b- and c- variants. FGFR1-3 IIIb and IIIc are generated from alternative exon used in ligand binding domain, therefore, ligand specificity of FGFR as well as biological functions may largely altered in IIIb and IIIc variants. Previous study shows that FGFR1-4 and their IIIb and IIIc variants can be activated at various efficiencies of different FGFs. Despite ligand-stimulated activation, unliganded FGFR can still form receptor dimers [ref]. By using FRET assays, Sarabipour and Hristova concluded that FGFR3 has highest unligand dimer among FGFR1-4 and,

even at low receptor concentration (10 receptors/μm^2), 50% of FGFR3 still form unliganded dimer.

FGFR alterations are found in multiple cancer types, including breast cancer. Using cBioPortal to analyze data from TCGA database showed that alterations of FGFR1-4 are found in multiple patient breast cancer patient cohorts (Fig. 11A) and is correlated with worse overall survival (p-value 0.007) (Fig. 11B).

(A)

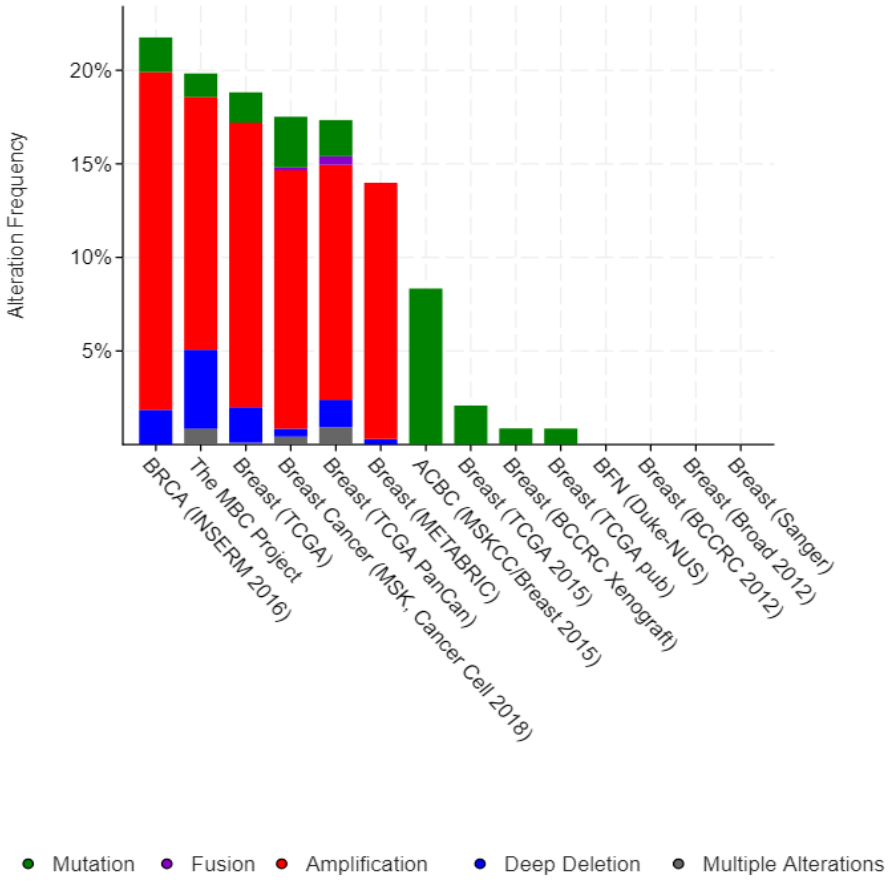

(B)

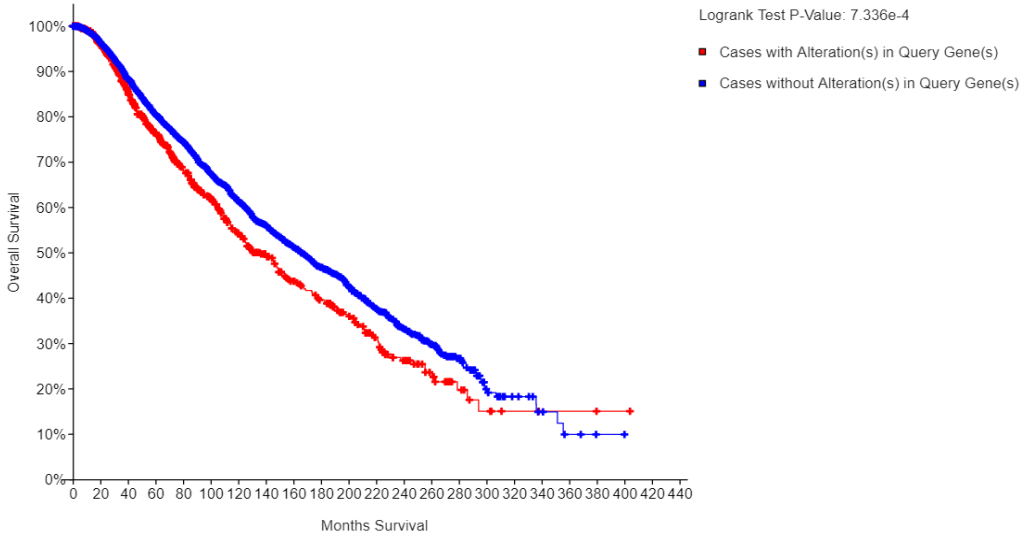

Figure 11. FGFR alterations in multiple breast cancer patients' cohorts. **(A)** FGFR1-4 gene alteration type and frequency in different breast cancer cohorts. Green: gene mutation; Red: gene amplification; Blue: gene deletion; Purple: gene fusion; Dark grey: multiple alterations. **(B)** Overall survival Kaplan-Meier estimate plot of 857 cases of FGFR1-4 altered patients with 334 patient deceased and median survival of 135.3 months; 5608 patients without FGFR1-4 alteration and 1555 patient deceased, medium survival 165.4 months.

There are around 10% of breast cancer patient exhibit FGFR1 gene amplification (chromosome 8p11-12), and this amplification is found predominantly in ER-positive breast cancers. Amplification of this region is positively correlated to lower metastasis-free survival, higher oncogene addiction and invasion of cancer cells. FGFR2 is amplified in 5%-10% of breast cancer tumors. *In vitro* study show that overexpressed FGFR2 contribute to resistance of cancer cells to

FGFR inhibitor. Mutations of FGFR2 has been reported in multiple cancer types, R203C, N550K, S588C and K660M are found in breast cancer. FGFR3 amplification is rare in breast cancer (around 1%) (reviewed in [205]). Despite low mutation rate of FGFRs in breast cancer, the aberrant activation of FGFR is one of the known antiangiogenic therapy-resistance mechanisms, and FGFR inhibition contributes to enhance endocrine therapy in breast cancer [205]. Therefore, FGFR inhibition is still one of the potential targeted therapies suitable for breast cancer treatment, and there are multiple FGFR inhibitors currently under clinical trial investigations in different solid tumors (Table 3).

Table 3. FGFR Inhibitors in Clinical Studies.

Inhibitor	Targets	Company	Clinical Trial Identify Number
AZD4547	FGFR1 FGFR2 FGFR3 KDR	AstraZeneca	Ph I/II: NCT01824901 (Lung cancer) Ph I/II: NCT01202591 (ER+ breast cancer) Ph II: NCT01795768 (Gastric cancer, Oesophageal cancer, Breast cancer, SCLC) Ph II: NCT01457846 (Gastro-oesophageal junction cancer, gastric Cancer Ph II/III: NCT02965378 (SCLC) Ph I/II: NCT01791985 (ER+ breast cancer)
Dovitinib (TKI-258)	FLT3 c-Kit FGFR3 VEGFR1 VEGFR2 VEGFR3	Novartis	Ph I/II: NCT01921673 (Gastric cancer) Ph II: NCT01719549 (Gastric cancer) Ph II: NCT01732107 (Bladder cancer) Ph II: NCT01676714 (NSCLC, Colorectal cancer) Ph II: NCT01831726 (Tumor) Ph II: NCT00958971 (HER2- breast cancer) Ph II: NCT01379534 (Endometrial cancer) Ph II: NCT00790426 (Urothelial cancer)

Erdafitinib (JNJ-42756493)	FGFR1 FGFR2 FGFR3 FGFR4	Janssen	Ph I: NCT03238196 (ER+/HER2- breast cancer) Ph I: NCT03825484 (Advanced cancers) Ph III: NCT03390504 (Urothelial cancer) Ph II: NCT02699606 (Urothelial cancer, Esophageal cancer, Cholangiocarcinoma) Ph II: NCT02365597 (Urothelial cancer) Ph II: NCT03827850 (Lung cancer) Ph I: NCT01703481 (Advanced or Refractory Solid Tumors or Lymphoma) Ph II: NCT03210714 (Relapsed or Refractory Advanced Solid Tumors, Non-Hodgkin Lymphoma) Ph I/II: NCT03473743 (Urothelial cancer)
BGJ398	FGFR1 FGFR2 FGFR3 FGFR4	Novartis	Ph II: NCT02160041 (Solid Tumor, Hematologic Malignancies) Ph I: NCT01004224 (Solid Tumor) Ph Ib: NCT01928459 (Solid Tumor) Ph I: NCT01697605 (Tumors)
Lucitanib (E-3810)	FGFR1 FGFR2 FGFR3 VEGFR1 VEGFR2 VEGFR3 PDGFRα PDGFRβ	Clovis Oncology	Ph II: NCT02053636 (ER+ breast cancer) Ph I/II: NCT01283945 (Solid tumor) Ph II: NCT02202746 (Breast cancer) Ph II: NCT02109016 (Lung cancer)
Rogaratinib	FGFR1 FGFR2 FGFR3 FGFR4	Bayer	Ph I: NCT03517956 (Advanced solid tumor) Ph I: NCT01976741 (Neoplasm) Ph I: NCT03788603 (Neoplasm) Ph II: NCT03762122 (NSCLC)
Ponatinib	FGFR1 FGFR2 FGFR3 FGFR4 PDGFRα VEGFR2 c-Src c-Kit Abl	ARIAD Pharmaceuticals	Ph II: NCT02272998 (Advanced cancers) Ph II/III: NCT01761747 (NSCLC, Head and neck cancer) Ph II: NCT02265341 (Advanced biliary cancer)

Pemigatinib	FGFR1 FGFR2 FGFR3	Incyte	Ph I: NCT03822117 (Advanced cancers) Ph II: NCT03011372 (Myeloproliferative neoplasms) Ph II: NCT02872714 (Urothelial Cancer)
Derazantinib ARQ-087	FGFR1 FGFR2 FGFR3 FGFR4 RET DDR2 PDG-FRβVEGFR c-KIT	ArQule	Ph I/II: NCT01752920 (Advanced solid tumor)
Nintedanib	FGFR1 FGFR2 FGFR3 FGFR4 VEGFR1 VEGFR2 VEGFR3 VEGFR4 PDGFRα PDGFRβ Src Lyn	Centro Nacional de Investigaciones Oncologicas CARLOS III	Ph II: NCT01948141 (NSCLC) Ph I: NCT02619162 (Breast cancer)
TAS-120	FGFR1 FGFR2 FGFR3 FGFR4	Taiho Oncology	Ph I/II: NCT02052778 (Cholangiocarcinoma, Brain Tumor, Urothelial Cancer)
Debio 1347	FGFR1 FGFR2 FGFR3 FGFR4	Debiopharm	Ph II: NCT03834220 (Solid tumor) Ph I: NCT01948297 (Solid tumor) Ph II: NCT03344536 (Breast cancer)
LY3076226	FGFR3	Eli Lilly	Ph I: NCT02529553 (Advanced cancer)
PRN1371	FGFR1 FGFR2 FGFR3 FGFR4	Principia Biopharma	Ph I: NCT02608125 (Solid tumor, Urothelial cancer)
Brivanib	FGFR1 VEFGR1 VEGFR2 Flk1	Bristol-Myers Squibb	Ph II: NCT01367275 (Colorectal cancer)

ASP5878	FGFR1 FGFR2 FGFR3 FGFR4	Astellas Pharma	Ph I: NCT02038673 (Solid tumors)

*Due to limited space, Ph I studies are not listed in this Table unless it focuses on breast cancer.

2. FGFR3 is highly activated in cells with acquired PARP-i resistance

To screen for activated RTKs between PARP-i-sensitive and resistant cells with similar genetic background, we developed a panel of 31 cell lines with acquired talazoparib-resistance (BR#01-#31) from the PARP-i–sensitive, *BRCA1*-mutated TNBC cell line SUM149 (Fig. 10). The half maximal inhibitory concentration (IC_{50}) of talazoparib in the pool of BR cells was more than 100-fold than that in parental cells in colony formation assays (SUM149: 0.5 nM; BR: 50 nM, Fig. 12) and in MTT assays (SUM149: 1 nM; BR: 10 µM, Fig. 13).

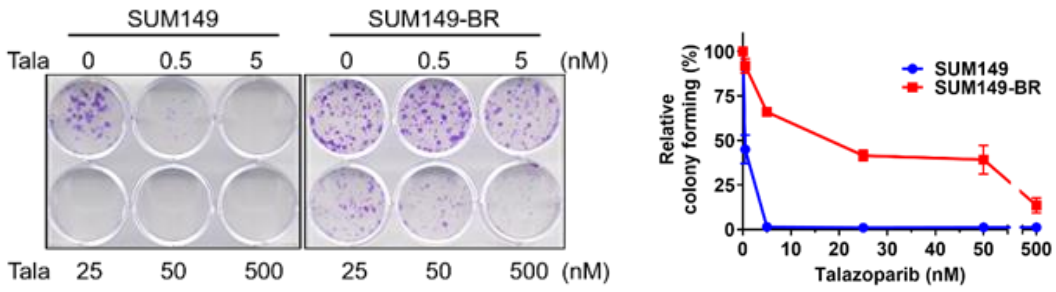

Figure 12. SUM149-BR is more resistant to talazoparib than SUM149 parental cell in colony formation assay.

Cells were seeded into 6-well plate and incubated overnight before treated with various concentrations of talazoparib for 10-14 days. Colonies were then stained with crystal violet and quantified. The number of colonies in the well without talazoparib treatment was designated to represent 100% relative colony forming rate. The number of colonies in wells treated with talazoparib were normalized to that of untreated well for calculating relative colony forming rate in response to talazoparib. Mean ± S.D. from 3 independent experiments were shown in the quantified figure.

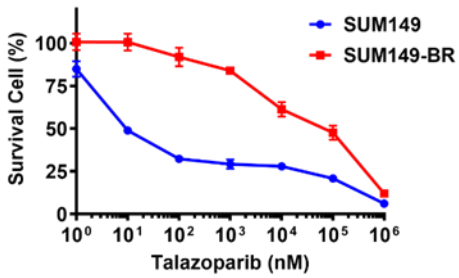

Figure 13. SUM149-BR is more resistant to talazoparib than SUM149 parental cell in MTT assay.

Cells plated into a 6-well plate and incubated overnight before treated with various concentrations of talazoparib for 5-6 days. Cell survival was then measured by using the value of optical density at 595 nm in MTT assays, the wells without talazoparib treatment were designated as 100% survival. Mean ± S.D. from 3 independent experiments were shown in the quantified figure.

As expected, the pool of BR cells showed cross-resistance to various PARP-is, including olaparib, rucaparib, and veliparib, with resistance capacity similar to that of intrinsic PARP-i resistant TNBC cells, including MDA-MB-231, BT-549, MDA-MB-468, HCC70, and HCC1937 (Fig. 14).

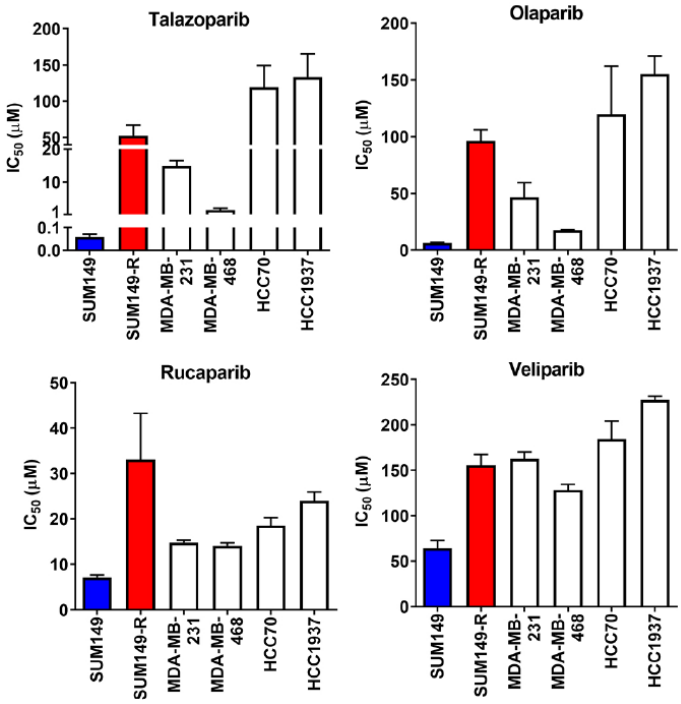

Figure 14. SUM149-BR cell shows resistance to four different PARP-is at a level comparable to known PARP-i-resistant TNBC cell lines.

The survival of cells in response to various concentrations of PARP-is indicated were measured by MTT assay. The cell survival curves were than used for calculating IC_{50} by using GraphPad Prism 8.0. Mean ± S.D. from 3 independent experiments were shown in the quantified figure.

We further determined the IC_{50} of four PARP-is in individual BR cells, and the cells showed a range of responses to these PARP-is; overall, the BR cells were more resistant to talazoparib and olaparib than to rucaparib and veliparib (Fig. 15).

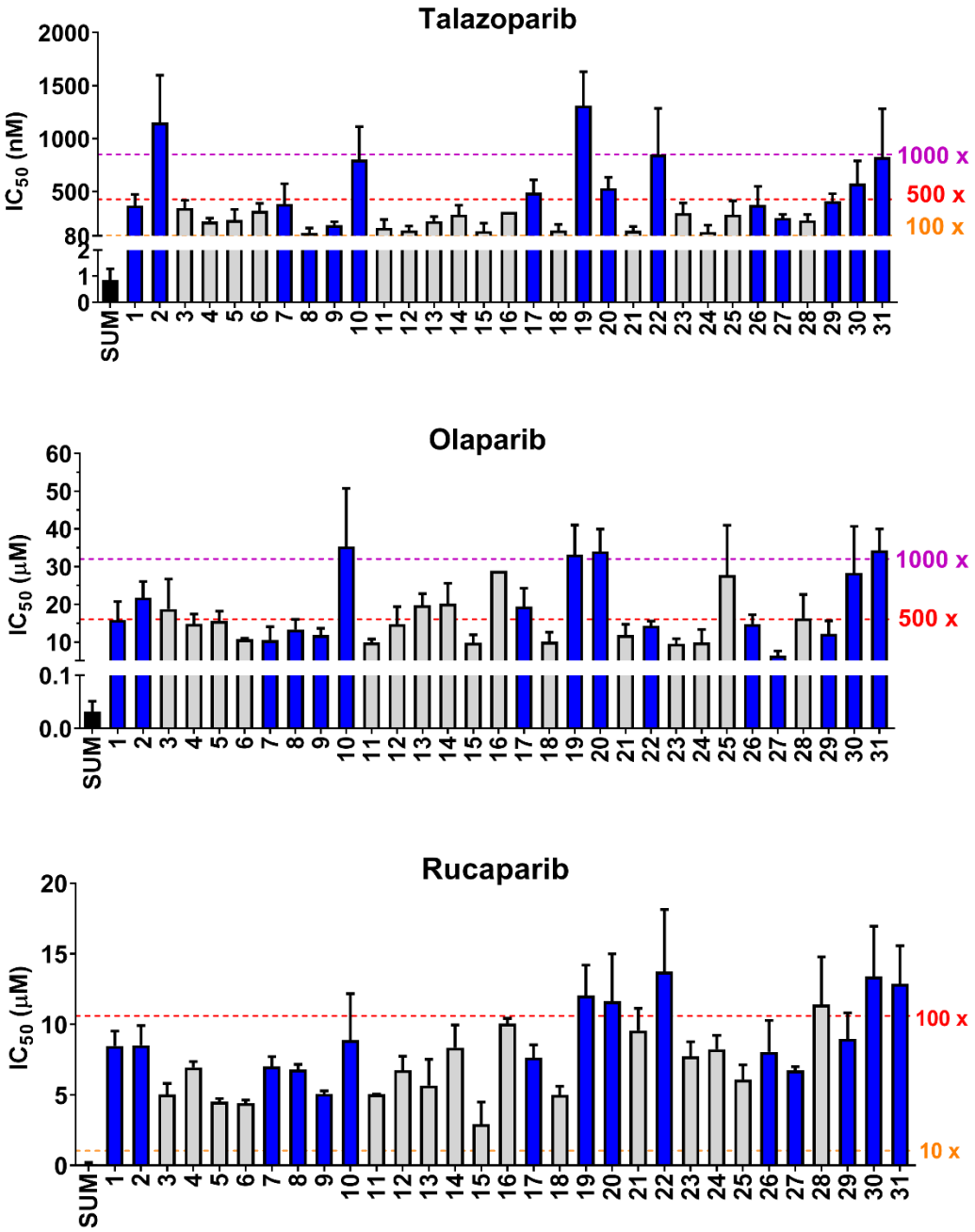
Talazoparib
IC50 (nM)
2000
1500
1000
500
80
2
1
0
1000 x
500 x
100 x
SUM
1 2 3 4 5 6 7 8 9 10 11 12 13 14 15 16 17 18 19 20 21 22 23 24 25 26 27 28 29 30 31
Olaparib
IC50 (μM)
60
50
40
30
20
10
0.1
0.0
1000 x
500 x
SUM
1 2 3 4 5 6 7 8 9 10 11 12 13 14 15 16 17 18 19 20 21 22 23 24 25 26 27 28 29 30 31
Rucaparib
IC50 (μM)
20
15
10
5
0
100 x
10 x
SUM
1 2 3 4 5 6 7 8 9 10 11 12 13 14 15 16 17 18 19 20 21 22 23 24 25 26 27 28 29 30 31

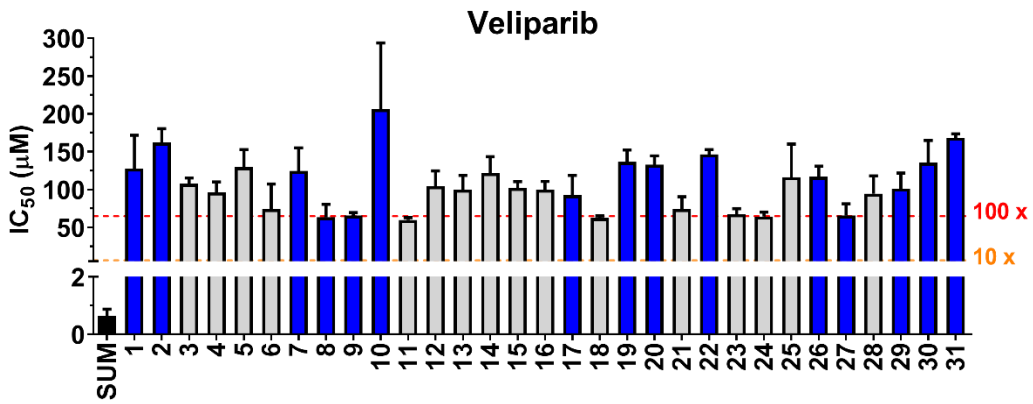

Figure 15. The IC50 of BR cells to PARP-is.

Cells were treated with various concentrations of PARP-is as indicated for 6 days before cell survival was analyzed by MTT assay. Fold (x) of IC_{50} was compared to that of SUM149 parental cell (SUM).

PARP-i–mediated cytotoxicity greatly relies on the involvement of PARP1 in DDR [206], to accentuate the rationale of including PARP-is in treatment strategy, we investigated the contribution of PARP1 to PARP-i-induced cytotoxicity in SUM149, BR#09, and BR#17 cells. We found that knocked-down endogenous PARP1 expression ($PARP1^{KD}$) in these cells, compared with the control cells carrying non-targeting shRNA, caused at least 10-fold more resistant to talazoparib (Fig. 16), indicating that PARP1 is still required for PARP-is-induced cytotoxicity in SUM149 and BR cells. Therefore, we deduced that PARP-i resistance in these cells is related to PARP1-mediated pathways, but is not due mainly to PARP-i efflux or loss of PARP1 [183, 206-209], and that PARP-is remain as reasonable therapeutic agent for BR cells.

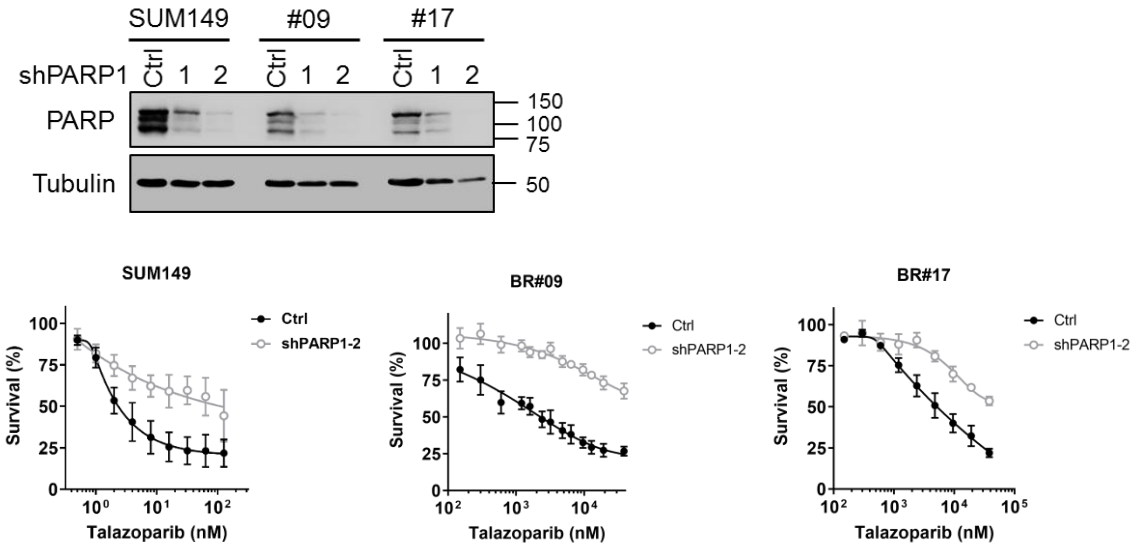

Figure 16. Knocking down PARP1 enhances talazoparib resistance in SUM149 and BR cells.

Endogenous PARP1 expression was knocked-down using two different short hairpin RNAs (shRNA) against PARP1 (shPARP1). Non-targeting shRNA was introduced as control (Ctrl). SUM149 and BR cells expressing control shRNA or shPARP1-2 were subjected to talazoparib treatment at various concentrations, and cell survival was measured by using MTT assay.

We selected 15 BR cells in order to identify common RTK targets, and sought specific RTK activations harbored in the majority of these cells, but not in SUM149 parental cell, with phospho-RTK antibody arrays (Fig. 17). Quantification data of the arrays showed that FGFR, IGFR and EGFR families were the most phosphorylated RTK families in BR cells, with phosphorylated FGFR3 had the highest prevalence of array signals that were at least 10-fold higher than in parental SUM149 cells (Fig. 17).

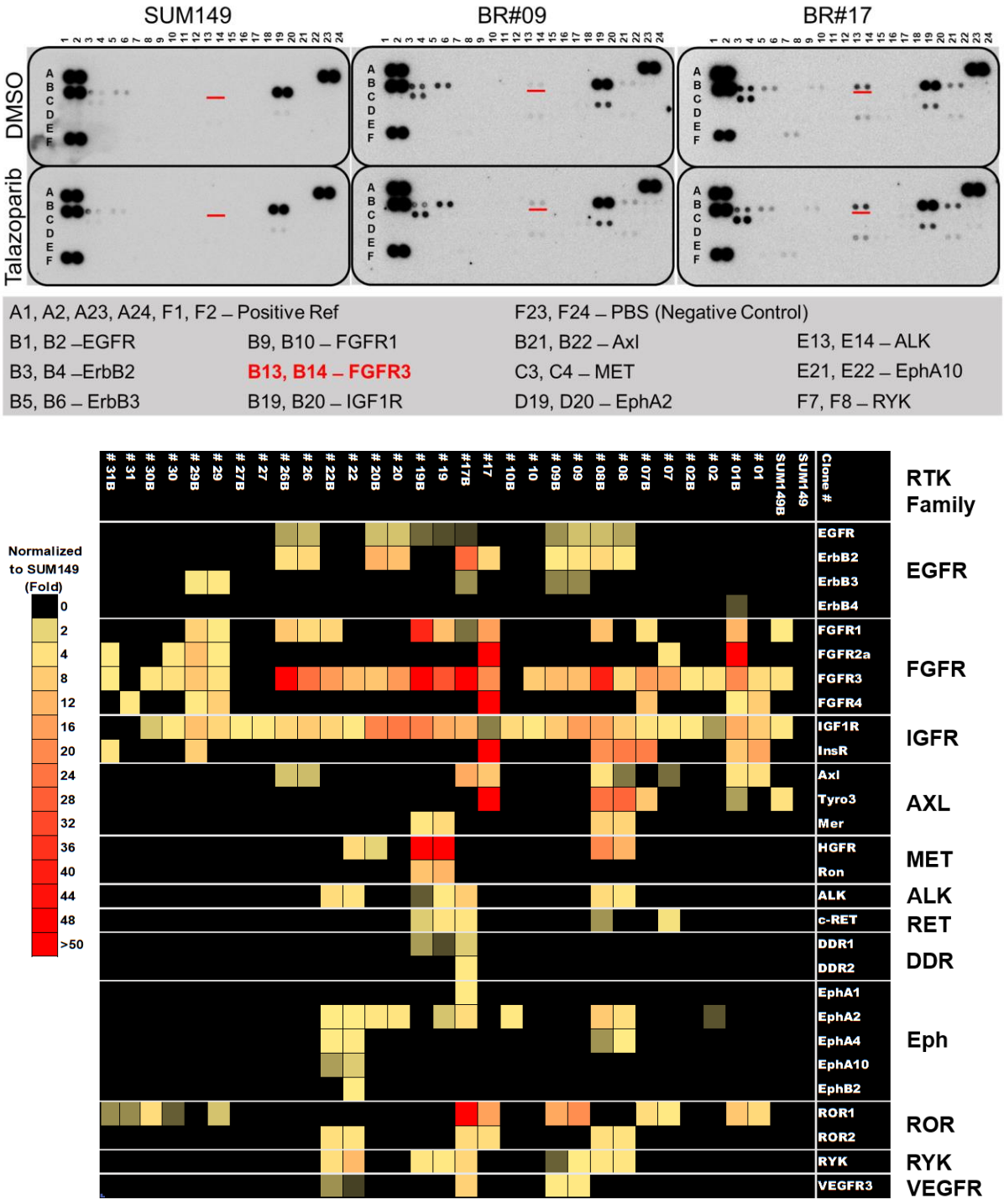

Figure 17. Antibody arrays of RTK activation in SUM149 and BR cells.

Cells indicated were treated with dimethyl sulfoxide (DMSO) or 100 nM talazoparib overnight and harvested for RTK antibody array analysis. Signal intensities on each array were normalized to the mean signal intensity of positive reference spots on each array and compared with the signal intensity of respective spots on SUM149 DMSO-treated array.

We validated the array data by Western blotting and found that, in about 50% of BR cells, FGFR3 phosphorylation and FGFR3 expression were higher than that in parental SUM149 cells (Fig. 18).

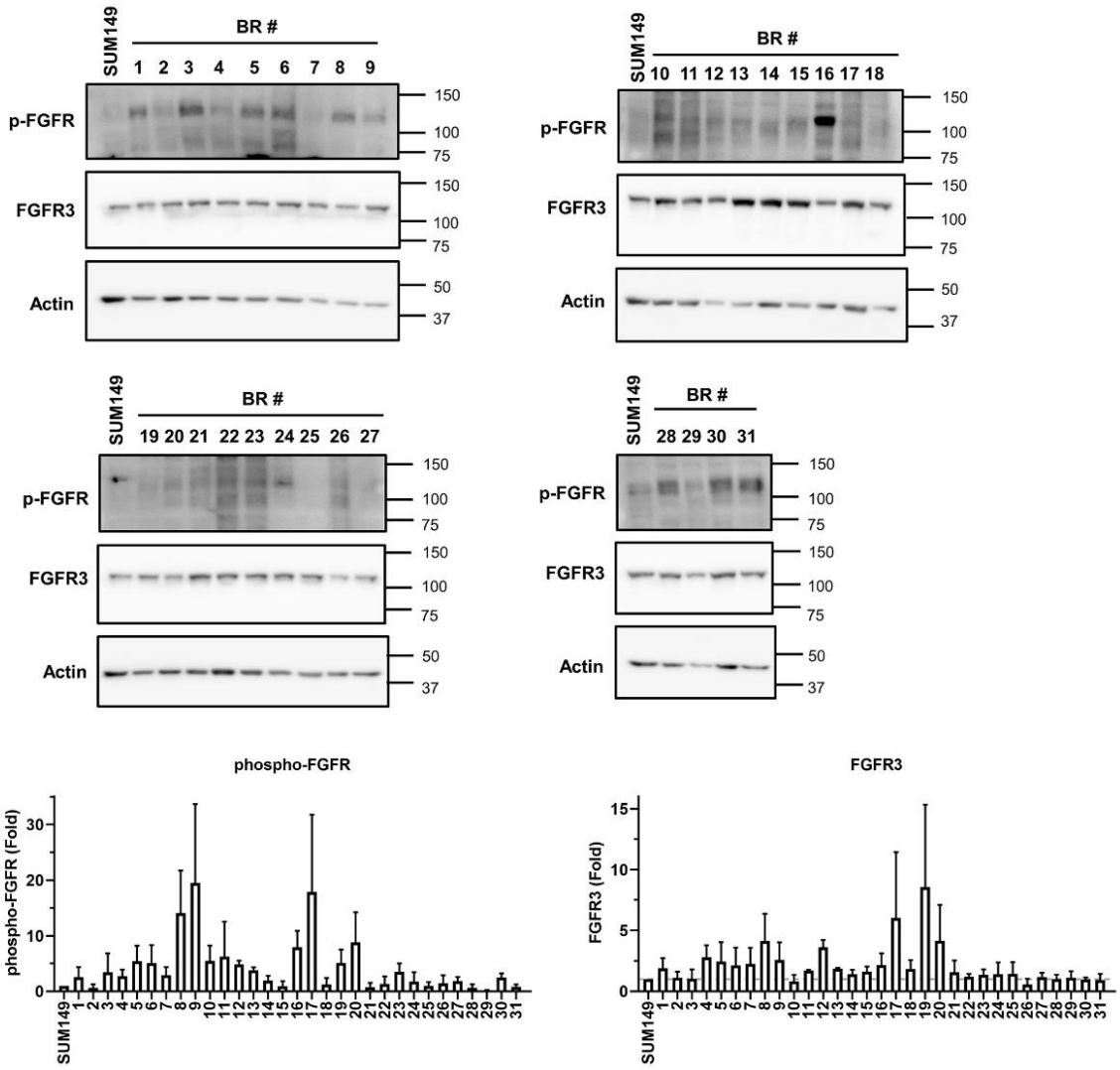

Figure 18. Expressions of phosphorylated FGFR3 and total FGFR3 proteins are higher in around half of the BR cells.

SUM149 and the 31 BR cells were treated with 100 nM talazoparib overnight before harvested for Western blotting analysis. Actin was chosen to serve as loading control. Signals of phosphorylated FGFR (p-FGFR) and FGFR3 were normalized to actin and then normalized to that of SUM149 (1-fold). Three independent repeats were performed and the quantitation histograms indicate mean ± S.D.

Furthermore, FGFR3 was also activated in acquired talazoparib resistant cells developed from HCC1806 TNBC cell (Fig. 19).

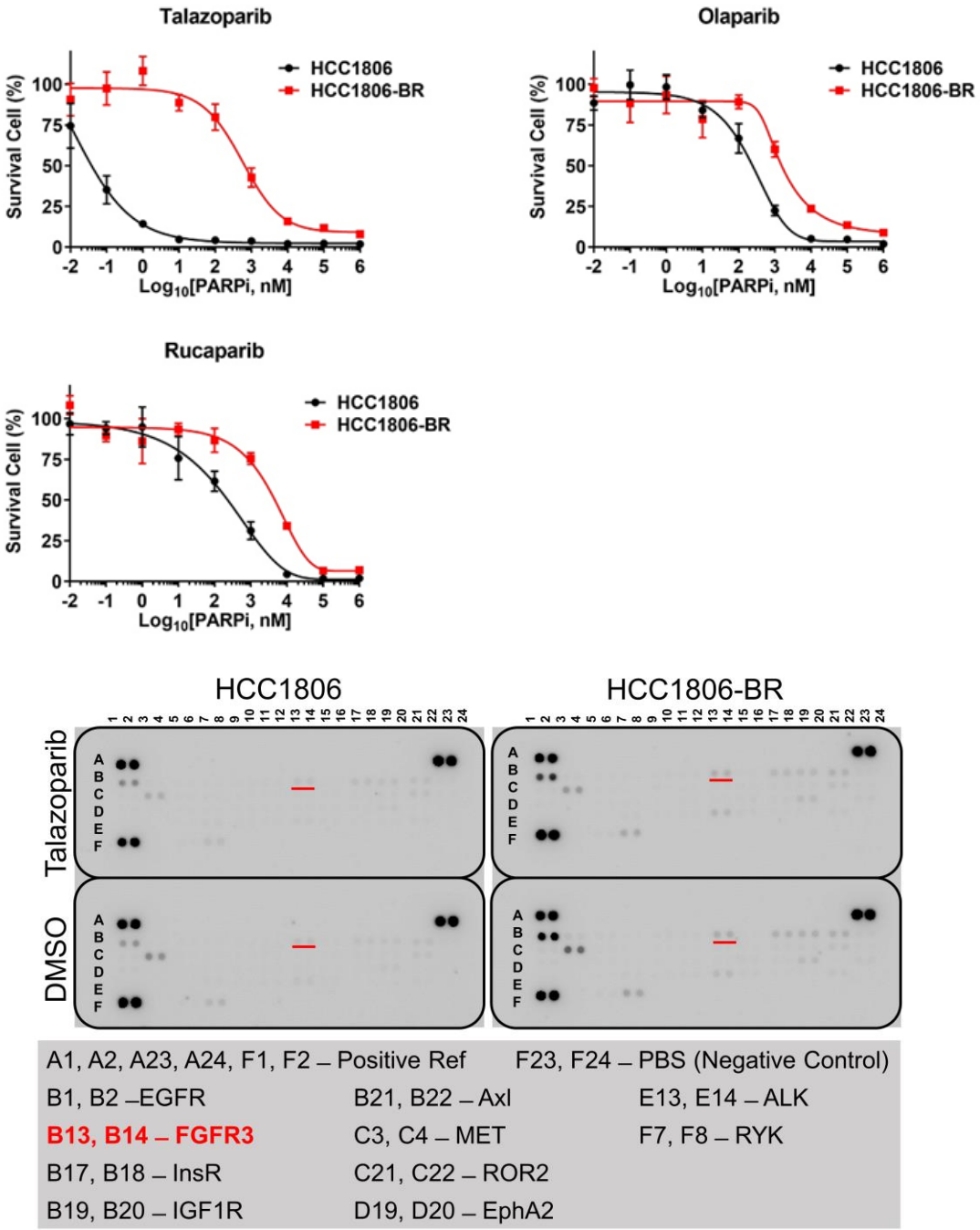

Figure 19. FGFR3 is activated in HCC1806-BR cells.

HCC1806-BR cell is more resistant to olaparib, talazoparib, and rucaparib than HCC1806 parental cells. Antibody arrays of RTK activation in HCC1806 parental cell and HCC1806-BR cells were performed with cells treated overnight with 1 μM talazoparib.

These results indicated that phosphorylated FGFR3 is common among acquired PARP-i–resistant TNBC cells. Therefore, we chose two BR cells (BR#09 and BR#17) that had high FGFR3 expression for studying the effects of FGFR3 on PARP-i resistance. To validate the involvement of FGFR3 in PARP-i resistance, we knocked-down endogenous FGFR3 expression ($FGFR3^{KD}$) in BR#09 and BR#17 cells. As expected, $FGFR3^{KD}$ strengthened talazoparib sensitivity in these cells, and that $FGFR3^{KD}$ cells rescued with wild-type FGFR3 ($FGFR3^{WT}$) exhibited restored resistance to talazoparib (Fig. 20).

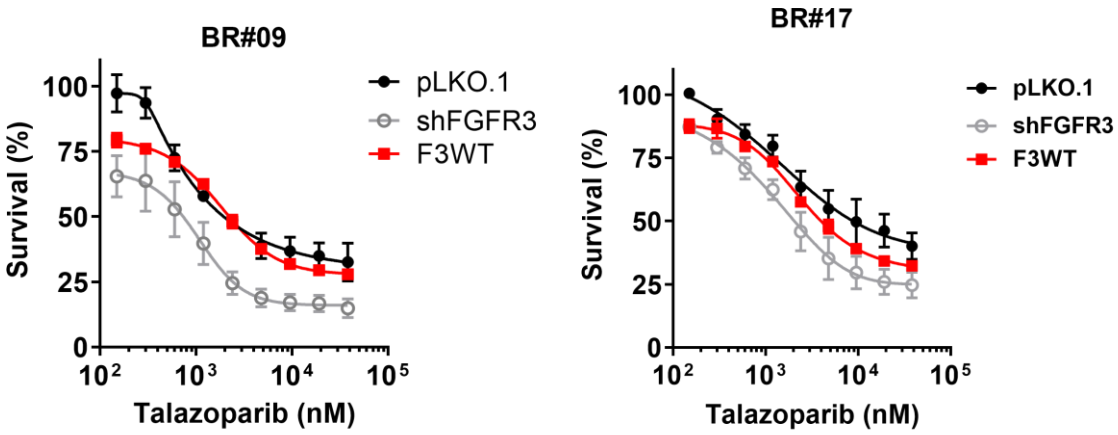

Figure 20. FGFR3 contributes to talazoparib resistance in BR cells. FGFR3 expression was knocked-down by shRNA in SUM149, BR#09, and BR#17 cells, and the expression of FGFR3 were examined by Western blotting.

Survival rate of the cells indicated in response to talazoparib was analyzed by MTT assay after 6 days of talazoparib treatment.

3. FGFR inhibition impedes DNA repair efficiency and has synergism with PARP-is

To elucidate role of FGFR3 in PARP-i-resistance, we first examined whether DNA damages can induce phosphorylation of FGFR3 by using alkylating agent methyl methanesulfonate (MMS) to damage DNA [207]. Indeed, both BR#09 and BR#17 cells elevated FGFR3 phosphorylation more than SUM149 cell in response to MMS and talazoparib treatment, and the FGFR phosphorylation can be inhibited by FGFR-is (Fig. 21).

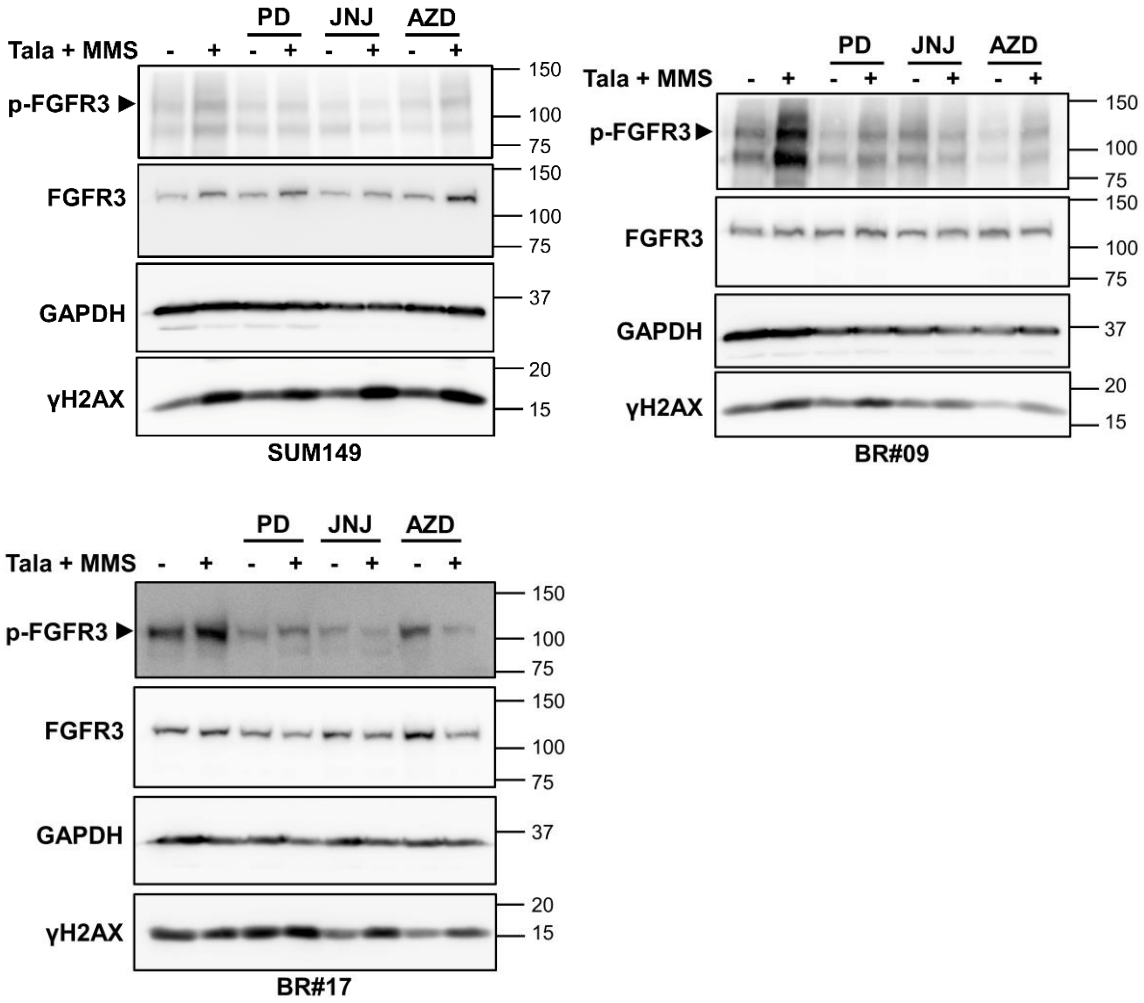

Figure 21. FGFR-is inhibited talazoparib-induced FGFR phosphorylation. Cells were treated with either 5 μM PD173074 (PD), erdafitinib (JNJ), or AZD4547 (AZD) for 4 h, and then further exposed to 100 nM talazoparib (Tala) and 0.01% MMS in combination with the FGFR-is indicated for another hour before harvested for Western blotting analysis.

While MMS induced similar amount of DNA damage in these cells, we found that BR cells have fewer DNA damages left than SUM149 at 3 h post-MMS treatment (Fig. 22).

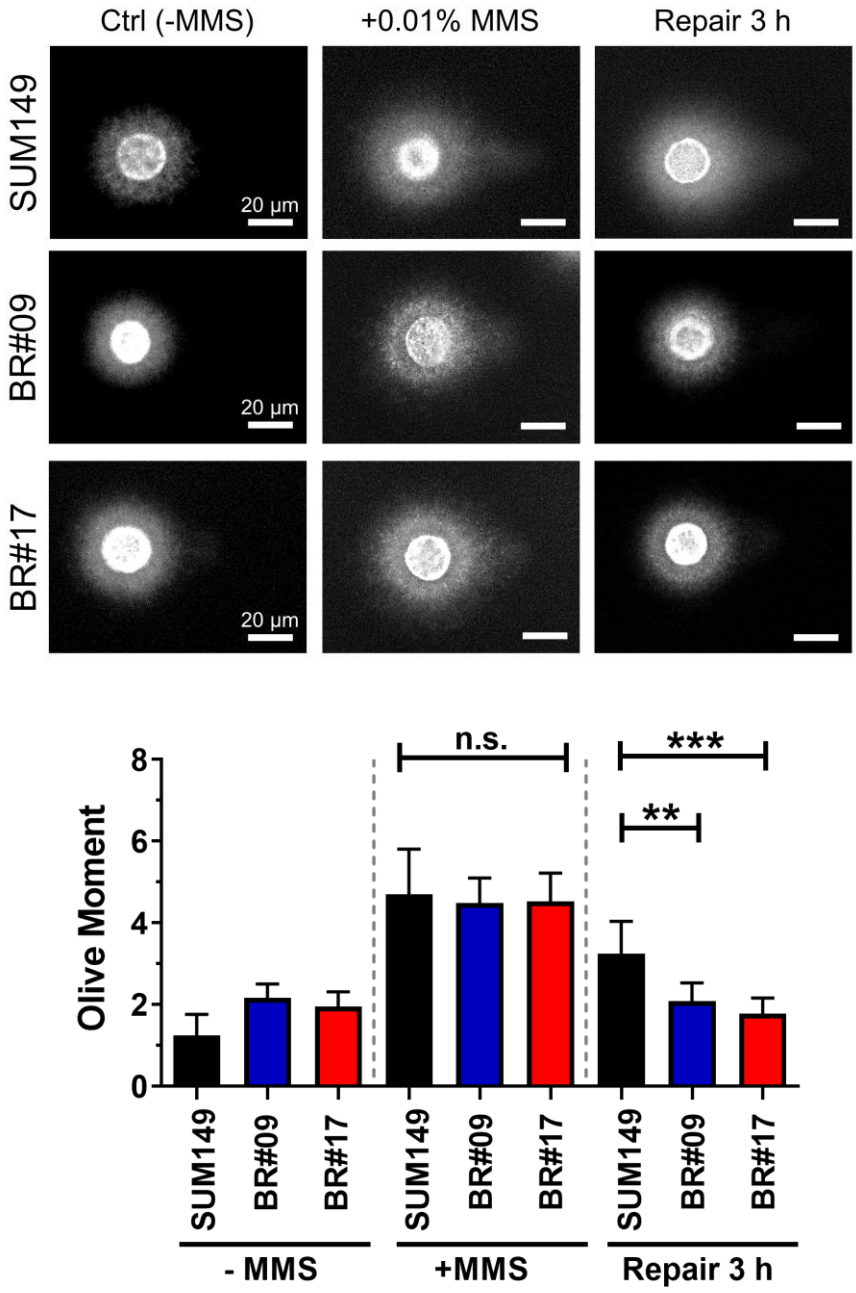

Figure 22. BR cells have higher DNA repair efficiency than SUM149. SUM149, BR#09, and BR#17 cells were treated with 0.01% MMS for 40 min (+MMS) to induce DNA damages. The cells were then released from MMS by refreshing cell culture medium to allow DNA repair for 3 h. The untreated group (-MMS) were harvested at the same time with the groups repaired after 3 h. DNA damages were then measured by alkaline comet assay using olive moment metric.

Because the confocal microscope analysis showed that FGFR3 co-localized with γH2AX DNA break foci (Fig. 23), we further investigated the effect of FGFR inhibition on DNA repair.

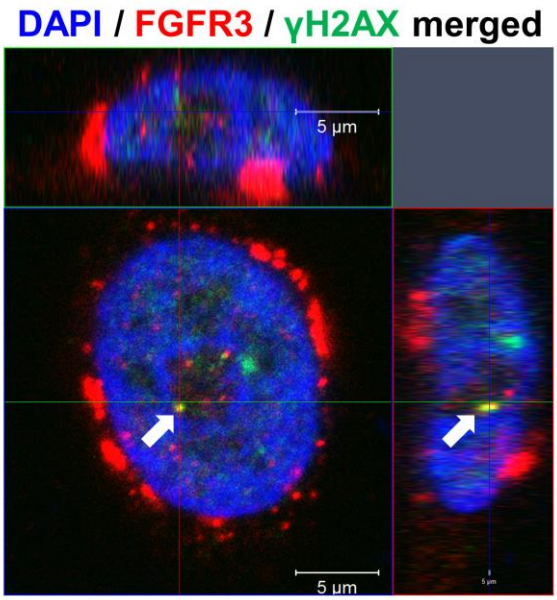

Figure 23. Co-localization of FGFR3 and γ H2AX in cell nucleus.

BR#17 cell were treated with 250 nM talazoparib and 0.01% MMS FGFR-is for an hour before fixed and subjected to immunofluorescence staining with antibodies against FGFR3 (TexasRed, red) and γ H2AX (FITC, green). DNA was counterstained with DAPI (4´6-diamidino-2-phenylindole) (blue). Z-stack images were captured using confocal microscope.

The γH2AX foci staining also show that, in absence of MMS, γH2AX foci formed in talazoparib treated cells is similar to that in cells treated with talazoparib and PD173074 combination (Fig. 24). Moreover, γH2AX foci significantly decreased from 4 to 8 hour treatment (p-value < 0.001) in untreated cells or cells treated with either talazoparib or PD173074 alone, but the amount of γH2AX foci remains unrepaired from 4 to 8 in combination treated group (Fig. 24).

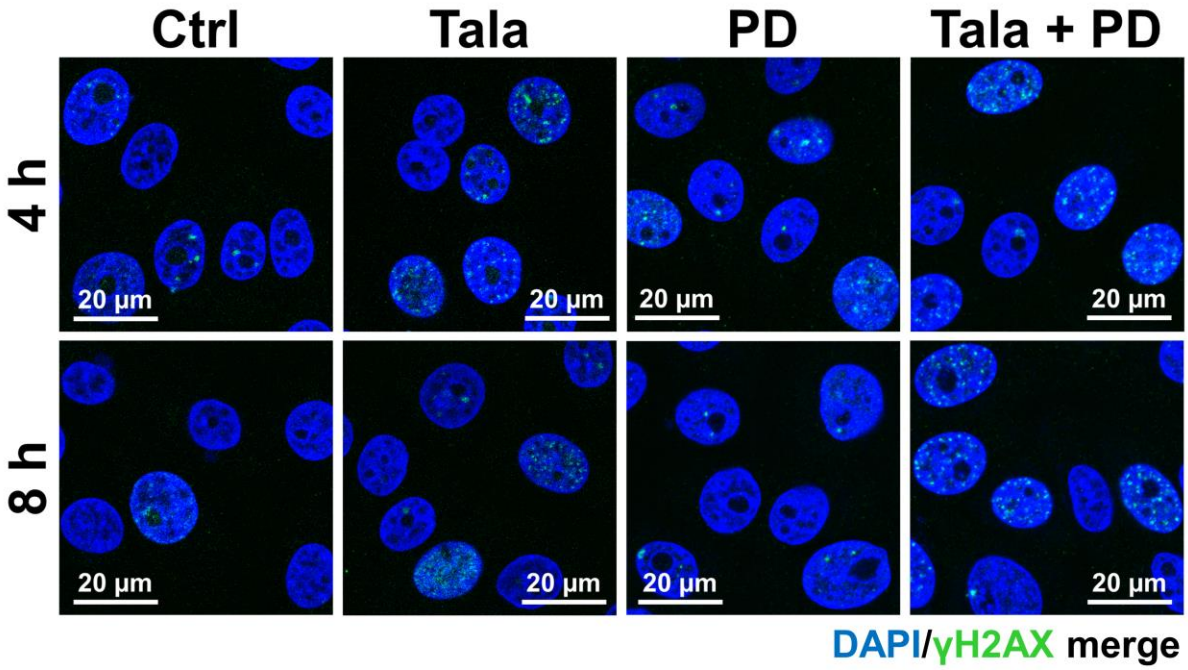

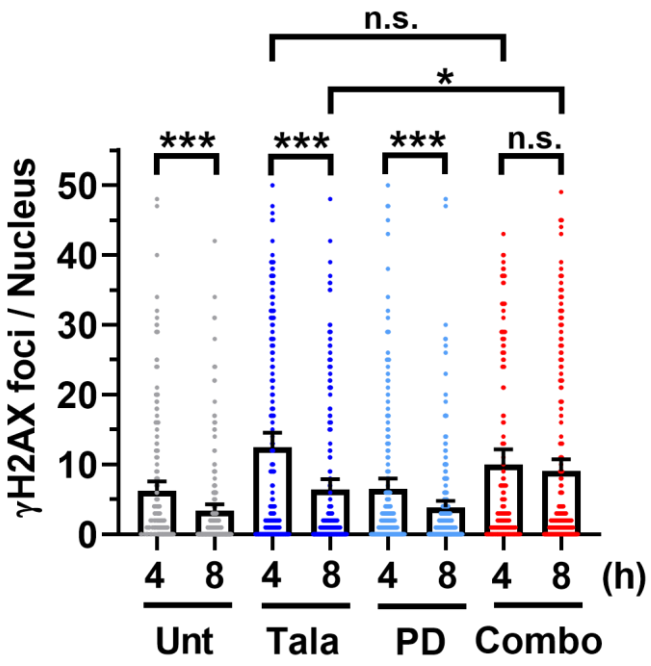

Figure 24. Combination of talazoparib and PD173074 delays repair of γH2AX foci.

BR#17 cells were treated for 1 hour with 0.01% MMS combined with 250 nM talazoparib (Tala) and 10 µM PD173074 (PD) as indicated. MMS was removed and cells were cultured in fresh culture medium (Ctrl), talazoparib, or PD173074 either alone or in combination for 4 h and 8 h before cells were fixed for immunofluorescence staining. DNA strand break γH2AX foci were detected using anti-γH2AX antibody (FITC, green) and DNA was counterstained with DAPI (blue). The γH2AX foci in each cell nucleus were counted using Blobfinder and the statistical analysis was performed using ANOVA, data from at least 150 individual cells were shown in dot, and the histogram showed mean ± 95% confident interval.

The same phenomenon was also observed in comet assay with MMS-induced DNA damages. We induced DNA damage in BR cells with MMS in the

presence of either talazoparib, PD173074, or combination of talazoparib and PD173074, and we found that combination of PD173074 and talazoparib did not induce more DNA damages than talazoparib treatment in comet assay (Fig. 25).

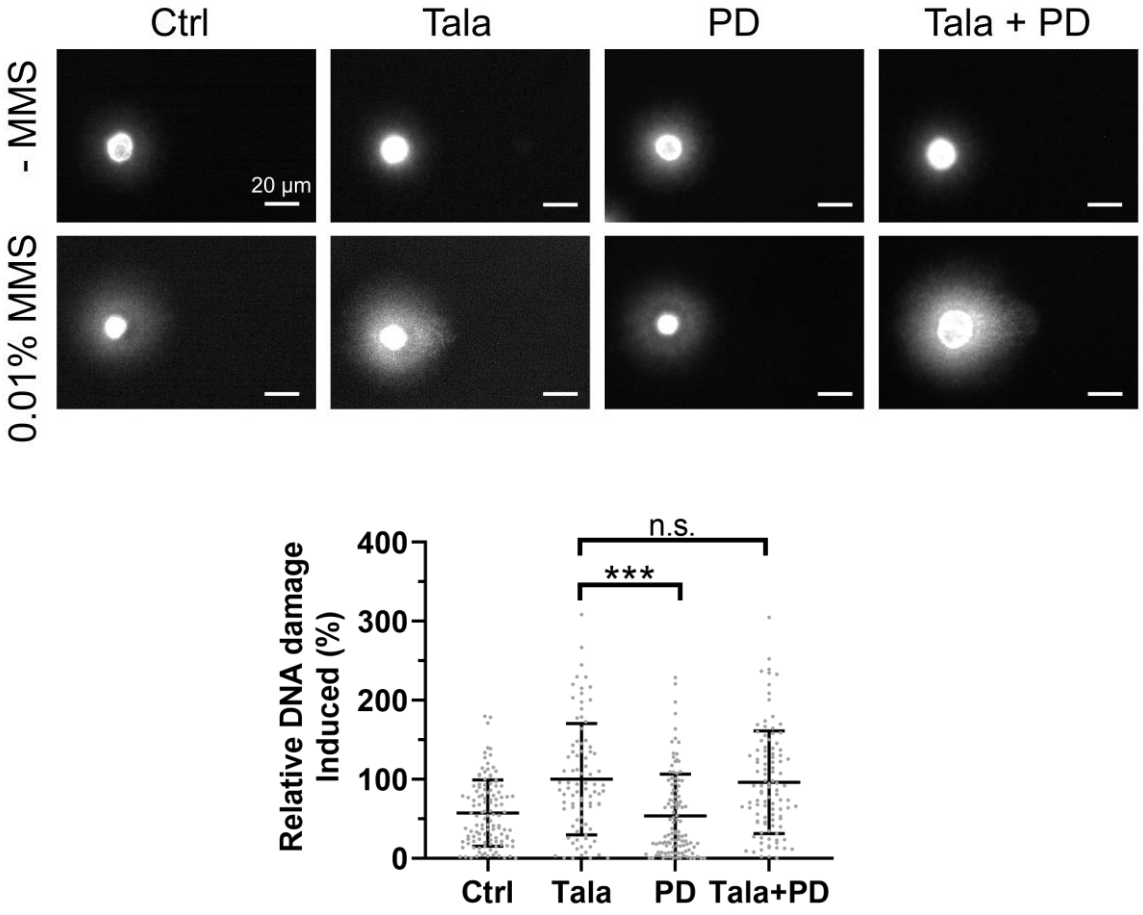

Figure 25. Combination of talazoparib and PD173074 does not increase DNA damage induction.

BR#09 cells were treated with 0.01% MMS, 100 nM talazoparib, and 10 μM PD173074 either alone or in combination for 1 h before harvested for alkaline comet assay. Among MMS treated groups, DNA damages in tail was quantified

using olive moment and normalized to that of talazoparib treated group. Statistical analysis was performed with ANOVA, data from at least 100 individual cells were shown in dot, and the mean ± standard deviation (S.D.) were shown.

Interestingly, while most of cells in control group eliminated DNA damage at 3 h after MMS removal, we found that BR cells in talazoparib treated group had similar unrepaired DNA damages as in PD173074 group, and that more DNA damages were left in cells repaired in combination of talazoparib and PD173074 (Fig. 26). Our comet assay and γH2AX foci staining data suggest that the combination treatment does not induce more DNA damages than talazoparib treatment, but the combination of talazoparib and PD173074 delays DNA repair efficiency, and thus, the combination may be more cytotoxic because it induces sustained burden of DNA breaks.

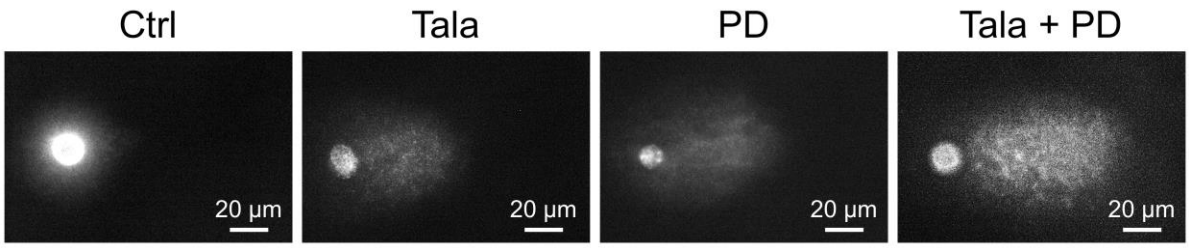

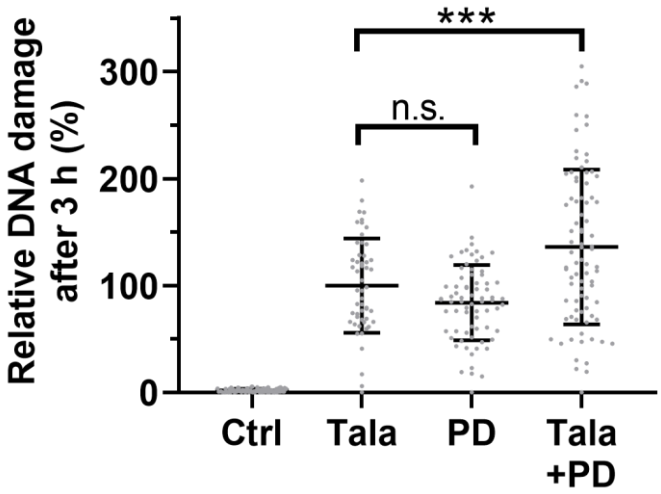

Figure 26. Combination of talazoparib and PD173074 delays DNA repair. BR#09 cells were treated with 0.01% MMS, 100 nM talazoparib, and 10 μM PD173074 either alone or in combination for 1 h. MMS was then removed and cells were incubated in talazoparib and PD173074 as indicated for 3 h before harvested for alkaline comet assay. DNA damages in tail was quantified using olive moment and normalized to that of talazoparib treated group. Statistical analysis was performed with ANOVA, data from at least 100 individual cells were shown in dot, and the mean ± standard deviation (S.D.) were shown.

We further examined the efficacies of combining PARP-is and FGFR-is in eliminating BR#09 and BR#17 cells. We evaluated the synergy between FGFR-is and PARP-is by measuring the combination index (CI) in these cells, in general, CI below 0.8 represents synergistic effect between inhibitors and CI below 0.3 indicates a strong synergism [210]. Considering the potential for study of this approach in clinical trials, we paired inhibitors developed by the same pharmaceutical companies, e.g. talazoparib combined with PD173074; olaparib combined with AZD4547. Using colony formation assay, we demonstrated that, in

BR#09 cell, combination of talazoparib and PD173074 had a moderate synergism (CI ranging from 0.3 to 0.9); in BR#17 cell, strong synergism between talazoparib and PD173074 was observed (CI below 0.07) (Fig. 27).

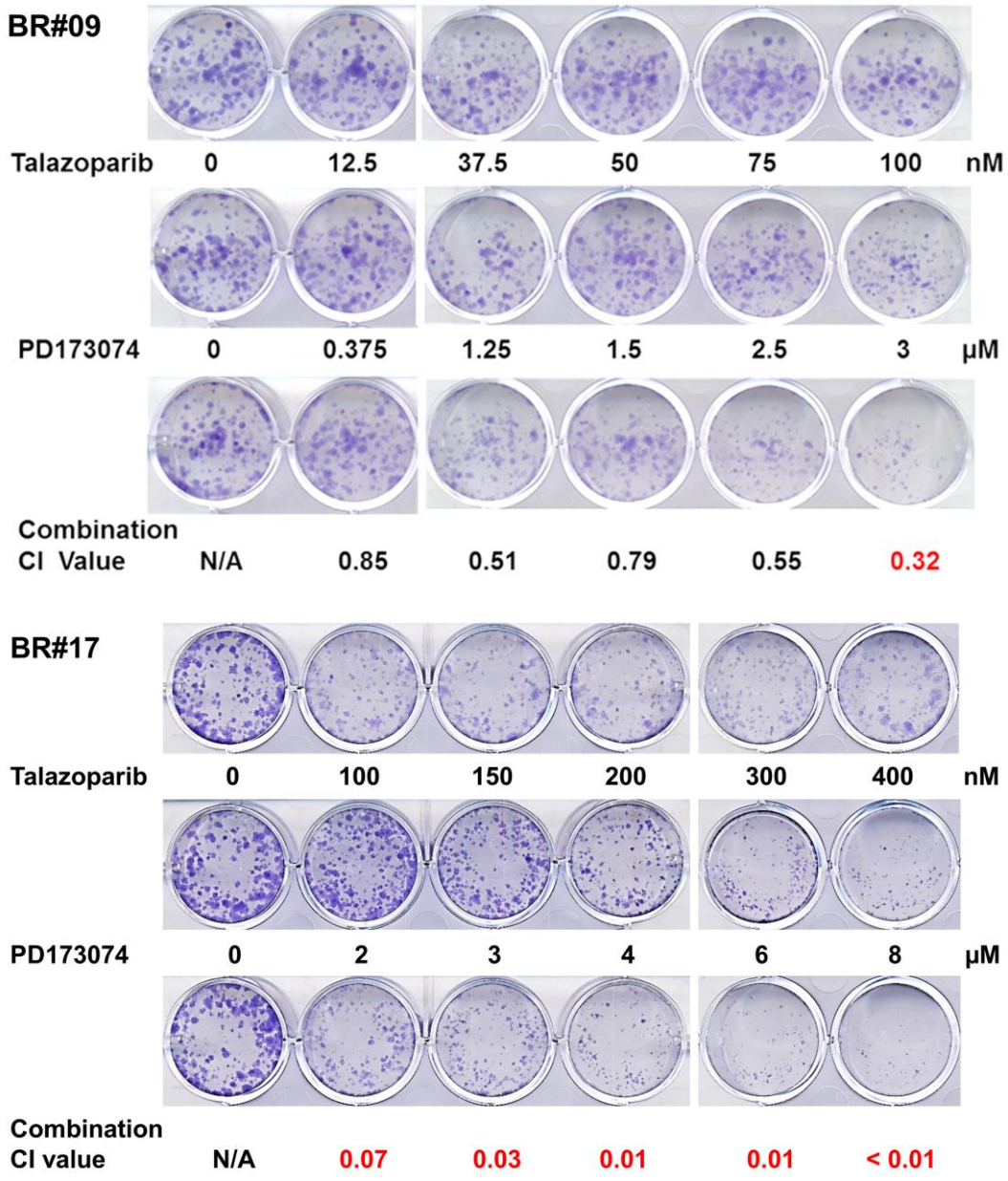

Figure 27. CI of talazoparib and PD173074 in BR#09 and BR#17 cells measured by colony formation assay.

Cells were treated with talazoparib and PD173074 at the concentrations indicated for 10-12 days, and then cells were fixed for colony formation assay. Number of colony formed was normalized to that in control group without talazoparib and PD173074 treatment, mean ± S.D. from at least 3 independent repeats were shown in histogram. CI was calculated using colony formation data obtained in the colony formation assay.

Because MTT assay is relatively more efficient in screening multiple ratios of drug combination than colony formation assay, we utilized MTT assay to evaluate synergism of PARP-is and FGFR-is BR and TNBC cells. In BR cells, the combination of talazoparib and PD173074 had a CI between 0.2 and 0.8 when eliminating more than 80% of the cells (Fa greater than 0.8) (Fig. 28), and the combination of olaparib and AZD4547 had a CI between 0.1 and 0.5 (Fig. 28).

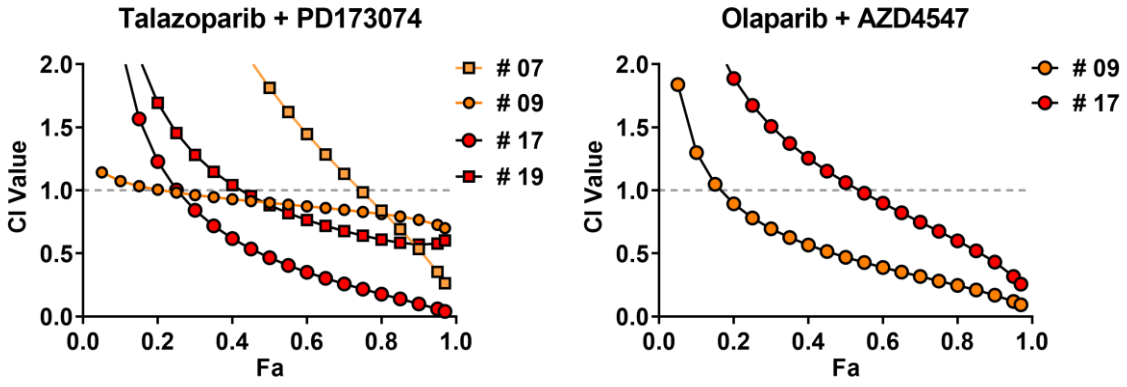

Figure 28. CI of the talazoparib and PD173074 combination or the olaparib and AZD4547 combination in multiple BR cells.

Cells were treated with various concentrations of talazoparib and PD173074 combinations or olaparib and AZD4547 combinations for 6 days before cell survival was measured by MTT assay. CI was then calculated by Compusyn software and MTT data of cell survival in response to treatments. Fa, fraction affected.

CI between 0.2 and 0.8 can also be reached in BT-549 and MDA-MB-157 cells with combinations of olaparib and AZD4547 (Fig. 29), suggesting the synergy of this combination is not limited to the BR cells we developed.

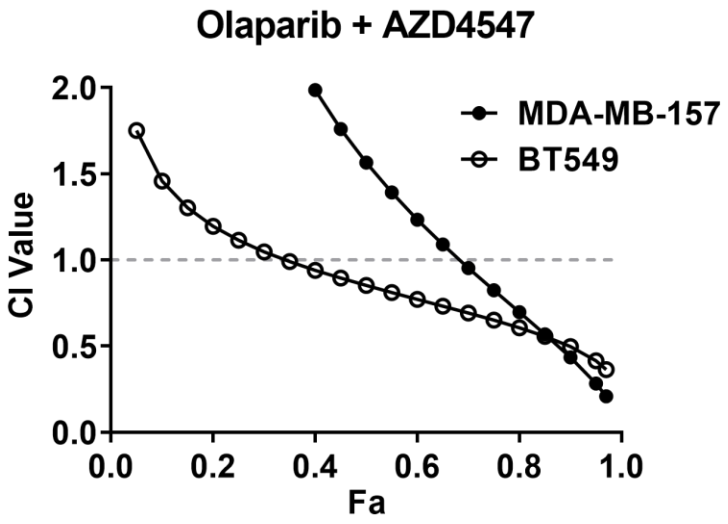

Figure 29. CI of the olaparib and AZD4547 combination in BT-549 and MDA-MB-157 cells.

Cells were treated with various concentrations of olaparib and AZD4547 combinations for 4 days before cell survival was measured by MTT assay. CI was then calculated by Compusyn software and MTT data of cell survival in response to treatments. Fa, fraction affected.

4. Inhibiting FGFR-mediated PARP1 Y158 phosphorylation reverses resistance to PARP-is

Since FGFR3 enhances PARP-i-resistance and FGFR inhibition affect DNA repair efficiency, we investigated whether FGFR3 exist in PARP1-interacting protein complex. We found that FGFR3 can be co-immunoprecipitated with PARP1 (Fig. 30), and our proximity ligation assay (PLA) data suggest FGFR3 and PARP1 can interact in cell nucleus (Fig. 31). Moreover, through PLA analysis, we found that the PLA signals of PARP1 and FGFR3 was less in cells treated with combination of talazoparib and PD173074 than in cells treated with either inhibitor alone (Fig. 31).

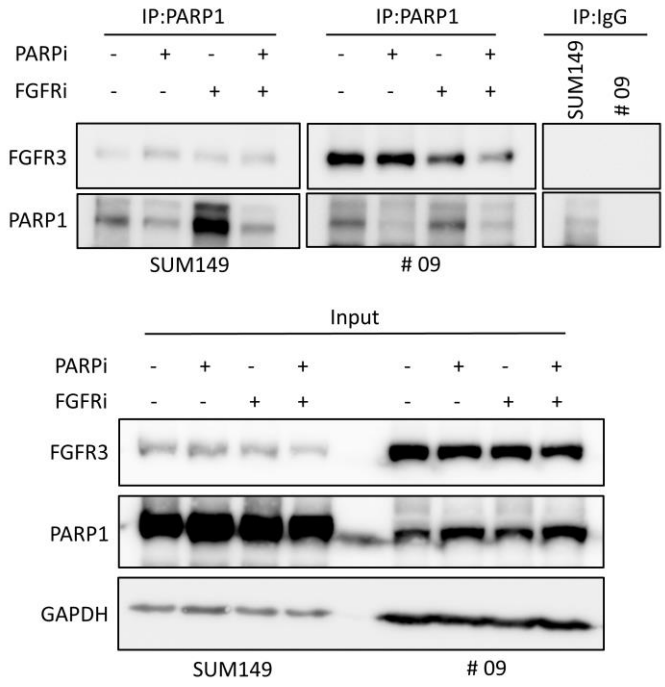

Figure 30. Co-immunoprecipitation of PARP1 and FGFR3.

SUM149 and BR#09 cells were treated with 100 nM talazoparib (PARPi) and 10 μM PD173074 (FGFRi) as indicated before harvested for PARP1 immunoprecipitation. For each sample, 500 μg total protein lysate was used for immunoprecipitation and 40 μg total protein were used for detecting target proteins in the cell lysate (input). The immunoprecipitated complex were then subjected to analyze the presence of FGFR3 by Western blotting.

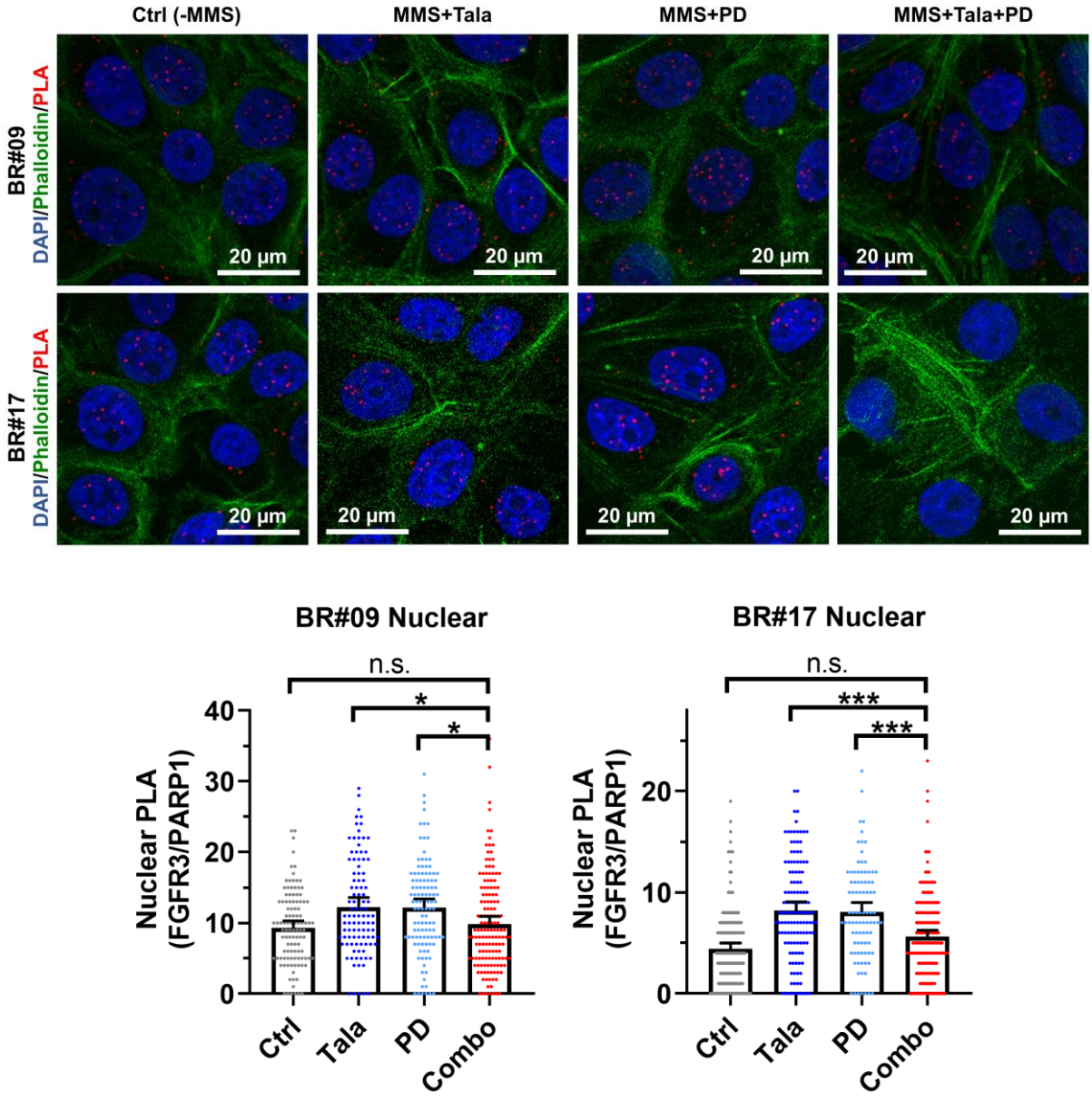

Figure 31. Combination of talazoparib and PD173074 decreases interaction between PARP1 and FGFR3.

FGFR3 and PARP1 PLA assays were performed with BR#09 and BR#17 cells treated with either 0.01% MMS, 100 nM talazoparib and 10 μM PD173074 either alone or in combination. Antibodies against FGFR3 and PARP1 were used and PLA signals (red) was detected using Duolink red assay and quantified by using Blobfinder. Phalloidin (green) was used to detect cytoskeleton and DNA was counterstained with DAPI (blue). Mean ± 95% confident interval of the number of PLA signals in each cell nucleus were shown in histogram. Individual cells were shown as dot and statistical analysis was performed using ANOVA with n > 100 in each group.

Followed our PLA results, we further hypothesized that FGFR3 may phosphorylate PARP1. Our *in vitro* kinase assay and mass spectrum analysis showed that FGFR phosphorylates PARP1 only at Y158 and Y176 amino acids (Fig. 32), which were predicted by motif scanning database to be phosphorylated by FGFR3 and FGFR1, respectively (Table 4).

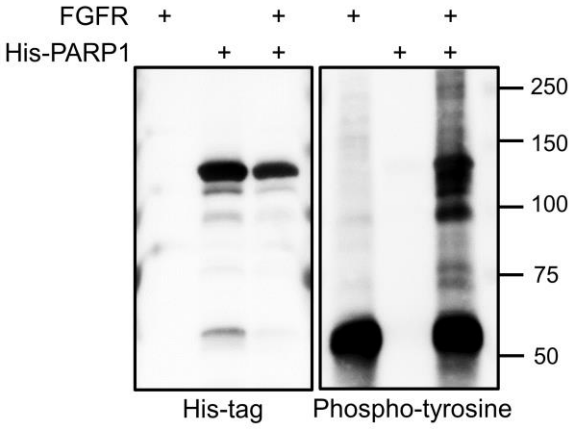

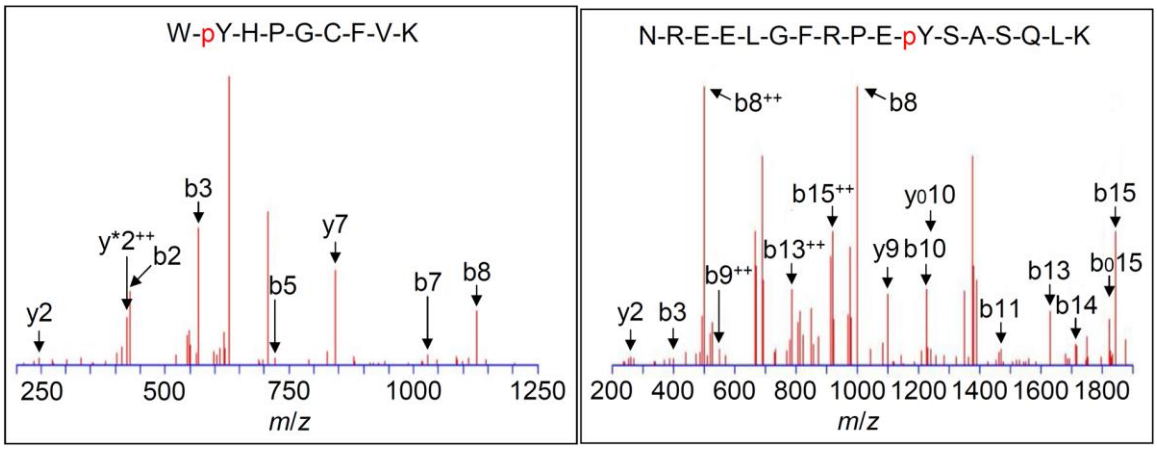

Figure 32. FGFR-mediated tyrosine phosphorylation of PARP1.

His-tagged PARP1 recombinant protein was incubated with activated FGFR kinase domain before half the samples were subjected to Western blotting analysis. Phosphorylated tyrosine residues were detected by antibodies against phospho-tyrosine (clone 4G10, PY20, and PY100) in Western blotting. The other half of the samples were separated on sodium dodecyl sulfate gel, and the p120 protein band was cut from the gel and sent for mass spectrum analysis. Phosphorylated tyrosine residues identified through mass spectrometry were aligned with PARP1 protein sequence and marked in red.

Table 4. Potential FGFR-mediated tyrosine phosphorylation sites on PARP1 predicted by motif scanning database

ID	Position	Code	Kinase	Peptide	Score	Cutoff	Source
PARP1	775	Y	TK	LLDIEVAYSLLRGGS	29.719	29.39	Pred.
PARP1	986	Y	TK	VNDTSLLYNEYIVYD	29.559	29.39	Pred.
PARP1	13	Y	TK/FGFR	DKLYRVEYAKSGRAS	368.288	330.368	Pred.
PARP1	310	Y	TK/FGFR	VFKSDAYYCTGDVTA	414.554	330.368	Pred.
PARP1	344	Y	TK/FGFR	KEFREISYLKKLKVK	681.814	330.368	Pred.
PARP1	689	Y	TK/FGFR	MKKAMVEYEIDLQKM	352.499	330.368	Pred.
PARP1	710	Y	TK/FGFR	KRQIQAAYSILSEVQ	389.106	330.368	Pred.
PARP1	13	Y	TK/FGFR/FGFR1	DKLYRVEYAKSGRAS	8.679	6.479	Pred.
PARP1	176	Y	TK/FGFR/FGFR1	ELGFRPEYSASQLKG	9.111	6.479	Pred.
PARP1	618	Y	TK/FGFR/FGFR1	IEHFMKLYEEKTGNA	6.492	6.479	Pred.
PARP1	710	Y	TK/FGFR/FGFR1	KRQIQAAYSILSEVQ	8.698	6.479	Pred.
PARP1	907	Y	TK/FGFR/FGFR1	MVSKSANYCHTSQGD	9.644	6.479	Pred.
PARP1	848	Y	TK/FGFR/FGFR2	REGECQRYKPFKQLH	1.62	1.409	Pred.
PARP1	9	Y	TK/FGFR/FGFR3	AESSDKLYRVEYAKS	3.61E-07	0.00E+00	Pred.
PARP1	13	Y	TK/FGFR/FGFR3	DKLYRVEYAKSGRAS	2.10E-07	0.00E+00	Pred.
PARP1	52	Y	TK/FGFR/FGFR3	DGKVPHWYHFSCFWK	5.17E-07	0.00E+00	Pred.
PARP1	158	Y	TK/FGFR/FGFR3	LGMIDRWYHPGCFVK	6.03E-07	0.00E+00	Pred.
PARP1	309	Y	TK/FGFR/FGFR3	LVFKSDAYYCTGDVT	7.03E-08	0.00E+00	Pred.
PARP1	310	Y	TK/FGFR/FGFR3	VFKSDAYYCTGDVTA	3.10E-07	0.00E+00	Pred.
PARP1	344	Y	TK/FGFR/FGFR3	KEFREISYLKKLKVK	7.57E-07	0.00E+00	Pred.
PARP1	569	Y	TK/FGFR/FGFR3	IVKGTNSYYKLQLLE	5.06E-07	0.00E+00	Pred.
PARP1	583	Y	TK/FGFR/FGFR3	EDDKENRYWIFRSWG	1.40E-06	0.00E+00	Pred.
PARP1	634	Y	TK/FGFR/FGFR3	HSKNFTKYPKKFYPL	7.25E-07	0.00E+00	Pred.
PARP1	639	Y	TK/FGFR/FGFR3	TKYPKKFYPLEIDYG	2.06E-07	0.00E+00	Pred.
PARP1	689	Y	TK/FGFR/FGFR3	MKKAMVEYEIDLQKM	4.65E-07	0.00E+00	Pred.
PARP1	710	Y	TK/FGFR/FGFR3	KRQIQAAYSILSEVQ	5.98E-07	0.00E+00	Pred.
PARP1	737	Y	TK/FGFR/FGFR3	LDLSNRFYTLIPHDF	2.50E-07	0.00E+00	Pred.
PARP1	775	Y	TK/FGFR/FGFR3	LLDIEVAYSLLRGGS	3.80E-07	0.00E+00	Pred.
PARP1	817	Y	TK/FGFR/FGFR3	EAEIIRKYVKNTHAT	1.35E-07	0.00E+00	Pred.
PARP1	848	Y	TK/FGFR/FGFR3	REGECQRYKPFKQLH	7.45E-07	0.00E+00	Pred.
PARP1	889	Y	TK/FGFR/FGFR3	PEAPVTGYMFGKGIY	8.10E-07	0.00E+00	Pred.
PARP1	907	Y	TK/FGFR/FGFR3	MVSKSANYCHTSQGD	1.06E-06	0.00E+00	Pred.
PARP1	986	Y	TK/FGFR/FGFR3	VNDTSLLYNEYIVYD	9.34E-07	0.00E+00	Pred.
PARP1	1001	Y	TK/FGFR/FGFR3	IAQVNLKYLLKLKFN	2.65E-07	0.00E+00	Pred.
PARP1	710	Y	TK/FGFR/FGFR4	KRQIQAAYSILSEVQ	1.922	1.821	Pred.
PARP1	775	Y	TK/FGFR/FGFR4	LLDIEVAYSLLRGGS	2.11	1.821	Pred.

Motif scanning database GPS 5.0 (http://gps.biocuckoo.cn)

We generated Y-to-phenylalanine (F) mutated PARP1 to mimic un-phosphorylated PARP1 and further examined contributions of these phosphorylation sites to PARP-i resistance and found that $PARP1^{Y158F}$ BR cells had talazoparib IC_{50} lower than that of $PARP1^{WT}$ cells in MTT assay (Fig. 33). However,

PARP1^{Y176F} did not show a significant impact on cell survival compared to PARP1^{WT} in response to talazoparib treatment (Fig. 33).

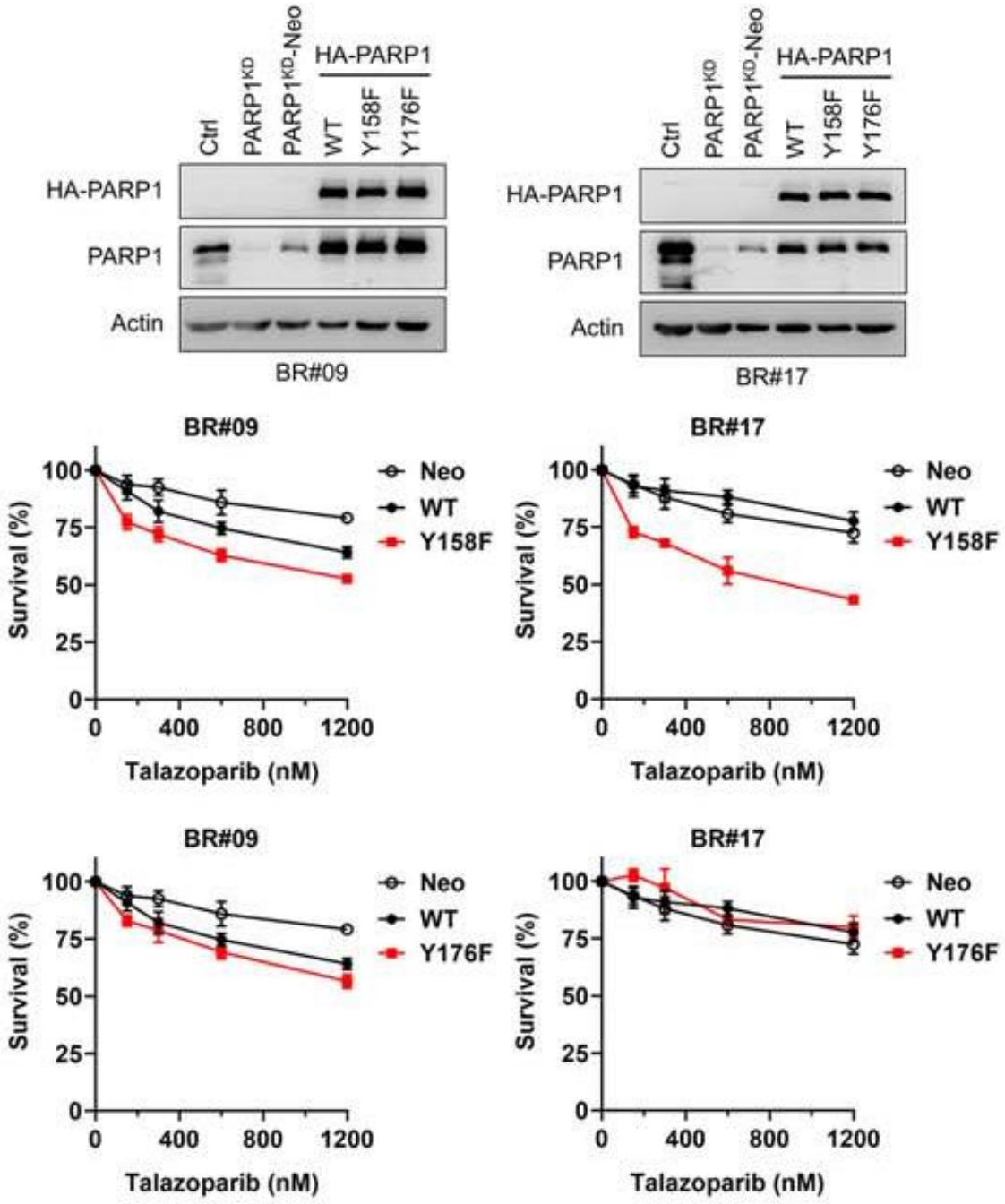

Figure 33. Effect of PARP1Y158F and PARP1Y176F mutants on cell survival in response to talazoparib.

PARP1 knock-down ($PARP1^{KD}$) BR#09 and BR#17 cells were exogenously expressed with hemagglutinin (HA)-tagged vector control (Neo), wild-type PARP1 (WT), and PARP1Y158F and PARP1Y176F mutants as indicated. Exogenous PARP1 expression was examined by Western blotting. Cells were treated with various concentrations of talazoparib for 6 days before cell survival rate was measured by MTT assay.

Using monoclonal antibody against Y158 phosphorylated PARP1 (p-Y158 PARP1), we showed that p-Y158 PARP1 can be diminished by treating BR cell with PD173074 (Fig. 34), and that synergism between talazoparib and PD173074 decreased in BR cells carrying $PARP1^{Y158F}$ mutant (Fig. 35). These results suggest the p-Y158-mediated cellular functions can indeed be inhibited by FGFR inhibition and contribute to FGFR-mediated PARP-i-resistance. Thus, we focused on studying DDR alteration between $PARP1^{WT}$ and $PARP1^{Y158F}$ mutants.

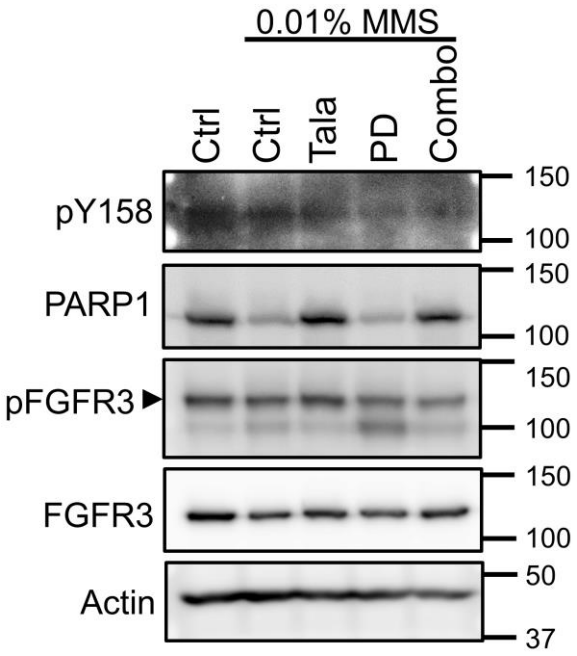

Figure 34. PARP1 Y158 phosphorylation can be inhibited by PD173074.
BR#17 cells were treated with MMS, 100 nM talazoparib (Tala), and 10 μM PD173074 (PD) as indicated before harvested for Western blotting analysis to detect p-Y158 PARP1 (pY158), PARP1, phosphorylated FGFR3 (pFGFR3), FGFR3, and actin.

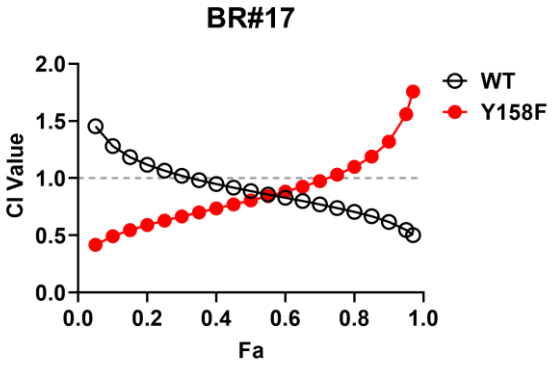

Figure 35. Synergism between talazoparib and PD173074 is affected by PARP1 Y158 phosphorylation.
CI of talazoparib and PD173074 in BR#17 cells expressing wild-type PARP1 (WT) or PARP1Y158F mutant (Y158F) with 6-day MTT assays.

We found that MMS is still capable of increasing PARylation signals in both PARP1^{WT} and PARP1^{Y158F} expressing BR cells and that PARP1^{WT} and PARP1^{Y158F} cells had similar PARP1 expression and PAR signals (Fig. 36), suggesting that PARylation activity of PARP1 is not compromised, and that PARP-i-resistance mediated by p-Y158 PARP1 does not positively correlate with PARP1 enzymatic activity.

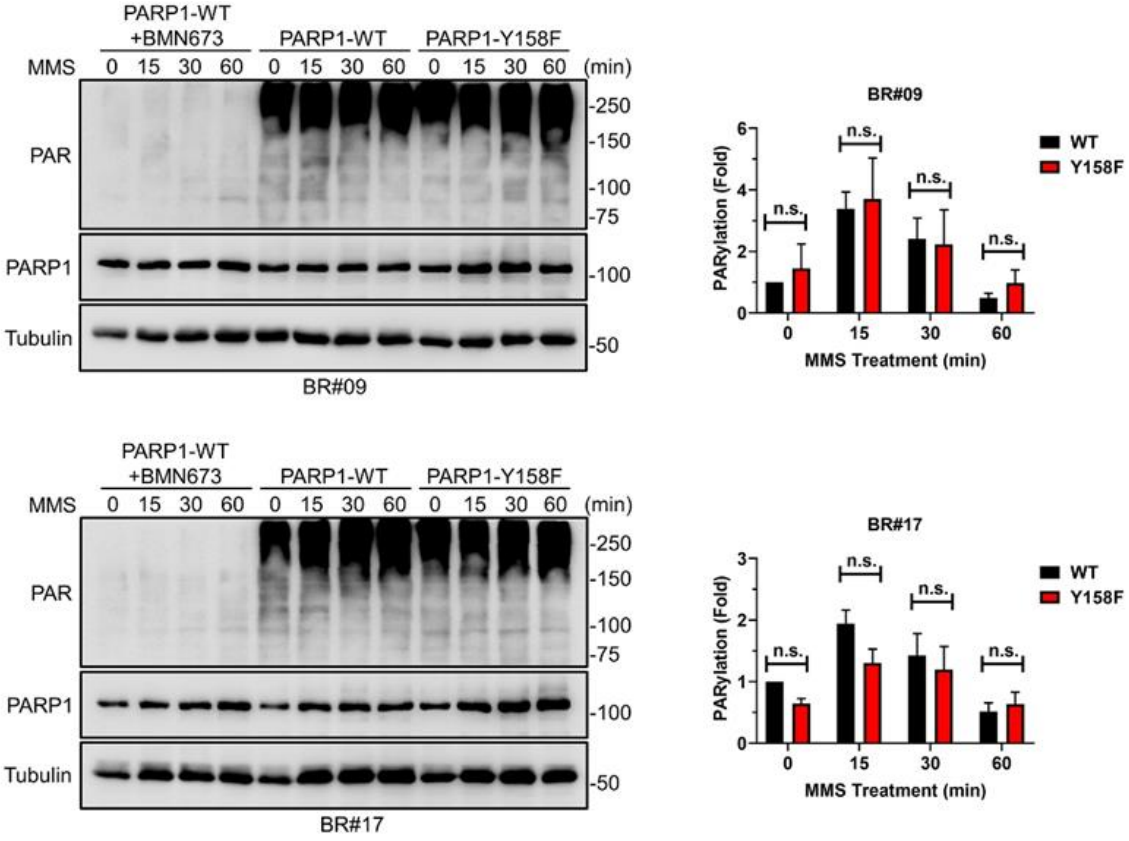

Figure 36. PARP1 Y158F mutant does not affect MMS-induced PARylation in BR cells.

BR#09 and BR#17 cells expressing either wild-type PARP1 (PARP1-WT) or PARP1^{Y158F} mutant were treated with 0.01% MMS for 1 h. PARP1 expression, PARylation (PAR), and tubulin were detected by Western blotting. PAR signal

intensity were normalized to tubulin signal intensity before compared to treated groups to wild-type PARP1 expressing cells treated with MMS (1-fold). Histograms show the mean ± S.D. from 3 independent repeats.

Therefore, we further examined the effect of p-Y158 PARP1 on PARP trapping. We found that more PARP1 was bound to chromatin in PARP1^{Y158F}-expressing cells than in PARP1^{WT}-expressing cells (Fig. 37), supporting our hypothesis that FGFR3 mediates PARP-i resistance by phosphorylating PARP1 at the Y158 residue.

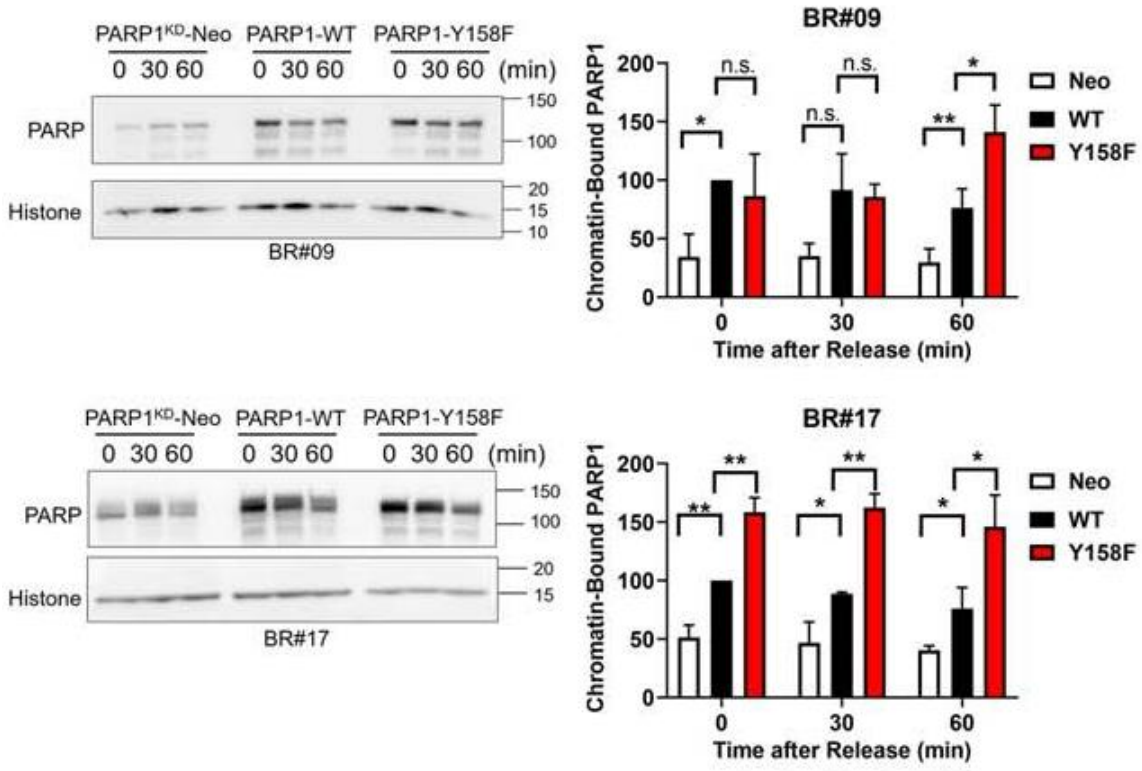

Figure 37. Effect of PARP1Y158F on PARP-trapping.

PARP1 knock-down cells expressing vector, wild-type PARP1, and PARP1Y158F mutants were treated with 100 nM talazoparib and 0.01% MMS for 40 min. Cells were harvested after removal of talazoparib and MMS for 0, 30, or 60 min and subjected to cell fractionation. Chromatin-bound PARP1 was then analyzed by Western blotting. PARP1 signal intensities were normalized to histone H4 and compared with that of PARP1 wild-type cells treated with talazoparib and MMS (PARP1-WT, 0 min). Mean ± S.D. from 3-5 individual repeats were shown in histogram and analyzed with ANOVA.

Moreover, we found that PD173074 can also prolonged talazoparib-induced PARP1 trapping in BR cells (Fig. 38). Therefore, we concluded that FGFR3 mediates PARP-i-resistance through phosphorylating PARP1 at Y158 residue to decrease PARP trapping caused by PARP-is.

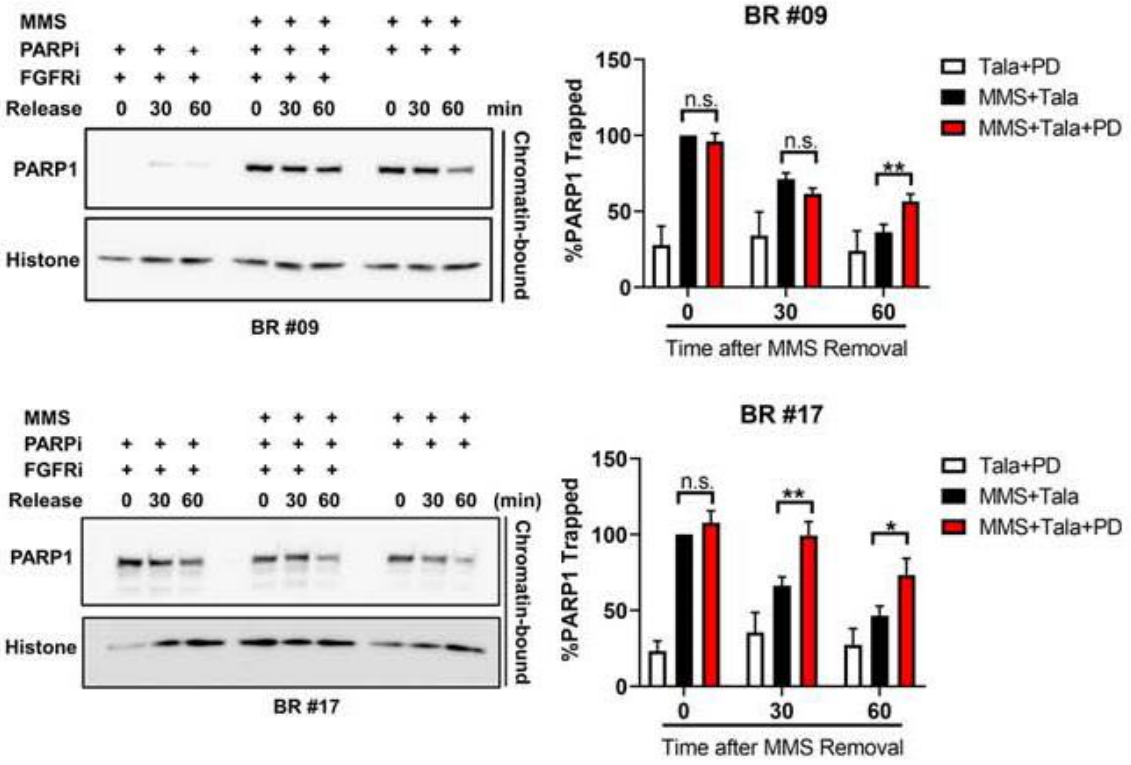

Figure 38. Effect of PD173074 on PARP-trapping.

As indicated, cells were pre-treated with 10 μM PD173074 for at least 2 h in FGFRi treated groups before treatment of 100 nM talazoparib and 0.01% MMS for another 40 min. Cells were harvested after removal of MMS and talazoparib for 0, 30, or 60 min and subjected to cell fractionation. Chromatin-bound PARP1 was then analyzed by Western blotting. PARP1 signal intensities were normalized to histone H4 and compared with that of cells treated with talazoparib and MMS (MMS +, PARPi +, FGFRi +, 0 min). Mean ± S.D. from 3-5 individual repeats were shown in histogram and analyzed with ANOVA.

5. Clinical application potent of targeting FGFR in PARPi-resistant TNBC

Xenograft mouse models with BR cells were employed to validate synergism of FGFR-i and PARP-i *in vivo.* Talazoparib treatment inhibited tumor

growth in the SUM149 model but not in BR#09 or BR#17 models (Fig. 39), confirming that BR cells remain PARP-i resistant in mouse models.

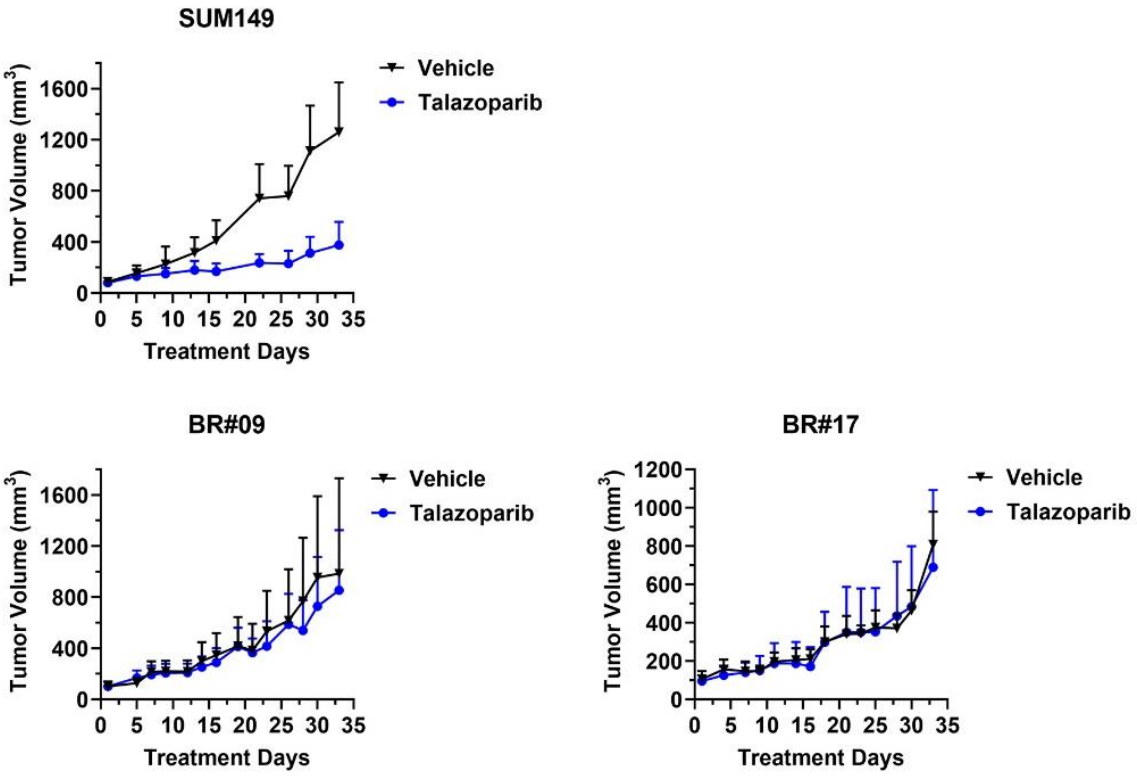

Figure 39. Talazoparib inhibits tumor growth in SUM149, but not in BR xenograft mouse models.

Two millions of SUM149, BR#09 and BR#17 cells were injected to the mammary fat pad of nude mice. Vehicle and talazoparib (0.25 m/k/d) daily treatment began at the time that the tumors reached an average size of 100 mm^3. For each model, 4-5 mice were included in each treatment group, and the figures show mean and S.D. of the tumors for 33 days of treatment.

For each inhibitor used in mouse treatment, concentration similar to or lower than those of the equivalent recommended dose for human [211-214]. As shown in both BR#09 and BR#17 xenograft mouse models, olaparib did not inhibit tumor growth as vehicle treatment, and AZD4547 slightly inhibited tumor growth only in BR#17 (p-value = 0.0192 at day 57). However, the combination of olaparirb and AZD4547 significantly inhibited tumor growth in both models (For BR#09, p-value < 0.0001 compared to vehicle and single agent treatments; for BR#17, p-value = 0.0046 compared to AZD4547 and p-value < 0.0001 to vehicle and olaparib treatment) (Fig. 40). Therefore, combination of olaparib and AZD4547 prolonged animal survival in both models (Fig. 40). Meanwhile, animal weight loss was not observed in both models (Fig. 40), suggesting the toxicity is tolerable during the treatment.

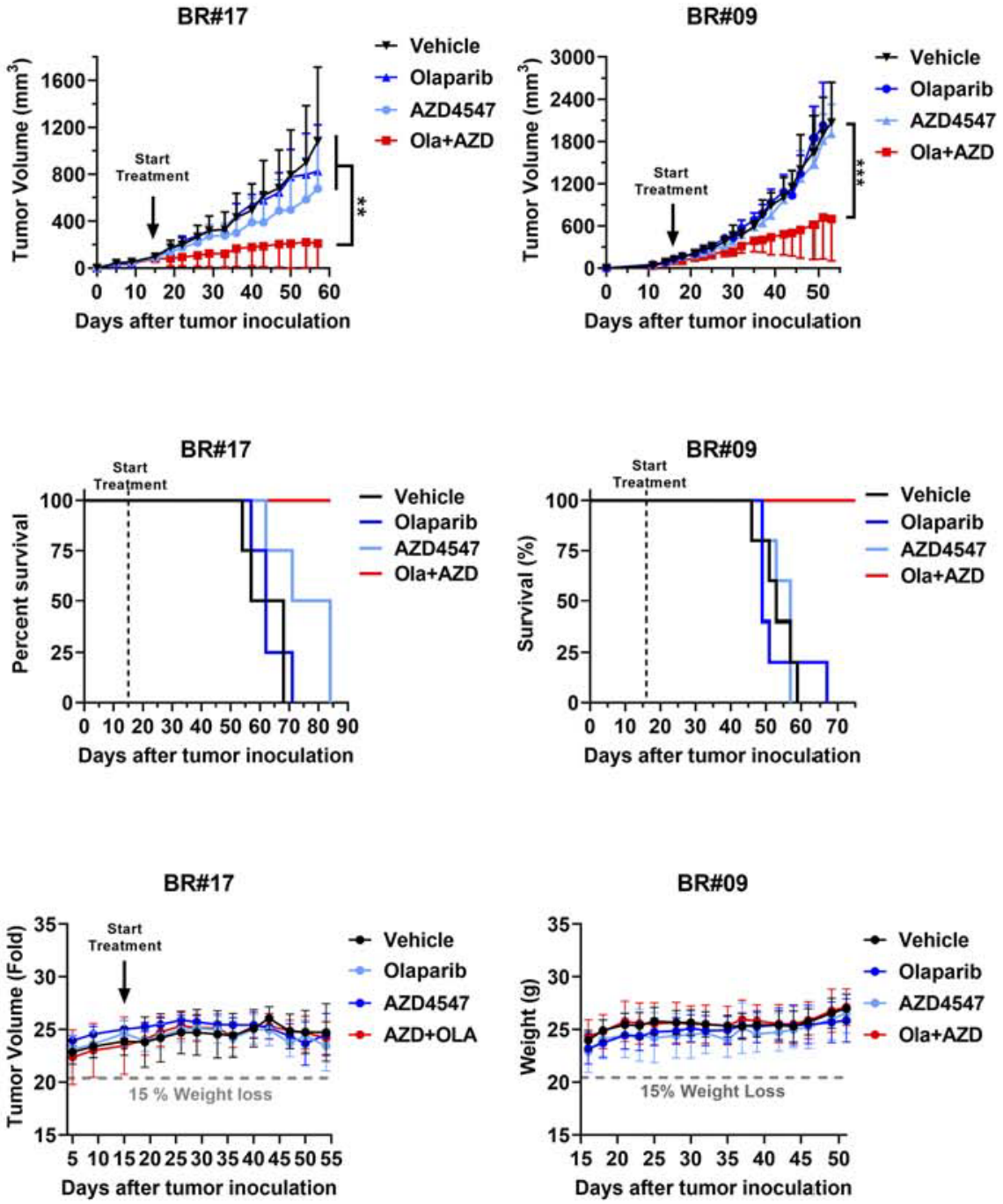

Figure 40. Synergy of FGFR-i and PARP-i in xenograft models.

BR#09 (n=5) and BR#17 (n=4) xenograft mouse models were treated with vehicle, olaparib (40 m/k/d), AZD4547 (8 m/k/d) either alone or in combination through oral gavage. Tumor volumes were measured at least twice a week and statistical analysis were performed using ANOVA (Upper panel). Survival days

of xenograft mouse models treated with olaparib and AZD4547 as described (Middle panel). Body weight (g) of mice treated (Lower panel).

Since PD173074 has not been investigated in clinical trial, we titrated its concentration for animal use by treating BR#09 xenograft mice with either 10 mg/kg/d or 20 mg/kg/d PD173074 with or without talazoparib. With tumors harvested after 3 days of treatments, we found that talazoparib induced FGFR3 phosphorylation, and the talazopairib-induced FGFR phosphorylation were inhibited by PD173074 at 10 mg/kg/d, and was inhibited further by 20 mg/kg PD173074 to less than the basal levels in the vehicle-treated control group (Fig. 41). However, 1/3 of mice treated with 20 mg/kg PD173074 combined with talazoparib experienced more than 10% weight loss (Fig. 41). Therefore, we chose 15 mg/kg/d PD173074 for our further animal studies to ensure FGFR inhibition while minimizing toxicity.

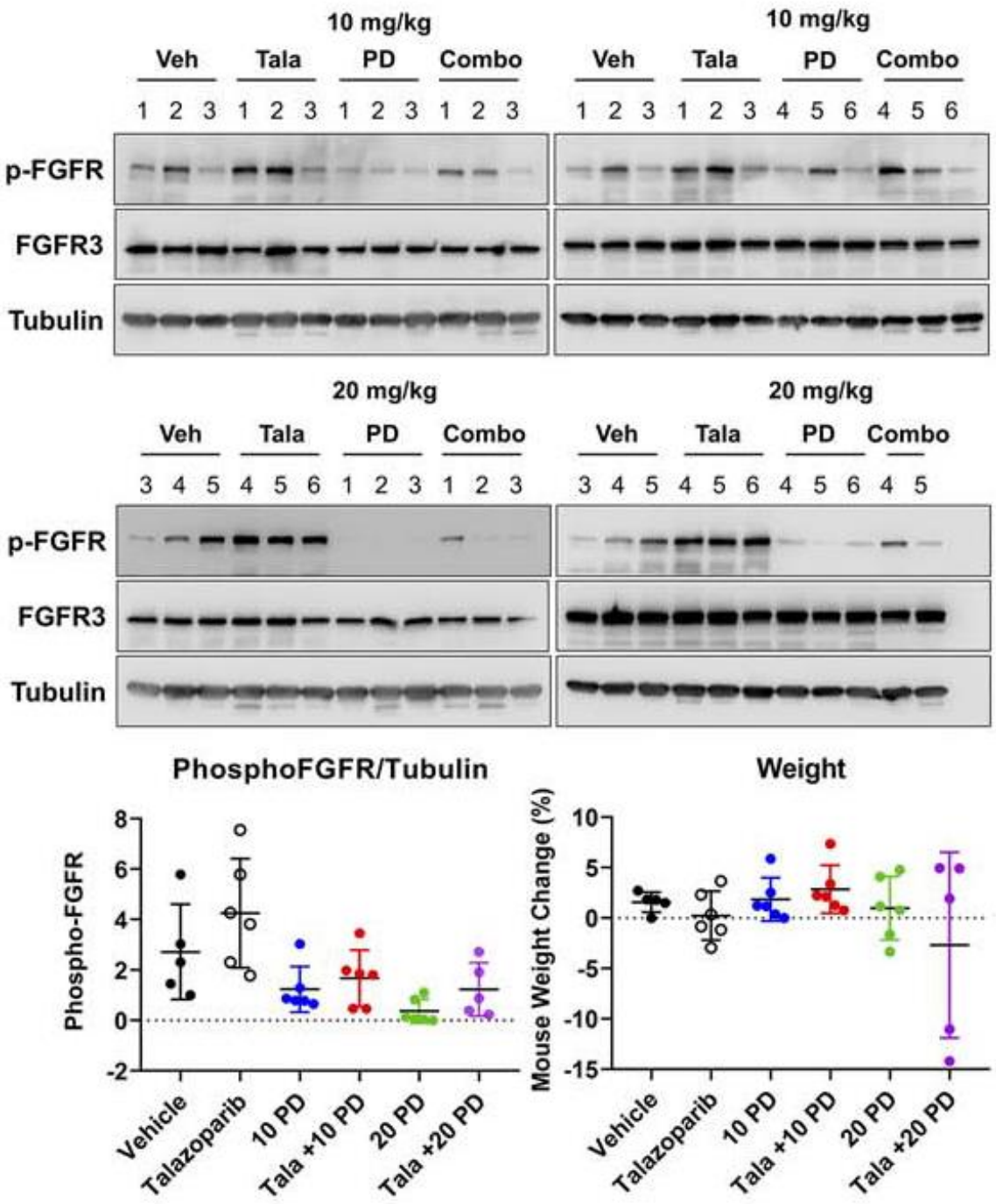

Figure 41. PD173074 treatment dose titration in xenograft mouse model. BR#09 xenograft mice (5-6 mice per group) were treated with PD173074 at 10 mg/kg or 20 mg/kg daily for 3 days before tumors were harvested for Western blotting analysis. Signal intensities of phosphorylated FGFR (p-FGFR) were normalized to that of tubulin and compared with the mean intensity in a vehicle-

treated group and shown in the quantitation panel (mean ± S.D.). Mouse body weight change (mean ± S.D.) after treatment was normalized to that of the mouse before treatment.

As expected, talazoparib and PD173074 single agent treatments did not inhibit tumor growth in both BR#09 and BR#17 models, while the combination of talazoparib and PD173074 significantly inhibited tumor growth (p-value < 0.0001 in both models) and prolonged animal survival (Fig 42).

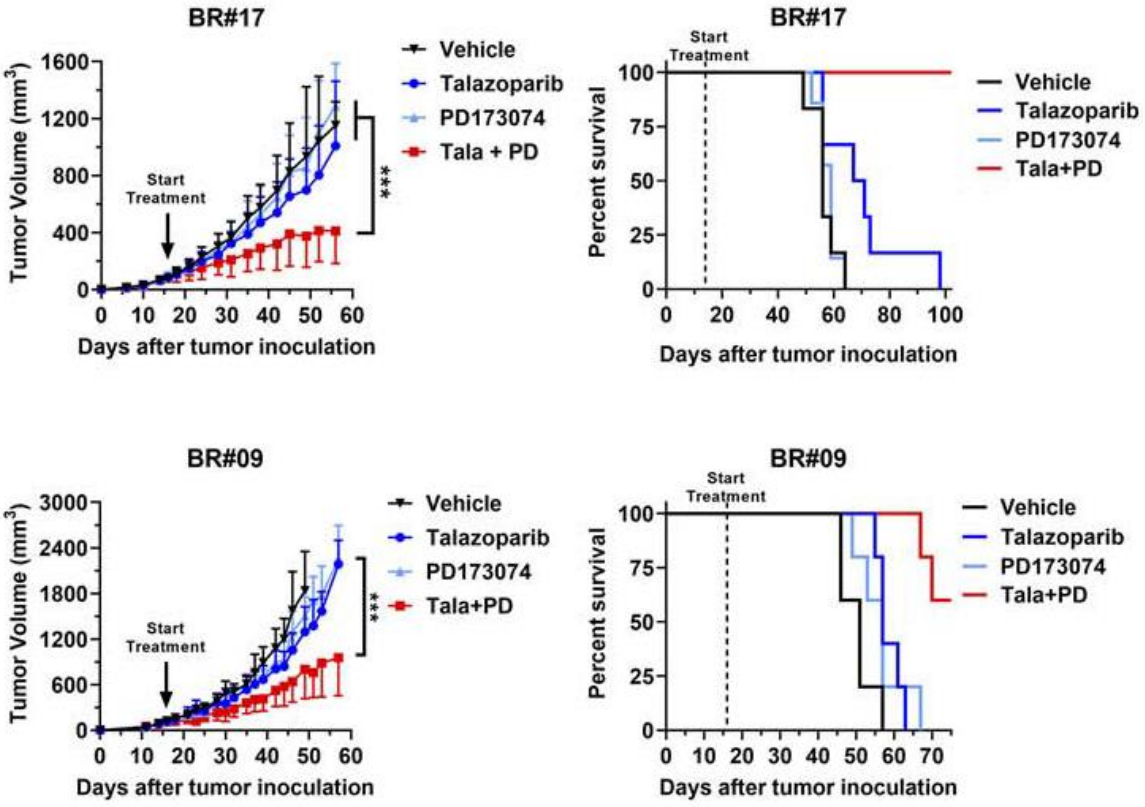

Figure 42. Combination of talazoparib and PD173074 suppress tumor growth and prolongs survival of BR xenograft mouse models.

Tumor growth and survival of the BR#09 (n=5) and BR#17 (n=6) xenograft models in response to talazoparib (0.25 m/k/d) and PD173074 (15 m/k/d) alone or in combination through oral gavage. Tumor volumes were measured 2-3 times every week.

To investigate the toxicity of the talazoparib and PD173074 combination, we chose the syngeneic 4T1 model to test the effects of talazoparib and PD173074 alone and in combination. In the 4T1 mice, the talazoparib and PD173074 combination inhibited tumor growth more than the talazoparib and PD173074 single-agent treatments did for two weeks of treatment before mice were sacrificed for toxicity tests. Blood chemical tests showed that the blood urea nitrogen (BUN), alanine aminotransferease (ALT), and aspartate aminotransferase (AST) levels in these animals were within the range of normal Balb/c mice (Fig. 43), indicating that the kidney and liver functions of these mice were not damaged by the treatments.

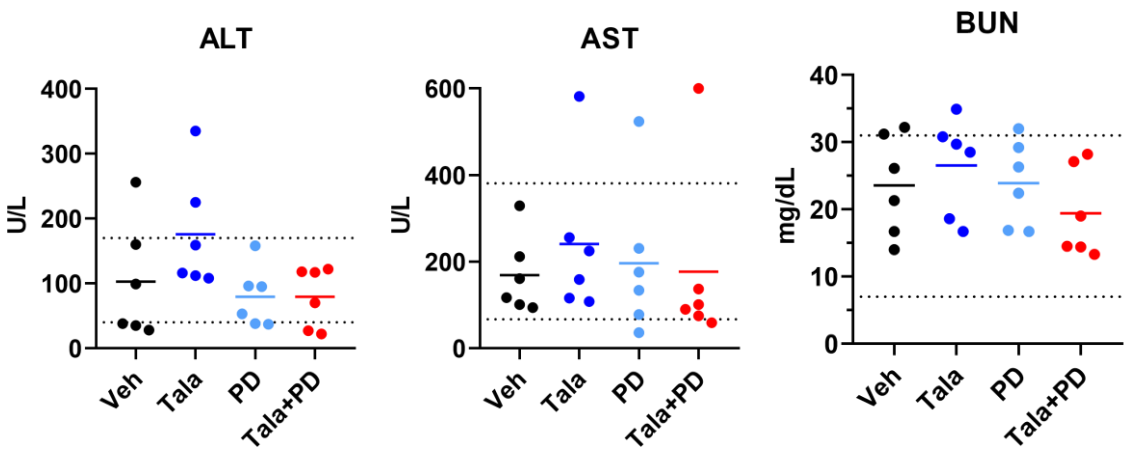

Figure 43. Blood chemical test of 4T1 mouse treated with talazoparib and PD173074.

Blood were collected by cardiac puncture after 12 days of treatment, and the concentrations of alanine aminotransferase (ALT), aspartate aminotransferase (AST), and blood urea nitrogen (BUN) were measured. Dot lines indicate the concentration of ALT, AST and BUN reported in North American colonies of Charles river BALC/C mouse (https://animalab.eu/sites/all/pliki/produkty-dopobrania/balb_c_Mouse_clinical_pathology_data.pdf).

As PARP-is are approved as maintenance therapy for platinum drug-sensitive tumors and the PARP-is shared similar resistance mechanisms with platinum resistance, we collected patient-derived xenograft (PDX) models with known PARP-is or platinum resistance as PARP-is are recently approved for breast cancer and there are limited breast cancer patients treated with long-term PARP-is. We further correlated p-FGFR signals to talazoparib resistance and platinum resistance using tissues of patient-derived xenograft (PDX) models developed from TNBC patients [202]. In 13 TNBC PDX tissues' IHC staining, we

found that talazoparib and platinum resistant PDX models has a slightly higher H-score of p-FGFR (H-score 251.4 ± 51.1) than the sensitive models (p-FGFR H-score 191.7 ± 48.6, p-value 0.0862) (Fig. 44).

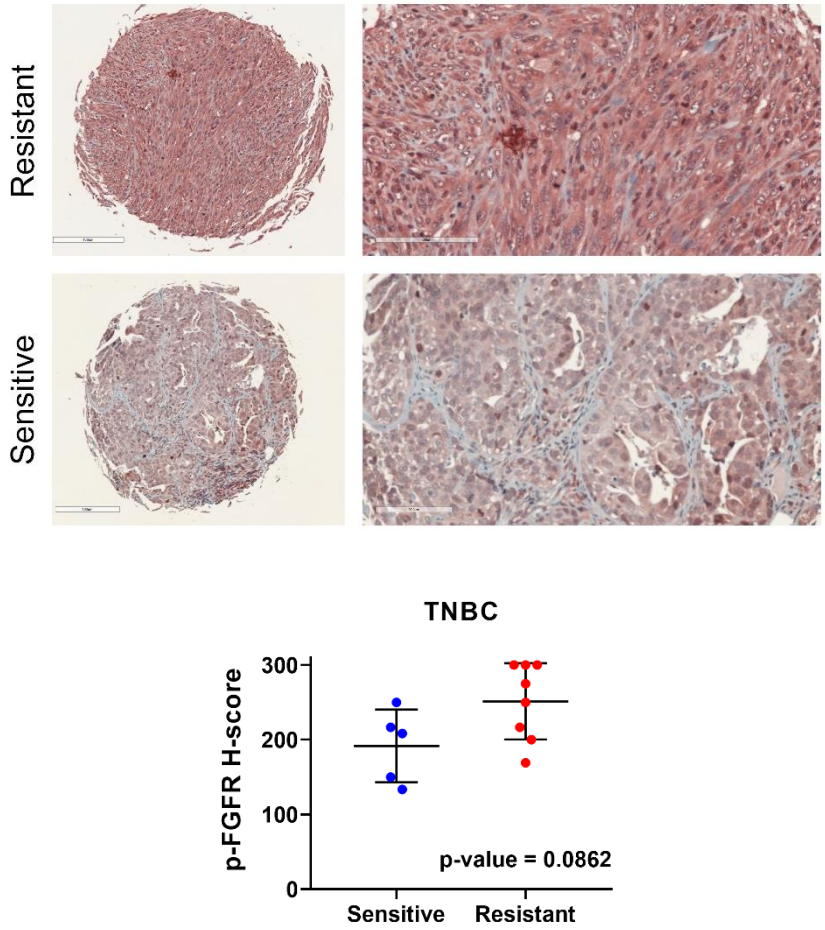

Figure 44. Immunohistochemistry staining of phosphorylated FGFR in TNBC PDX tumors.

TNBC PDX tissue microarray was collected by Dr. Coya Tapia and the response of these PDX models to talazoparib and platinum agents were performed by laboratory of Dr. Funda Meric-Bernstam . Immunohistochemistry staining and H-

score calculation was performed by Dr. Weiya Xia. The statistical p-value is calculated using Mann-Whitney test (two-tailed) in GraphPad Prism 8.

Moreover, we also found significant higher of p-FGFR H-score in platinum resistant ovarian cancer PDX models (H-score 186.5 ± 49.6) than the sensitive models (H-score 120.0 ± 13.9, p-value 0.0093) (Fig. 45).This correlation suggests that p-FGFR and p-Y158 PARP1 have the potential to serve as biomarkers in indicating patients with FGFR-mediated PARP-i-resistance.

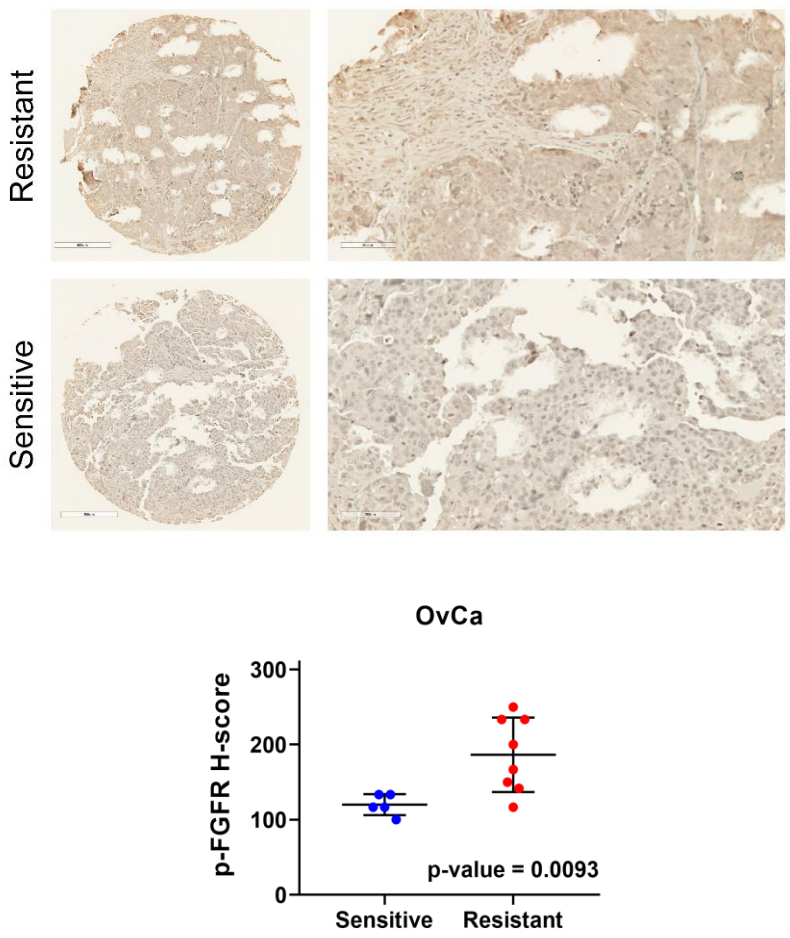

Figure 45. Immunohistochemistry staining of phosphorylated FGFR in Ovarian Cancer PDX tumors.

Ovarian cancer PDX tissue microarray was collected, and the patient responses to platinum agents were provided by laboratory of by Dr. Jinsong Liu. Immuno-histochemistry staining and H-score calculation was performed by Dr. Weiya Xia. The statistical p-value is calculated using Mann-Whitney test (two-tailed) in GraphPad Prism 8.

Chapter IV. Discussion

In this study, we concluded that inhibition of FGFR3 reinstates PARP-i sensitivity through prolonging PARP trapping. We found FGFR phosphorylates PARP1 at Y158 amino acid, and that PARP1 Y158 non-phosphorylated mutant ($PARP1^{Y158F}$) was trapped longer than $PARP1^{WT}$ in BR cells, indicating this FGFR-mediated PARP1 phosphorylation contributes to resolve PARP trapping in these cells. The prolonged PARP trapping decreases efficiency of DNA repair and hence increase DNA damage burden in cells. We also demonstrated that FGFR-i and PARP-i synergistically inhibit growth of tumor cells in animal models, and that the toxicity of combination is manageable. Furthermore, using PDX models, we showed that p-FGFR and p-Y158 PARP1 can serve as biomarkers for stratifying patients for FGFR-i and PARP-i combination treatment.

Previous artificial introduced CRISPR-Cas9 mutagenesis screen study showed that PARP1 ZF1 domain F44I mutation contributes to PARP-i-resistance because it is spared from PARP trapping [215]. Since structural studies showed that ZF1 and ZF2 domains form a functional unit to recognize DNA strand break [159], Y158F mutation-induced prolong of PARP trapping may be explained from aspect of protein conformation. Structurally, Y158 amino acid locates adjacent to PARP1 ZF2 domain's zinc ion binding residues (C125, C128, H159 and C162) and the DNA interacting residues (L151/I156)[216, 217], indicating that Y158 may also involve in protein structure stabilization. Therefore, there is possibility that p-Y158 PARP1 disrupts the dissociation of PARP1 from DNA by altering the structural stability of the PARP1 dimer. This protein structure aspect can also provide a reason for our finding that Y176F mutation did not enhance PARP-i sensitivity, because Y176 locates away

from DNA binding core residues. However, detailed studies regarding impacts of p-Y158 on PARP1 conformation and dimerization should be further pursued.

We previously reported that MET also contributes to PARP inhibitor resistance through phosphorylating PARP1[157]. However, FGFR3 and MET phosphorylate PARP1 at different domains, and thus, the two RTKs have different impacts on DDR and may enhance therapeutic efficacies of PARP-is in different patient populations. MET phosphorylates $PARP1^{Y907}$ at catalytic domain, and thus increasing PARP1 enzymatic activity while decreasing interaction between PARP-i and PARP1[157]. In contrast, we found that inhibition of FGFR decreases solving of PARP-trapping through phosphorylate $PARP1^{Y158}$ at DNA-binding domain, but this p-Y158 PARP1 has similar enzymatic activity to its non-phosphorylated mutant ($PARP1^{Y158F}$). Therefore, we deduced that FGFR-i and PARP-i combination will benefit patients bearing tumors that solve PARP-i-induced PARP trapping efficiently, and that combination of MET inhibitor and PARP-is will benefit patients carrying tumors in which PARP-is failed to inhibit PARP1 enzymatic activity. We further FGFR-is may be more suitable that MET inhibitors in the PARP-is combination strategies for patients with acquired resistance to PARP trapping-inducing PARP-is such as talazoparib and olaparib. In the future, we aim on developing efficient p-Y158 PARP1 and p-FGFR screening method and promoting targeted PARP-i combination therapeutic strategies using the biomarker-kinase pairs we discovered as references to guide personalized PARP-i therapy in cancer treatment.

Appendix

1. Plasmid Map and Sequence of pCDH-EF1-HA-PARP1-Neo

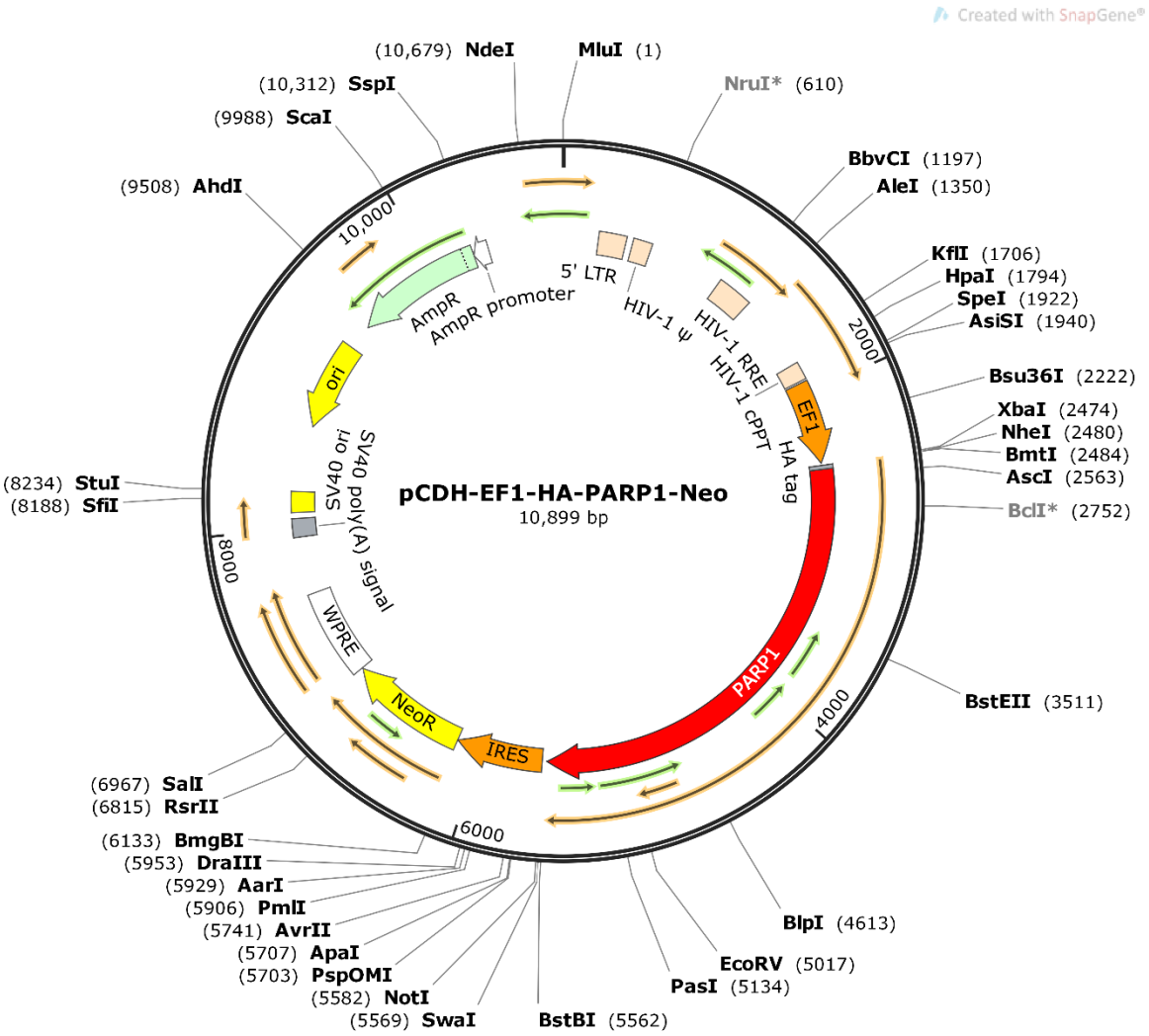

Amino Acid Sequence of HA-PARP1

(GenBank: AAH37545.1)

Met Y P Y D V P D Y A A E S S D K L Y R V E Y A K S G R A S C K K C S E S I P K D S L R Met A I Met V Q S P Met F D G K V P H W Y H F S C F W K V G H S I R H P D V E V D G F S E L R W D D Q Q K V K K T A E A G G V T G K G Q D G I G S K

A E K T L G D F A A E Y A K S N R S T C K G C Met E K I E K G Q V R L S K K Met V

D P E K P Q L G Met I D R W Y H P G C F V K N R E E L G F R P E Y S A S Q L K

G F S L L A T E D K E A L K K Q L P G V K S E G K R K G D E V D G V D E V A K K K

S K K E K D K D S K L E K A L K A Q N D L I W N I K D E L K K V C S T N D L K E L L

I F N K Q Q V P S G E S A I L D R V A D G Met V F G A L L P C E E C S G Q L V F K

S D A Y Y C T G D V T A W T K C Met V K T Q T P N R K E W V T P K E F R E I S Y L

K K L K V K K Q D R I F P P E T S A S V A A T P P P S T A S A P A A V N S S A S A

D K P L S N Met K I L T L G K L S R N K D E V K A Met I E K L G G K L T G T A N K A

S L C I S T K K E V E K Met N K K Met E E V K E A N I R V V S E D F L Q D V S A S T

K S L Q E L F L A H I L S P W G A E V K A E P V E V V A P R G K S G A A L S K K S

K G Q V K E E G I N K S E K R Met K L T L K G G A A V D P D S G L E H S A H V L E

K G G K V F S A T L G L V D I V K G T N S Y Y K L Q L L E D D K E N R Y W I F R S

W G R V G T V I G S N K L E Q Met P S K E D A I E H F Met K L Y E E K T G N A W H

S K N F T K Y P K K F Y P L E I D Y G Q D E E A V K K L T V N P G T K S K L P K P

V Q D L I K Met I F D V E S Met K K A Met V E Y E I D L Q K Met P L G K L S K R Q I

Q A A Y S I L S E V Q Q A V S Q G S S D S Q I L D L S N R F Y T L I P H D F G Met K

K P P L L N N A D S V Q A K A E Met L D N L L D I E V A Y S L L R G G S D D S S K

D P I D V N Y E K L K T D I K V V D R D S E E A E I I R K Y V K N T H A T T H N A Y

D L E V I D I F K I E R E G E C Q R Y K P F K Q L H N R R L L W H G S R T T N F A

G I L S Q G L R I A P P E A P V T G Y Met F G K G I Y F A D Met V S K S A N Y C H T

S Q G D P I G L I L L G E V A L G N Met Y E L K H A S H I S K L P K G K H S V K G L

G K T T P D P S A N I S L D G V D V P L G T G I S S G V N D T S L L Y N E Y I V Y D

I A Q V N L K Y L L K L K F N F K T S L W Stop

HA Tag-ZnF1-ZnF2-NLS-ZnF3-BRCT-WGR-PARP a-helical-Catalytic Domain

Met: M, Methionine

Y: Phospho-tyrosine detected by mass spectrometry

Bibliography

1. Prat A, Pineda E, Adamo B, Galvan P, Fernandez A, Gaba L, Diez M, Viladot M, Arance A, Munoz M: **Clinical implications of the intrinsic molecular subtypes of breast cancer**. *Breast* 2015, **24 Suppl 2**:S26-35.
2. Russnes HG, Lingjaerde OC, Borresen-Dale AL, Caldas C: **Breast Cancer Molecular Stratification: From Intrinsic Subtypes to Integrative Clusters**. *Am J Pathol* 2017, **187**(10):2152-2162.
3. Onitilo AA, Engel JM, Greenlee RT, Mukesh BN: **Breast cancer subtypes based on ER/PR and Her2 expression: comparison of clinicopathologic features and survival**. *Clin Med Res* 2009, **7**(1-2):4-13.
4. Parise CA, Bauer KR, Brown MM, Caggiano V: **Breast cancer subtypes as defined by the estrogen receptor (ER), progesterone receptor (PR), and the human epidermal growth factor receptor 2 (HER2) among women with invasive breast cancer in California, 1999-2004**. *Breast J* 2009, **15**(6):593-602.
5. Fokter Dovnik N, Dovnik A, Cas Sikosek N, Ravnik M, Arko D, Takac I: **Prognostic Role of HER2 Status and Adjuvant Trastuzumab Treatment in Lymph Node-Negative Breast Cancer Patients - a Retrospective Single Center Analysis**. *Breast Care (Basel)* 2016, **11**(6):406-410.
6. Menard S, Fortis S, Castiglioni F, Agresti R, Balsari A: **HER2 as a prognostic factor in breast cancer**. *Oncology* 2001, **61 Suppl 2**:67-72.

7. Sapino A, Goia M, Recupero D, Marchio C: **Current Challenges for HER2 Testing in Diagnostic Pathology: State of the Art and Controversial Issues**. *Front Oncol* 2013, **3**:129.

8. Aysola K, Desai A, Welch C, Xu J, Qin Y, Reddy V, Matthews R, Owens C, Okoli J, Beech DJ *et al*: **Triple Negative Breast Cancer - An Overview**. *Hereditary Genet* 2013, **2013**(Suppl 2).

9. Schneider R, Barakat A, Pippen J, Osborne C: **Aromatase inhibitors in the treatment of breast cancer in post-menopausal female patients: an update**. *Breast Cancer (Dove Med Press)* 2011, **3**:113-125.

10. Tong CWS, Wu M, Cho WCS, To KKW: **Recent Advances in the Treatment of Breast Cancer**. *Front Oncol* 2018, **8**:227.

11. Carey L, Winer E, Viale G, Cameron D, Gianni L: **Triple-negative breast cancer: disease entity or title of convenience?** *Nat Rev Clin Oncol* 2010, **7**(12):683-692.

12. Garrido-Castro AC, Lin NU, Polyak K: **Insights into Molecular Classifications of Triple-Negative Breast Cancer: Improving Patient Selection for Treatment**. *Cancer Discov* 2019, **9**(2):176-198.

13. Yeo SK, Guan JL: **Breast Cancer: Multiple Subtypes within a Tumor?** *Trends Cancer* 2017, **3**(11):753-760.

14. Molyneux G, Geyer FC, Magnay FA, McCarthy A, Kendrick H, Natrajan R, Mackay A, Grigoriadis A, Tutt A, Ashworth A *et al*: **BRCA1 basal-like breast cancers originate from luminal epithelial progenitors and not from basal stem cells**. *Cell Stem Cell* 2010, **7**(3):403-417.

15. Inic Z, Zegarac M, Inic M, Markovic I, Kozomara Z, Djurisic I, Inic I, Pupic G, Jancic S: **Difference between Luminal A and Luminal B Subtypes According to Ki-67, Tumor Size, and Progesterone Receptor Negativity Providing Prognostic Information**. *Clin Med Insights Oncol* 2014, **8**:107-111.

16. Lemmon MA, Schlessinger J: **Cell signaling by receptor tyrosine kinases**. *Cell* 2010, **141**(7):1117-1134.

17. Favelyukis S, Till JH, Hubbard SR, Miller WT: **Structure and autoregulation of the insulin-like growth factor 1 receptor kinase**. *Nature structural biology* 2001, **8**(12):1058-1063.

18. Furdui CM, Lew ED, Schlessinger J, Anderson KS: **Autophosphorylation of FGFR1 kinase is mediated by a sequential and precisely ordered reaction**. *Molecular cell* 2006, **21**(5):711-717.

19. Honegger AM, Kris RM, Ullrich A, Schlessinger J: **Evidence that autophosphorylation of solubilized receptors for epidermal growth factor is mediated by intermolecular cross-phosphorylation**. *Proceedings of the National Academy of Sciences of the United States of America* 1989, **86**(3):925-929.

20. Cobb MH, Sang BC, Gonzalez R, Goldsmith E, Ellis L: **Autophosphorylation activates the soluble cytoplasmic domain of the insulin receptor in an intermolecular reaction**. *The Journal of biological chemistry* 1989, **264**(31):18701-18706.

21. Krauss G: **Biochemistry of Signal Transduction and Regulation**. In., 5th edn. Hoboken: Wiley; 2014: 1 online resource (845 p.).

22. Volinsky N, Kholodenko BN: **Complexity of receptor tyrosine kinase signal processing**. *Cold Spring Harbor perspectives in biology* 2013, **5**(8):a009043.

23. Carpenter G, Liao HJ: **Receptor tyrosine kinases in the nucleus**. *Cold Spring Harbor perspectives in biology* 2013, **5**(10):a008979.

24. Wang YN, Hung MC: **Nuclear functions and subcellular trafficking mechanisms of the epidermal growth factor receptor family**. *Cell & bioscience* 2012, **2**(1):13.

25. Liccardi G, Hartley JA, Hochhauser D: **EGFR nuclear translocation modulates DNA repair following cisplatin and ionizing radiation treatment**. *Cancer research* 2011, **71**(3):1103-1114.

26. Jaganathan S, Yue P, Paladino DC, Bogdanovic J, Huo Q, Turkson J: **A functional nuclear epidermal growth factor receptor, SRC and Stat3 heteromeric complex in pancreatic cancer cells**. *PloS one* 2011, **6**(5):e19605.

27. Lee HJ, Lan L, Peng G, Chang WC, Hsu MC, Wang YN, Cheng CC, Wei L, Nakajima S, Chang SS *et al*: **Tyrosine 370 phosphorylation of ATM positively regulates DNA damage response**. *Cell research* 2015.

28. Kuo HY, Huang YS, Tseng CH, Chen YC, Chang YW, Shih HM, Wu CW: **PML represses lung cancer metastasis by suppressing the nuclear EGFR-mediated transcriptional activation of MMP2**. *Cell cycle* 2014, **13**(19):3132-3142.

29. Traynor AM, Weigel TL, Oettel KR, Yang DT, Zhang C, Kim K, Salgia R, Iida M, Brand TM, Hoang T *et al*: **Nuclear EGFR protein expression predicts poor survival in early stage non-small cell lung cancer**. *Lung cancer* 2013, **81**(1):138-141.

30. Coleman SJ, Chioni AM, Ghallab M, Anderson RK, Lemoine NR, Kocher HM, Grose RP: **Nuclear translocation of FGFR1 and FGF2 in pancreatic stellate cells facilitates pancreatic cancer cell invasion**. *EMBO molecular medicine* 2014, **6**(4):467-481.

31. Chioni AM, Grose R: **FGFR1 cleavage and nuclear translocation regulates breast cancer cell behavior**. *The Journal of cell biology* 2012, **197**(6):801-817.

32. Hadzisejdic I, Mustac E, Jonjic N, Petkovic M, Grahovac B: **Nuclear EGFR in ductal invasive breast cancer: correlation with cyclin-D1 and prognosis**. *Modern pathology : an official journal of the United States and Canadian Academy of Pathology, Inc* 2010, **23**(3):392-403.

33. El-Sayed A, Harashima H: **Endocytosis of gene delivery vectors: from clathrin-dependent to lipid raft-mediated endocytosis**. *Molecular therapy : the journal of the American Society of Gene Therapy* 2013, **21**(6):1118-1130.

34. Wandinger-Ness A, Zerial M: **Rab proteins and the compartmentalization of the endosomal system**. *Cold Spring Harbor perspectives in biology* 2014, **6**(11):a022616.

35. Bonifacino JS: **Adaptor proteins involved in polarized sorting**. *The Journal of cell biology* 2014, **204**(1):7-17.

36. Goh LK, Huang F, Kim W, Gygi S, Sorkin A: **Multiple mechanisms collectively regulate clathrin-mediated endocytosis of the epidermal growth factor receptor**. *The Journal of cell biology* 2010, **189**(5):871-883.

37. Sorkin A, Fortian A: **Endocytosis and Endosomal Sorting of Receptor Tyrosine Kinases**. In: *Receptor Tyrosine Kinases: Structure, Functions and Role in Human Disease.* Edited by Wheeler DL, Yarden Y: Springer New York; 2015: 133-161.

38. Kelly BT, Graham SC, Liska N, Dannhauser PN, Honing S, Ungewickell EJ, Owen DJ: **Clathrin adaptors. AP2 controls clathrin polymerization with a membrane-activated switch**. *Science* 2014, **345**(6195):459-463.

39. Traub LM, Bonifacino JS: **Cargo recognition in clathrin-mediated endocytosis**. *Cold Spring Harbor perspectives in biology* 2013, **5**(11):a016790.

40. Huang F, Jiang X, Sorkin A: **Tyrosine phosphorylation of the beta2 subunit of clathrin adaptor complex AP-2 reveals the role of a di-leucine motif in the epidermal growth factor receptor trafficking**. *The Journal of biological chemistry* 2003, **278**(44):43411-43417.

41. Sigismund S, Woelk T, Puri C, Maspero E, Tacchetti C, Transidico P, Di Fiore PP, Polo S: **Clathrin-independent endocytosis of ubiquitinated cargos**. *Proceedings of the National Academy of Sciences of the United States of America* 2005, **102**(8):2760-2765.

42. Goh LK, Sorkin A: **Endocytosis of receptor tyrosine kinases**. *Cold Spring Harbor perspectives in biology* 2013, **5**(5):a017459.

43. Boucrot E, Ferreira AP, Almeida-Souza L, Debard S, Vallis Y, Howard G, Bertot L, Sauvonnet N, McMahon HT: **Endophilin marks and controls a clathrin-independent endocytic pathway**. *Nature* 2015, **517**(7535):460-465.

44. Renard HF, Simunovic M, Lemiere J, Boucrot E, Garcia-Castillo MD, Arumugam S, Chambon V, Lamaze C, Wunder C, Kenworthy AK *et al*: **Endophilin-A2 functions in membrane scission in clathrin-independent endocytosis**. *Nature* 2015, **517**(7535):493-496.

45. Sorkin A, Krolenko S, Kudrjavtceva N, Lazebnik J, Teslenko L, Soderquist AM, Nikolsky N: **Recycling of epidermal growth factor-receptor complexes in A431 cells: identification of dual pathways**. *The Journal of cell biology* 1991, **112**(1):55-63.

46. Hsu VW, Prekeris R: **Transport at the recycling endosome**. *Current opinion in cell biology* 2010, **22**(4):528-534.

47. Du Y, Shen J, Hsu JL, Han Z, Hsu MC, Yang CC, Kuo HP, Wang YN, Yamaguchi H, Miller SA *et al*: **Syntaxin 6-mediated Golgi translocation plays an important role in nuclear functions of EGFR through microtubule-dependent trafficking**. *Oncogene* 2014, **33**(6):756-770.

48. Parachoniak CA, Luo Y, Abella JV, Keen JH, Park M: **GGA3 functions as a switch to promote Met receptor recycling, essential for sustained ERK and cell migration**. *Developmental cell* 2011, **20**(6):751-763.

49. Myers JM, Martins GG, Ostrowski J, Stachowiak MK: **Nuclear trafficking of FGFR1: a role for the transmembrane domain**. *Journal of cellular biochemistry* 2003, **88**(6):1273-1291.

50. Wang YN, Wang H, Yamaguchi H, Lee HJ, Lee HH, Hung MC: **COPI-mediated retrograde trafficking from the Golgi to the ER regulates EGFR nuclear transport**. *Biochemical and biophysical research communications* 2010, **399**(4):498-504.

51. Wang YN, Lee HH, Lee HJ, Du Y, Yamaguchi H, Hung MC: **Membrane-bound trafficking regulates nuclear transport of integral epidermal growth factor receptor (EGFR) and ErbB-2**. *The Journal of biological chemistry* 2012, **287**(20):16869-16879.

52. Giri DK, Ali-Seyed M, Li LY, Lee DF, Ling P, Bartholomeusz G, Wang SC, Hung MC: **Endosomal transport of ErbB-2: mechanism for nuclear entry of the cell surface receptor**. *Molecular and cellular biology* 2005, **25**(24):11005-11018.

53. Lo HW, Ali-Seyed M, Wu Y, Bartholomeusz G, Hsu SC, Hung MC: **Nuclear-cytoplasmic transport of EGFR involves receptor endocytosis, importin beta1 and CRM1**. *Journal of cellular biochemistry* 2006, **98**(6):1570-1583.

54. Gorlich D, Vogel F, Mills AD, Hartmann E, Laskey RA: **Distinct functions for the two importin subunits in nuclear protein import**. *Nature* 1995, **377**(6546):246-248.

55. Wang YN, Yamaguchi H, Huo L, Du Y, Lee HJ, Lee HH, Wang H, Hsu JM, Hung MC: **The translocon Sec61beta localized in the inner nuclear**

membrane transports membrane-embedded EGF receptor to the nucleus. *The Journal of biological chemistry* 2010, **285**(49):38720-38729.

56. Stachowiak MK, Fang X, Myers JM, Dunham SM, Berezney R, Maher PA, Stachowiak EK: **Integrative nuclear FGFR1 signaling (INFS) as a part of a universal "feed-forward-and-gate" signaling module that controls cell growth and differentiation**. *Journal of cellular biochemistry* 2003, **90**(4):662-691.

57. Friedberg EC: **DNA repair and mutagenesis**, 2nd edn. Washington, D.C: ASM Press; 2006.

58. Johnson RE, Washington MT, Prakash S, Prakash L: **Fidelity of human DNA polymerase eta**. *J Biol Chem* 2000, **275**(11):7447-7450.

59. Schaaper RM: **Base selection, proofreading, and mismatch repair during DNA replication in Escherichia coli**. *J Biol Chem* 1993, **268**(32):23762-23765.

60. Kuzminov A: **Single-strand interruptions in replicating chromosomes cause double-strand breaks**. *Proc Natl Acad Sci U S A* 2001, **98**(15):8241-8246.

61. Jackson AL, Loeb LA: **The contribution of endogenous sources of DNA damage to the multiple mutations in cancer**. *Mutation research* 2001, **477**(1-2):7-21.

62. Jackson SP, Bartek J: **The DNA-damage response in human biology and disease**. *Nature* 2009, **461**(7267):1071-1078.

63. Hoeijmakers JH: **Genome maintenance mechanisms are critical for preventing cancer as well as other aging-associated diseases**. *Mechanisms of ageing and development* 2007, **128**(7-8):460-462.

64. Goode EL, Ulrich CM, Potter JD: **Polymorphisms in DNA repair genes and associations with cancer risk**. *Cancer epidemiology, biomarkers & prevention : a publication of the American Association for Cancer Research, cosponsored by the American Society of Preventive Oncology* 2002, **11**(12):1513-1530.

65. Peltomaki P: **Role of DNA mismatch repair defects in the pathogenesis of human cancer**. *Journal of clinical oncology : official journal of the American Society of Clinical Oncology* 2003, **21**(6):1174-1179.

66. Ortega J, Li JY, Lee S, Tong D, Gu L, Li GM: **Phosphorylation of PCNA by EGFR inhibits mismatch repair and promotes misincorporation during DNA synthesis**. *Proc Natl Acad Sci U S A* 2015, **112**(18):5667-5672.

67. Chen DJ, Nirodi CS: **The epidermal growth factor receptor: a role in repair of radiation-induced DNA damage**. *Clinical cancer research : an official journal of the American Association for Cancer Research* 2007, **13**(22 Pt 1):6555-6560.

68. Medova M, Aebersold DM, Zimmer Y: **The Molecular Crosstalk between the MET Receptor Tyrosine Kinase and the DNA Damage Response-Biological and Clinical Aspects**. *Cancers* 2013, **6**(1):1-27.

69. Skorski T: **Oncogenic tyrosine kinases and the DNA-damage response**. *Nature reviews Cancer* 2002, **2**(5):351-360.

70. Eckstein N, Roper L, Haas B, Potthast H, Hermes U, Unkrig C, Naumann-Winter F, Enzmann H: **Clinical pharmacology of tyrosine kinase inhibitors becoming generic drugs: the regulatory perspective**. *Journal of experimental & clinical cancer research : CR* 2014, **33**:15.

71. Scott CL, Swisher EM, Kaufmann SH: **Poly (ADP-ribose) polymerase inhibitors: recent advances and future development**. *Journal of clinical oncology : official journal of the American Society of Clinical Oncology* 2015, **33**(12):1397-1406.

72. Ame JC, Spenlehauer C, de Murcia G: **The PARP superfamily**. *BioEssays : news and reviews in molecular, cellular and developmental biology* 2004, **26**(8):882-893.

73. Jungmichel S, Rosenthal F, Altmeyer M, Lukas J, Hottiger MO, Nielsen ML: **Proteome-wide identification of poly(ADP-Ribosyl)ation targets in different genotoxic stress responses**. *Molecular cell* 2013, **52**(2):272-285.

74. Nojima H: **G1 and S-phase checkpoints, chromosome instability, and cancer**. *Methods Mol Biol* 2004, **280**:3-49.

75. Zhou BB, Elledge SJ: **The DNA damage response: putting checkpoints in perspective**. *Nature* 2000, **408**(6811):433-439.

76. Crick F: **The double helix: a personal view**. *Nature* 1974, **248**(5451):766-769.

77. Lomax ME, Folkes LK, O'Neill P: **Biological consequences of radiation-induced DNA damage: relevance to radiotherapy**. *Clin Oncol (R Coll Radiol)* 2013, **25**(10):578-585.

78. Huitema AD, Smits KD, Mathot RA, Schellens JH, Rodenhuis S, Beijnen JH: **The clinical pharmacology of alkylating agents in high-dose chemotherapy**. *Anti-cancer drugs* 2000, **11**(7):515-533.

79. Hoeijmakers JH: **Genome maintenance mechanisms for preventing cancer**. *Nature* 2001, **411**(6835):366-374.

80. Yu H, Liu Z, Huang YJ, Yin M, Wang LE, Wei Q: **Association between single nucleotide polymorphisms in ERCC4 and risk of squamous cell carcinoma of the head and neck**. *PLoS One* 2012, **7**(7):e41853.

81. Li C, Hu Z, Lu J, Liu Z, Wang LE, El-Naggar AK, Sturgis EM, Spitz MR, Wei Q: **Genetic polymorphisms in DNA base-excision repair genes ADPRT, XRCC1, and APE1 and the risk of squamous cell carcinoma of the head and neck**. *Cancer* 2007, **110**(4):867-875.

82. Wang M, Qin C, Zhu J, Yuan L, Fu G, Zhang Z, Yin C: **Genetic variants of XRCC1, APE1, and ADPRT genes and risk of bladder cancer**. *DNA and cell biology* 2010, **29**(6):303-311.

83. Hu D, Lin X, Zhang H, Zheng X, Niu W: **APEX nuclease (multifunctional DNA repair enzyme) 1 gene Asp148Glu polymorphism and cancer risk: a meta-analysis involving 58 articles and 48903 participants**. *PLoS One* 2013, **8**(12):e83527.

84. Divine KK, Gilliland FD, Crowell RE, Stidley CA, Bocklage TJ, Cook DL, Belinsky SA: **The XRCC1 399 glutamine allele is a risk factor for adenocarcinoma of the lung**. *Mutation research* 2001, **461**(4):273-278.

85. Schneider J, Classen V, Helmig S: **XRCC1 polymorphism and lung cancer risk**. *Expert review of molecular diagnostics* 2008, **8**(6):761-780.

86. Krokan HE, Bjoras M: **Base excision repair**. *Cold Spring Harb Perspect Biol* 2013, **5**(4):a012583.

87. King BS, Cooper KL, Liu KJ, Hudson LG: **Poly(ADP-ribose) contributes to an association between poly(ADP-ribose) polymerase-1 and xeroderma pigmentosum complementation group A in nucleotide excision repair**. *J Biol Chem* 2012, **287**(47):39824-39833.

88. Herceg Z, Wang ZQ: **Functions of poly(ADP-ribose) polymerase (PARP) in DNA repair, genomic integrity and cell death**. *Mutation research* 2001, **477**(1-2):97-110.

89. Strom CE, Johansson F, Uhlen M, Szigyarto CA, Erixon K, Helleday T: **Poly (ADP-ribose) polymerase (PARP) is not involved in base excision repair but PARP inhibition traps a single-strand intermediate**. *Nucleic acids research* 2011, **39**(8):3166-3175.

90. Montoni A, Robu M, Pouliot E, Shah GM: **Resistance to PARP-Inhibitors in Cancer Therapy**. *Front Pharmacol* 2013, **4**:18.

91. Lee JM, Ledermann JA, Kohn EC: **PARP Inhibitors for BRCA1/2 mutation-associated and BRCA-like malignancies**. *Annals of oncology : official journal of the European Society for Medical Oncology / ESMO* 2014, **25**(1):32-40.

92. Audeh MW, Carmichael J, Penson RT, Friedlander M, Powell B, Bell-McGuinn KM, Scott C, Weitzel JN, Oaknin A, Loman N *et al*: **Oral poly(ADP-**

ribose) polymerase inhibitor olaparib in patients with BRCA1 or BRCA2 mutations and recurrent ovarian cancer: a proof-of-concept trial. *Lancet* 2010, **376**(9737):245-251.

93. Bixel K, Hays JL: **Olaparib in the management of ovarian cancer**. *Pharmacogenomics and personalized medicine* 2015, **8**:127-135.

94. Scott AD, Waters R: **Inducible nucleotide excision repair (NER) of UV-induced cyclobutane pyrimidine dimers in the cell cycle of the budding yeast Saccharomyces cerevisiae: evidence that inducible NER is confined to the G1 phase of the mitotic cell cycle**. *Molecular & general genetics : MGG* 1997, **254**(1):43-53.

95. Reed E: **Platinum-DNA adduct, nucleotide excision repair and platinum based anti-cancer chemotherapy**. *Cancer treatment reviews* 1998, **24**(5):331-344.

96. Hess MT, Gunz D, Luneva N, Geacintov NE, Naegeli H: **Base pair conformation-dependent excision of benzo[a]pyrene diol epoxide-guanine adducts by human nucleotide excision repair enzymes**. *Molecular and cellular biology* 1997, **17**(12):7069-7076.

97. Kraemer KH, Lee MM, Andrews AD, Lambert WC: **The role of sunlight and DNA repair in melanoma and nonmelanoma skin cancer. The xeroderma pigmentosum paradigm**. *Archives of dermatology* 1994, **130**(8):1018-1021.

98. Lai JP, Liu YC, Alimchandani M, Liu Q, Aung PP, Matsuda K, Lee CC, Tsokos M, Hewitt S, Rushing EJ *et al*: **The influence of DNA repair on neurological degeneration, cachexia, skin cancer and internal**

neoplasms: autopsy report of four xeroderma pigmentosum patients (XP-A, XP-C and XP-D). *Acta neuropathologica communications* 2013, **1**:4.

99. Poulogiannis G, Frayling IM, Arends MJ: **DNA mismatch repair deficiency in sporadic colorectal cancer and Lynch syndrome**. *Histopathology* 2010, **56**(2):167-179.

100. Elsayed FA, Kets CM, Ruano D, van den Akker B, Mensenkamp AR, Schrumpf M, Nielsen M, Wijnen JT, Tops CM, Ligtenberg MJ *et al*: **Germline variants in POLE are associated with early onset mismatch repair deficient colorectal cancer**. *European journal of human genetics : EJHG* 2015, **23**(8):1080-1084.

101. Assasi N, Blackhouse G, Campbell K, Weeks L, Levine M. In: *Mismatch Repair Deficiency Testing for Patients with Colorectal Cancer: A Clinical and Cost-Effectiveness Evaluation.* Ottawa (ON); 2015.

102. Cheung-Ong K, Giaever G, Nislow C: **DNA-damaging agents in cancer chemotherapy: serendipity and chemical biology**. *Chem Biol* 2013, **20**(5):648-659.

103. Deriano L, Roth DB: **Modernizing the nonhomologous end-joining repertoire: alternative and classical NHEJ share the stage**. *Annu Rev Genet* 2013, **47**:433-455.

104. Aravind L, Koonin EV: **Prokaryotic homologs of the eukaryotic DNA-end-binding protein Ku, novel domains in the Ku protein and prediction of a prokaryotic double-strand break repair system**. *Genome Res* 2001, **11**(8):1365-1374.

105. Gu J, Lieber MR: **Mechanistic flexibility as a conserved theme across 3 billion years of nonhomologous DNA end-joining**. *Genes Dev* 2008, **22**(4):411-415.

106. Lieber MR: **The mechanism of double-strand DNA break repair by the nonhomologous DNA end-joining pathway**. *Annu Rev Biochem* 2010, **79**:181-211.

107. Krajewska M, Fehrmann RS, de Vries EG, van Vugt MA: **Regulators of homologous recombination repair as novel targets for cancer treatment**. *Frontiers in genetics* 2015, **6**:96.

108. Shibata A, Moiani D, Arvai AS, Perry J, Harding SM, Genois MM, Maity R, van Rossum-Fikkert S, Kertokalio A, Romoli F *et al*: **DNA double-strand break repair pathway choice is directed by distinct MRE11 nuclease activities**. *Molecular cell* 2014, **53**(1):7-18.

109. Lafrance-Vanasse J, Williams GJ, Tainer JA: **Envisioning the dynamics and flexibility of Mre11-Rad50-Nbs1 complex to decipher its roles in DNA replication and repair**. *Progress in biophysics and molecular biology* 2015, **117**(2-3):182-193.

110. Li X, Heyer WD: **Homologous recombination in DNA repair and DNA damage tolerance**. *Cell Res* 2008, **18**(1):99-113.

111. Noguchi M, Yu D, Hirayama R, Ninomiya Y, Sekine E, Kubota N, Ando K, Okayasu R: **Inhibition of homologous recombination repair in irradiated tumor cells pretreated with Hsp90 inhibitor 17-allylamino-17-**

demethoxygeldanamycin. *Biochem Biophys Res Commun* 2006, **351**(3):658-663.

112. Adimoolam S, Sirisawad M, Chen J, Thiemann P, Ford JM, Buggy JJ: **HDAC inhibitor PCI-24781 decreases RAD51 expression and inhibits homologous recombination**. *Proc Natl Acad Sci U S A* 2007, **104**(49):19482-19487.

113. Toss A, Tomasello C, Razzaboni E, Contu G, Grandi G, Cagnacci A, Schilder RJ, Cortesi L: **Hereditary ovarian cancer: not only BRCA 1 and 2 genes**. *Biomed Res Int* 2015, **2015**:341723.

114. Wittersheim M, Buttner R, Markiefka B: **Genotype/Phenotype correlations in patients with hereditary breast cancer**. *Breast Care (Basel)* 2015, **10**(1):22-26.

115. Taniguchi T, Tischkowitz M, Ameziane N, Hodgson SV, Mathew CG, Joenje H, Mok SC, D'Andrea AD: **Disruption of the Fanconi anemia-BRCA pathway in cisplatin-sensitive ovarian tumors**. *Nat Med* 2003, **9**(5):568-574.

116. Byrski T, Gronwald J, Huzarski T, Grzybowska E, Budryk M, Stawicka M, Mierzwa T, Szwiec M, Wisniowski R, Siolek M *et al*: **Response to neo-adjuvant chemotherapy in women with BRCA1-positive breast cancers**. *Breast Cancer Res Treat* 2008, **108**(2):289-296.

117. Byrski T, Gronwald J, Huzarski T, Grzybowska E, Budryk M, Stawicka M, Mierzwa T, Szwiec M, Wisniowski R, Siolek M *et al*: **Pathologic complete response rates in young women with BRCA1-positive breast cancers**

after neoadjuvant chemotherapy. *Journal of clinical oncology : official journal of the American Society of Clinical Oncology* 2010, **28**(3):375-379.

118. Benafif S, Hall M: **An update on PARP inhibitors for the treatment of cancer**. *Onco Targets Ther* 2015, **8**:519-528.

119. Muggia F, Safra T: **'BRCAness' and its implications for platinum action in gynecologic cancer**. *Anticancer Res* 2014, **34**(2):551-556.

120. Al-Minawi AZ, Saleh-Gohari N, Helleday T: **The ERCC1/XPF endonuclease is required for efficient single-strand annealing and gene conversion in mammalian cells**. *Nucleic acids research* 2008, **36**(1):1-9.

121. Pastink A, Eeken JC, Lohman PH: **Genomic integrity and the repair of double-strand DNA breaks**. *Mutation research* 2001, **480-481**:37-50.

122. Montagut C, Settleman J: **Targeting the RAF-MEK-ERK pathway in cancer therapy**. *Cancer letters* 2009, **283**(2):125-134.

123. Feng Z, Hu W, Chen JX, Pao A, Li H, Rom W, Hung MC, Tang MS: **Preferential DNA damage and poor repair determine ras gene mutational hotspot in human cancer**. *Journal of the National Cancer Institute* 2002, **94**(20):1527-1536.

124. Grabocka E, Pylayeva-Gupta Y, Jones MJ, Lubkov V, Yemanaberhan E, Taylor L, Jeng HH, Bar-Sagi D: **Wild-type H- and N-Ras promote mutant K-Ras-driven tumorigenesis by modulating the DNA damage response**. *Cancer Cell* 2014, **25**(2):243-256.

125. Hahnel PS, Enders B, Sasca D, Roos WP, Kaina B, Bullinger L, Theobald M, Kindler T: **Targeting components of the alternative NHEJ pathway**

sensitizes KRAS mutant leukemic cells to chemotherapy. *Blood* 2014, **123**(15):2355-2366.

126. Xu N, Hegarat N, Black EJ, Scott MT, Hochegger H, Gillespie DA: **Akt/PKB suppresses DNA damage processing and checkpoint activation in late G2**. *J Cell Biol* 2010, **190**(3):297-305.

127. Xu N, Lao Y, Zhang Y, Gillespie DA: **Akt: a double-edged sword in cell proliferation and genome stability**. *J Oncol* 2012, **2012**:951724.

128. Wei Z, Song X, Shaikh ZA: **Cadmium promotes the proliferation of triple-negative breast cancer cells through EGFR-mediated cell cycle regulation**. *Toxicology and applied pharmacology* 2015, **289**(1):98-108.

129. Weidhaas JB, Eisenmann DM, Holub JM, Nallur SV: **A conserved RAS/mitogen-activated protein kinase pathway regulates DNA damage-induced cell death postirradiation in Radelegans**. *Cancer Res* 2006, **66**(21):10434-10438.

130. Yacoub A, McKinstry R, Hinman D, Chung T, Dent P, Hagan MP: **Epidermal growth factor and ionizing radiation up-regulate the DNA repair genes XRCC1 and ERCC1 in DU145 and LNCaP prostate carcinoma through MAPK signaling**. *Radiat Res* 2003, **159**(4):439-452.

131. Yacoub A, Park JS, Qiao L, Dent P, Hagan MP: **MAPK dependence of DNA damage repair: ionizing radiation and the induction of expression of the DNA repair genes XRCC1 and ERCC1 in DU145 human prostate carcinoma cells in a MEK1/2 dependent fashion**. *Int J Radiat Biol* 2001, **77**(10):1067-1078.

132. Toulany M, Dittmann K, Fehrenbacher B, Schaller M, Baumann M, Rodemann HP: **PI3K-Akt signaling regulates basal, but MAP-kinase signaling regulates radiation-induced XRCC1 expression in human tumor cells in vitro**. *DNA Repair (Amst)* 2008, **7**(10):1746-1756.

133. Chou RH, Wang YN, Hsieh YH, Li LY, Xia W, Chang WC, Chang LC, Cheng CC, Lai CC, Hsu JL *et al*: **EGFR modulates DNA synthesis and repair through Tyr phosphorylation of histone H4**. *Developmental cell* 2014, **30**(2):224-237.

134. Tong D, Ortega J, Kim C, Huang J, Gu L, Li GM: **Arsenic Inhibits DNA Mismatch Repair by Promoting EGFR Expression and PCNA Phosphorylation**. *J Biol Chem* 2015, **290**(23):14536-14541.

135. Wang SC, Nakajima Y, Yu YL, Xia W, Chen CT, Yang CC, McIntush EW, Li LY, Hawke DH, Kobayashi R *et al*: **Tyrosine phosphorylation controls PCNA function through protein stability**. *Nat Cell Biol* 2006, **8**(12):1359-1368.

136. Yu YL, Chou RH, Liang JH, Chang WJ, Su KJ, Tseng YJ, Huang WC, Wang SC, Hung MC: **Targeting the EGFR/PCNA signaling suppresses tumor growth of triple-negative breast cancer cells with cell-penetrating PCNA peptides**. *PLoS One* 2013, **8**(4):e61362.

137. Lee HJ, Lan L, Peng G, Chang WC, Hsu MC, Wang YN, Cheng CC, Wei L, Nakajima S, Chang SS *et al*: **Tyrosine 370 phosphorylation of ATM positively regulates DNA damage response**. *Cell Res* 2015, **25**(2):225-236.

138. Nowsheen S, Cooper T, Stanley JA, Yang ES: **Synthetic lethal interactions between EGFR and PARP inhibition in human triple negative breast cancer cells**. *PLoS One* 2012, **7**(10):e46614.

139. Al-Ejeh F, Shi W, Miranda M, Simpson PT, Vargas AC, Song S, Wiegmans AP, Swarbrick A, Welm AL, Brown MP *et al*: **Treatment of triple-negative breast cancer using anti-EGFR-directed radioimmunotherapy combined with radiosensitizing chemotherapy and PARP inhibitor**. *Journal of nuclear medicine : official publication, Society of Nuclear Medicine* 2013, **54**(6):913-921.

140. Sui H, Shi C, Yan Z, Li H: **Combination of erlotinib and a PARP inhibitor inhibits growth of A2780 tumor xenografts due to increased autophagy**. *Drug design, development and therapy* 2015, **9**:3183-3190.

141. Dittmann K, Mayer C, Kehlbach R, Rothmund MC, Peter Rodemann H: **Radiation-induced lipid peroxidation activates src kinase and triggers nuclear EGFR transport**. *Radiother Oncol* 2009, **92**(3):379-382.

142. Dittmann K, Mayer C, Kehlbach R, Rodemann HP: **Radiation-induced caveolin-1 associated EGFR internalization is linked with nuclear EGFR transport and activation of DNA-PK**. *Mol Cancer* 2008, **7**:69.

143. Wanner G, Mayer C, Kehlbach R, Rodemann HP, Dittmann K: **Activation of protein kinase Cepsilon stimulates DNA-repair via epidermal growth factor receptor nuclear accumulation**. *Radiother Oncol* 2008, **86**(3):383-390.

144. Yu YL, Chou RH, Wu CH, Wang YN, Chang WJ, Tseng YJ, Chang WC, Lai CC, Lee HJ, Huo L *et al*: **Nuclear EGFR suppresses ribonuclease activity of polynucleotide phosphorylase through DNAPK-mediated phosphorylation at serine 776**. *J Biol Chem* 2012, **287**(37):31015-31026.

145. Dittmann K, Mayer C, Kehlbach R, Rodemann HP: **The radioprotector Bowman-Birk proteinase inhibitor stimulates DNA repair via epidermal growth factor receptor phosphorylation and nuclear transport**. *Radiother Oncol* 2008, **86**(3):375-382.

146. Dittmann K, Mayer C, Wanner G, Kehlbach R, Rodemann HP: **The radioprotector O-phospho-tyrosine stimulates DNA-repair via epidermal growth factor receptor- and DNA-dependent kinase phosphorylation**. *Radiother Oncol* 2007, **84**(3):328-334.

147. Bandyopadhyay D, Mandal M, Adam L, Mendelsohn J, Kumar R: **Physical interaction between epidermal growth factor receptor and DNA-dependent protein kinase in mammalian cells**. *J Biol Chem* 1998, **273**(3):1568-1573.

148. Huang SM, Harari PM: **Modulation of radiation response after epidermal growth factor receptor blockade in squamous cell carcinomas: inhibition of damage repair, cell cycle kinetics, and tumor angiogenesis**. *Clinical cancer research : an official journal of the American Association for Cancer Research* 2000, **6**(6):2166-2174.

149. Dittmann K, Mayer C, Rodemann HP: **Inhibition of radiation-induced EGFR nuclear import by C225 (Cetuximab) suppresses DNA-PK activity**. *Radiother Oncol* 2005, **76**(2):157-161.

150. Chinnaiyan P, Huang S, Vallabhaneni G, Armstrong E, Varambally S, Tomlins SA, Chinnaiyan AM, Harari PM: **Mechanisms of enhanced radiation response following epidermal growth factor receptor signaling inhibition by erlotinib (Tarceva)**. *Cancer Res* 2005, **65**(8):3328-3335.

151. Huang SM, Bock JM, Harari PM: **Epidermal growth factor receptor blockade with C225 modulates proliferation, apoptosis, and radiosensitivity in squamous cell carcinomas of the head and neck**. *Cancer Res* 1999, **59**(8):1935-1940.

152. Tan M, Jing T, Lan KH, Neal CL, Li P, Lee S, Fang D, Nagata Y, Liu J, Arlinghaus R *et al*: **Phosphorylation on tyrosine-15 of p34(Cdc2) by ErbB2 inhibits p34(Cdc2) activation and is involved in resistance to taxol-induced apoptosis**. *Molecular cell* 2002, **9**(5):993-1004.

153. Li C, Brand TM, Iida M, Huang S, Armstrong EA, van der Kogel A, Wheeler DL: **Human epidermal growth factor receptor 3 (HER3) blockade with U3-1287/AMG888 enhances the efficacy of radiation therapy in lung and head and neck carcinoma**. *Discov Med* 2013, **16**(87):79-92.

154. Li C, Huang S, Armstrong EA, Francis DM, Werner LR, Sliwkowski MX, van der Kogel A, Harari PM: **Antitumor Effects of MEHD7945A, a Dual-Specific Antibody against EGFR and HER3, in Combination with Radiation in**

Lung and Head and Neck Cancers. *Mol Cancer Ther* 2015, **14**(9):2049-2059.

155. Huang S, Li C, Armstrong EA, Peet CR, Saker J, Amler LC, Sliwkowski MX, Harari PM: **Dual targeting of EGFR and HER3 with MEHD7945A overcomes acquired resistance to EGFR inhibitors and radiation**. *Cancer Res* 2013, **73**(2):824-833.

156. Chen JT, Huang CY, Chiang YY, Chen WH, Chiou SH, Chen CY, Chow KC: **HGF increases cisplatin resistance via down-regulation of AIF in lung cancer cells**. *Am J Respir Cell Mol Biol* 2008, **38**(5):559-565.

157. Du Y, Yamaguchi H, Wei Y, Hsu JL, Wang HL, Hsu YH, Lin WC, Yu WH, Leonard PG, Lee GRt *et al*: **Blocking c-Met-mediated PARP1 phosphorylation enhances anti-tumor effects of PARP inhibitors**. *Nat Med* 2016, **22**(2):194-201.

158. Zhao H, Chen MS, Lo YH, Waltz SE, Wang J, Ho PC, Vasiliauskas J, Plattner R, Wang YL, Wang SC: **The Ron receptor tyrosine kinase activates c-Abl to promote cell proliferation through tyrosine phosphorylation of PCNA in breast cancer**. *Oncogene* 2014, **33**(11):1429-1437.

159. Ali AAE, Timinszky G, Arribas-Bosacoma R, Kozlowski M, Hassa PO, Hassler M, Ladurner AG, Pearl LH, Oliver AW: **The zinc-finger domains of PARP1 cooperate to recognize DNA strand breaks**. *Nat Struct Mol Biol* 2012, **19**(7):685-692.

160. Alemasova EE, Lavrik OI: **Poly(ADP-ribosyl)ation by PARP1: reaction mechanism and regulatory proteins**. *Nucleic Acids Res* 2019, **47**(8):3811-3827.

161. Ray Chaudhuri A, Nussenzweig A: **The multifaceted roles of PARP1 in DNA repair and chromatin remodelling**. *Nat Rev Mol Cell Biol* 2017, **18**(10):610-621.

162. Hanahan D, Weinberg RA: **Hallmarks of cancer: the next generation**. *Cell* 2011, **144**(5):646-674.

163. Jiang X, Li W, Li X, Bai H, Zhang Z: **Current status and future prospects of PARP inhibitor clinical trials in ovarian cancer**. *Cancer Manag Res* 2019, **11**:4371-4390.

164. Exman P, Barroso-Sousa R, Tolaney SM: **Evidence to date: talazoparib in the treatment of breast cancer**. *Onco Targets Ther* 2019, **12**:5177-5187.

165. Shen Y, Aoyagi-Scharber M, Wang B: **Trapping Poly(ADP-Ribose) Polymerase**. *J Pharmacol Exp Ther* 2015, **353**(3):446-457.

166. Murai J, Pommier Y: **PARP Trapping Beyond Homologous Recombination and Platinum Sensitivity in Cancers**. *Annual Review of Cancer Biology* 2019, **3**(1):131-150.

167. Murai J, Huang SY, Das BB, Renaud A, Zhang Y, Doroshow JH, Ji J, Takeda S, Pommier Y: **Trapping of PARP1 and PARP2 by Clinical PARP Inhibitors**. *Cancer Res* 2012, **72**(21):5588-5599.

168. Kotsopoulos J: **BRCA Mutations and Breast Cancer Prevention**. *Cancers (Basel)* 2018, **10**(12).

169. Greenup R, Buchanan A, Lorizio W, Rhoads K, Chan S, Leedom T, King R, McLennan J, Crawford B, Kelly Marcom P *et al*: **Prevalence of BRCA mutations among women with triple-negative breast cancer (TNBC) in a genetic counseling cohort**. *Ann Surg Oncol* 2013, **20**(10):3254-3258.

170. Chen H, Wu J, Zhang Z, Tang Y, Li X, Liu S, Cao S, Li X: **Association Between BRCA Status and Triple-Negative Breast Cancer: A Meta-Analysis**. *Front Pharmacol* 2018, **9**:909.

171. Byrum AK, Vindigni A, Mosammaparast N: **Defining and Modulating 'BRCAness'**. *Trends Cell Biol* 2019, **29**(9):740-751.

172. Tian T, Shan L, Yang W, Zhou X, Shui R: **Evaluation of the BRCAness phenotype and its correlations with clinicopathological features in triple-negative breast cancers**. *Hum Pathol* 2019, **84**:231-238.

173. Papadimitriou M, Mountzios G, Papadimitriou CA: **The role of PARP inhibition in triple-negative breast cancer: Unraveling the wide spectrum of synthetic lethality**. *Cancer Treat Rev* 2018, **67**:34-44.

174. Noordermeer SM, van Attikum H: **PARP Inhibitor Resistance: A Tug-of-War in BRCA-Mutated Cells**. *Trends Cell Biol* 2019, **29**(10):820-834.

175. Gogola E, Rottenberg S, Jonkers J: **Resistance to PARP Inhibitors: Lessons from Preclinical Models of BRCA-Associated Cancer**. *Annual Review of Cancer Biology* 2019, **3**(1):235-254.

176. Norquist B, Wurz KA, Pennil CC, Garcia R, Gross J, Sakai W, Karlan BY, Taniguchi T, Swisher EM: **Secondary somatic mutations restoring**

BRCA1/2 predict chemotherapy resistance in hereditary ovarian carcinomas. *J Clin Oncol* 2011, **29**(22):3008-3015.

177. Waks AG, Cohen O, Kochupurakkal B, Kim D, Dunn CE, Buendia JB, Wander S, Helvie K, Lloyd MR, Marini L *et al*: **Reversion and non-reversion mechanisms of resistance to PARP inhibitor or platinum chemotherapy in BRCA1/2-mutant metastatic breast cancer**. *Annals of Oncology* 2020.

178. Cao L, Xu X, Bunting SF, Liu J, Wang RH, Cao LL, Wu JJ, Peng TN, Chen J, Nussenzweig A *et al*: **A selective requirement for 53BP1 in the biological response to genomic instability induced by Brca1 deficiency**. *Mol Cell* 2009, **35**(4):534-541.

179. Bouwman P, Aly A, Escandell JM, Pieterse M, Bartkova J, van der Gulden H, Hiddingh S, Thanasoula M, Kulkarni A, Yang Q *et al*: **53BP1 loss rescues BRCA1 deficiency and is associated with triple-negative and BRCA-mutated breast cancers**. *Nat Struct Mol Biol* 2010, **17**(6):688-695.

180. Bunting SF, Callen E, Wong N, Chen HT, Polato F, Gunn A, Bothmer A, Feldhahn N, Fernandez-Capetillo O, Cao L *et al*: **53BP1 inhibits homologous recombination in Brca1-deficient cells by blocking resection of DNA breaks**. *Cell* 2010, **141**(2):243-254.

181. Rottenberg S, Jaspers JE, Kersbergen A, van der Burg E, Nygren AO, Zander SA, Derksen PW, de Bruin M, Zevenhoven J, Lau A *et al*: **High sensitivity of BRCA1-deficient mammary tumors to the PARP inhibitor AZD2281 alone and in combination with platinum drugs**. *Proc Natl Acad Sci U S A* 2008, **105**(44):17079-17084.

182. Callaghan R, Luk F, Bebawy M: **Inhibition of the multidrug resistance P-glycoprotein: time for a change of strategy?** *Drug Metab Dispos* 2014, **42**(4):623-631.

183. Dufour R, Daumar P, Mounetou E, Aubel C, Kwiatkowski F, Abrial C, Vatoux C, Penault-Llorca F, Bamdad M: **BCRP and P-gp relay overexpression in triple negative basal-like breast cancer cell line: a prospective role in resistance to Olaparib**. *Sci Rep* 2015, **5**:12670.

184. Oplustil O'Connor L, Rulten SL, Cranston AN, Odedra R, Brown H, Jaspers JE, Jones L, Knights C, Evers B, Ting A *et al*: **The PARP Inhibitor AZD2461 Provides Insights into the Role of PARP3 Inhibition for Both Synthetic Lethality and Tolerability with Chemotherapy in Preclinical Models**. *Cancer Res* 2016, **76**(20):6084-6094.

185. Johnson N, Li YC, Walton ZE, Cheng KA, Li D, Rodig SJ, Moreau LA, Unitt C, Bronson RT, Thomas HD *et al*: **Compromised CDK1 activity sensitizes BRCA-proficient cancers to PARP inhibition**. *Nat Med* 2011, **17**(7):875-882.

186. Blazek D, Kohoutek J, Bartholomeeusen K, Johansen E, Hulinkova P, Luo Z, Cimermancic P, Ule J, Peterlin BM: **The Cyclin K/Cdk12 complex maintains genomic stability via regulation of expression of DNA damage response genes**. *Genes Dev* 2011, **25**(20):2158-2172.

187. Joshi PM, Sutor SL, Huntoon CJ, Karnitz LM: **Ovarian cancer-associated mutations disable catalytic activity of CDK12, a kinase that promotes homologous recombination repair and resistance to cisplatin and**

poly(ADP-ribose) polymerase inhibitors. *J Biol Chem* 2014, **289**(13):9247-9253.

188. Bajrami I, Frankum JR, Konde A, Miller RE, Rehman FL, Brough R, Campbell J, Sims D, Rafiq R, Hooper S *et al*: **Genome-wide profiling of genetic synthetic lethality identifies CDK12 as a novel determinant of PARP1/2 inhibitor sensitivity**. *Cancer Res* 2014, **74**(1):287-297.

189. Johnson SF, Cruz C, Greifenberg AK, Dust S, Stover DG, Chi D, Primack B, Cao S, Bernhardy AJ, Coulson R *et al*: **CDK12 Inhibition Reverses De Novo and Acquired PARP Inhibitor Resistance in BRCA Wild-Type and Mutated Models of Triple-Negative Breast Cancer**. *Cell Rep* 2016, **17**(9):2367-2381.

190. Mishra B, Zhang S, Zhao H, Darzynkiewicz Z, Lee EYC, Lee M, Zhang Z: **Discovery of a novel DNA polymerase inhibitor and characterization of its antiproliferative properties**. *Cancer Biol Ther* 2019, **20**(4):474-486.

191. Mak JPY, Ma HT, Poon RYC: **Synergism between ATM and PARP1 Inhibition Involves DNA Damage and Abrogating the G2 DNA Damage Checkpoint**. *Mol Cancer Ther* 2020, **19**(1):123-134.

192. Lallo A, Frese KK, Morrow CJ, Sloane R, Gulati S, Schenk MW, Trapani F, Simms N, Galvin M, Brown S *et al*: **The Combination of the PARP Inhibitor Olaparib and the WEE1 Inhibitor AZD1775 as a New Therapeutic Option for Small Cell Lung Cancer**. *Clin Cancer Res* 2018, **24**(20):5153-5164.

193. Yazinski SA, Comaills V, Buisson R, Genois MM, Nguyen HD, Ho CK, Todorova Kwan T, Morris R, Lauffer S, Nussenzweig A *et al*: **ATR inhibition**

disrupts rewired homologous recombination and fork protection pathways in PARP inhibitor-resistant BRCA-deficient cancer cells. *Genes Dev* 2017, **31**(3):318-332.

194. Ceccaldi R, Liu JC, Amunugama R, Hajdu I, Primack B, Petalcorin MI, O'Connor KW, Konstantinopoulos PA, Elledge SJ, Boulton SJ *et al*: **Homologous-recombination-deficient tumours are dependent on Poltheta-mediated repair**. *Nature* 2015, **518**(7538):258-262.

195. Pilie PG, Tang C, Mills GB, Yap TA: **State-of-the-art strategies for targeting the DNA damage response in cancer**. *Nat Rev Clin Oncol* 2019, **16**(2):81-104.

196. Chen MK, Du Y, Sun L, Hsu JL, Wang YH, Gao Y, Huang J, Hung MC: **H2O2 induces nuclear transport of the receptor tyrosine kinase c-MET in breast cancer cells via a membrane-bound retrograde trafficking mechanism**. *J Biol Chem* 2019, **294**(21):8516-8528.

197. Allalou A, Wahlby C: **BlobFinder, a tool for fluorescence microscopy image cytometry**. *Comput Methods Programs Biomed* 2009, **94**(1):58-65.

198. Okada M, Fukagawa T: **Purification of a protein complex that associates with chromatin**. In., vol. PROTOCOL (Version 1), 15 December 2006 edn: Protocol Exchange; 2006.

199. Johannessen CM, Boehm JS, Kim SY, Thomas SR, Wardwell L, Johnson LA, Emery CM, Stransky N, Cogdill AP, Barretina J *et al*: **COT drives resistance to RAF inhibition through MAP kinase pathway reactivation**. *Nature* 2010, **468**(7326):968-972.

200. Kim E, Ilic N, Shrestha Y, Zou L, Kamburov A, Zhu C, Yang X, Lubonja R, Tran N, Nguyen C *et al*: **Systematic Functional Interrogation of Rare Cancer Variants Identifies Oncogenic Alleles**. *Cancer Discov* 2016, **6**(7):714-726.

201. Chen MK, Tsai YC, Li PY, Liou CC, Taniga ES, Chang DW, Mori T, Liu YC: **Delay of gap filling during nucleotide excision repair by base excision repair: the concept of competition exemplified by the effect of propolis**. *Toxicol Sci* 2011, **122**(2):339-348.

202. Evans KW, Yuca E, Akcakanat A, Scott SM, Arango NP, Zheng X, Chen K, Tapia C, Tarco E, Eterovic AK *et al*: **A Population of Heterogeneous Breast Cancer Patient-Derived Xenografts Demonstrate Broad Activity of PARP Inhibitor in BRCA1/2 Wild-Type Tumors**. *Clin Cancer Res* 2017, **23**(21):6468-6477.

203. Chou TC: **Theoretical basis, experimental design, and computerized simulation of synergism and antagonism in drug combination studies**. *Pharmacol Rev* 2006, **58**(3):621-681.

204. Farrell B, Breeze AL: **Structure, activation and dysregulation of fibroblast growth factor receptor kinases: perspectives for clinical targeting**. *Biochem Soc Trans* 2018, **46**(6):1753-1770.

205. Perez-Garcia J, Munoz-Couselo E, Soberino J, Racca F, Cortes J: **Targeting FGFR pathway in breast cancer**. *Breast* 2018, **37**:126-133.

206. Pommier Y, O'Connor MJ, de Bono J: **Laying a trap to kill cancer cells: PARP inhibitors and their mechanisms of action**. *Sci Transl Med* 2016, **8**(362):362ps317.

207. Pachkowski BF, Tano K, Afonin V, Elder RH, Takeda S, Watanabe M, Swenberg JA, Nakamura J: **Cells deficient in PARP-1 show an accelerated accumulation of DNA single strand breaks, but not AP sites, over the PARP-1-proficient cells exposed to MMS**. *Mutat Res* 2009, **671**(1-2):93-99.

208. Lombard AP, Liu C, Armstrong CM, D'Abronzo LS, Lou W, Chen H, Dall'Era M, Ghosh PM, Evans CP, Gao AC: **Overexpressed ABCB1 Induces Olaparib-Taxane Cross-Resistance in Advanced Prostate Cancer**. *Transl Oncol* 2019, **12**(7):871-878.

209. Vaidyanathan A, Sawers L, Gannon AL, Chakravarty P, Scott AL, Bray SE, Ferguson MJ, Smith G: **ABCB1 (MDR1) induction defines a common resistance mechanism in paclitaxel- and olaparib-resistant ovarian cancer cells**. *Br J Cancer* 2016, **115**(4):431-441.

210. Chou TC: **Drug combination studies and their synergy quantification using the Chou-Talalay method**. *Cancer Res* 2010, **70**(2):440-446.

211. de Bono J, Ramanathan RK, Mina L, Chugh R, Glaspy J, Rafii S, Kaye S, Sachdev J, Heymach J, Smith DC *et al*: **Phase I, Dose-Escalation, Two-Part Trial of the PARP Inhibitor Talazoparib in Patients with Advanced Germline BRCA1/2 Mutations and Selected Sporadic Cancers**. *Cancer Discov* 2017, **7**(6):620-629.

212. Paik PK, Shen R, Berger MF, Ferry D, Soria JC, Mathewson A, Rooney C, Smith NR, Cullberg M, Kilgour E *et al*: **A Phase Ib Open-Label Multicenter Study of AZD4547 in Patients with Advanced Squamous Cell Lung Cancers**. *Clin Cancer Res* 2017, **23**(18):5366-5373.

213. Robson M, Im SA, Senkus E, Xu B, Domchek SM, Masuda N, Delaloge S, Li W, Tung N, Armstrong A *et al*: **Olaparib for Metastatic Breast Cancer in Patients with a Germline BRCA Mutation**. *N Engl J Med* 2017, **377**(6):523-533.

214. Litton JK, Rugo HS, Ettl J, Hurvitz SA, Goncalves A, Lee KH, Fehrenbacher L, Yerushalmi R, Mina LA, Martin M *et al*: **Talazoparib in Patients with Advanced Breast Cancer and a Germline BRCA Mutation**. *N Engl J Med* 2018, **379**(8):753-763.

215. Pettitt SJ, Krastev DB, Brandsma I, Drean A, Song F, Aleksandrov R, Harrell MI, Menon M, Brough R, Campbell J *et al*: **Genome-wide and high-density CRISPR-Cas9 screens identify point mutations in PARP1 causing PARP inhibitor resistance**. *Nat Commun* 2018, **9**(1):1849.

216. Langelier MF, Planck JL, Roy S, Pascal JM: **Crystal structures of poly(ADP-ribose) polymerase-1 (PARP-1) zinc fingers bound to DNA: structural and functional insights into DNA-dependent PARP-1 activity**. *J Biol Chem* 2011, **286**(12):10690-10701.

217. Eustermann S, Videler H, Yang JC, Cole PT, Gruszka D, Veprintsev D, Neuhaus D: **The DNA-binding domain of human PARP-1 interacts with**

DNA single-strand breaks as a monomer through its second zinc finger.

J Mol Biol 2011, **407**(1):149-170.

Vita

Mei-Kuang Chen was born in Changhua city, Taiwan, the daughter of Shu-Chin Wang and Shan-Tarng Chen. After completing her work at National Taichung Girl's Senior High School, Taichung, Taiwan in 2005, she entered Department of Life Science, College of Life Science at National Tsing Hua University, Hsinchu, Taiwan. She finished her undergraduate thesis and received the degree of Bachelor of Science in June 2009 with a major in Life Science. She entered Institute of Molecular Medicine, College of Life Science at National Tsing Hua University in 2009. She received the degree of Master of Science in July, 2011. In the next year, she worked as administration assistant and research assistant in Department of Life Science at National Tsing Hua University. She then entered The University of Texas Graduate School of Biomedical Sciences at Houston and received the degree of Master of Science in July, 2012. In August of 2012, she entered into PhD program at The University of Texas MD Anderson Cancer Center UTHealth Graduate School of Biomedical Sciences; The University of Texas MD Anderson Cancer Center at Houston.